Phenology of anther development of dwarf mistletoe (*Arceuthobium americanum* Nutt. *ex* Engelm.): an anatomical investigation of microsporogenesis and microgametogenesis

by

Karen Yvonne Sereda

A Thesis
Submitted to the Faculty of Graduate Studies
in Partial Fulfillment of the Requirements
for the Degree of

MASTER OF SCIENCE

Department of Botany
The University of Manitoba
Winnipeg, Manitoba R3T 2N2

THE UNIVERSITY OF MANITOBA

FACULTY OF GRADUATE STUDIES

*****

COPYRIGHT PERMISSION PAGE

Phenology of anther development of dwarf mistletoe (*Arceuthobium americanum* Nutt. *ex* Engelm.): an anatomical investigation of microsporogenesis and microgametogenesis

BY

Karen Yvonne Sereda

A Thesis/Practicum submitted to the Faculty of Graduate Studies of The University of Manitoba in partial fulfillment of the requirements of the degree of Master of Science

Abstract

Vegetative meristems of *Arceuthobium americanum* have a typical tunica-corpus dome shape. Conversion to a floral meristem occurs in early May at Belair, Manitoba, and is indicated by an alteration to a flattened shape. By late May, perianth segments are present and continue to elongate into the month of June, when stamen primordia are initiated. Protodermal and hypodermal cells divide periclinally and anticlinally to result initially in a uniseriate epidermis and primary parietal layer surrounding a single region of sporogenous cells. A second division by the primary parietal layer produces an inner tapetal layer bounded by an ephemeral middle layer. There is no endothecium. The epidermis later develops wall thickenings and serves as an exothecium for pollen dehiscence. Proliferation of the sporogenous tissue eventually results in a cup-shaped sporangium around a central, sterile columella. By mid-August, mitotic divisions have ceased and the sporogenous cells are now referred to as the microsporocytes. The middle layer is crushed between the epidermis and tapetum and is eventually completely resorbed. Many vacuolate cells are present within the anther and especially in the tapetum, although these cells are quite organelle-rich. Cytomictic channels are found both between microsporocytes and tapetal cells, but not between the two cell types. The third week in August, microsporocytes become more spherical and develop thickened, callose-containing cell walls. An artifactual periplasmic space becomes quite prominent at this stage of development, and cytomictic channels are still present. By late August, meiosis has concluded and tetrahedral tetrads, still in their callose-rich walls are found. It is around the time of meiosis when presumed cytoplasmically male sterile anthers are first observed. Cytokinesis appears to be simultaneous and is probably via in-furrowing. Separated microspores are seen by the end of August and are vacuolate early on. Later, they become more cytoplasmically dense, develop a sporopollenin wall and enlarge in size. The tapetum releases small tubular structures, as well as larger osmiophilic material via orbicules and bigger tapetal extrusions. Microspore mitosis occurs in early September and initially both nuclei are spherical and centrally located. The vegetative nucleus becomes more elongate in shape, but the generative remains round and is distinguishable from the vegetative because of its enveloping cell wall. Both cells contain mitochondria and amyloplasts. The spiny pollen grains have three colpae alternating with three pseudocolpae. The intine thickens beneath each aperture, whereas the exine thins in these same areas. A layer of pollenkitt is also present over the entire mature grain's papillate surface. Mature bicellular grains overwinter within intact floral buds until anthesis early the next spring. The *in vitro* germination of mature pollen was found to be more influenced by temperature than by sucrose concentration, but date of sampling and pollen source also had some effect. Pollen germinated at a higher rate at 20°C, however, the overall percent of pollen grains to germinate was low. Pollen tube lengths tended to be longer for each successive sampling date, and those germinated at 20°C had longer tubes than those incubated at 30°C. There was a very weak positive correlation between percent germination and pollen tube length.

Acknowledgements

Financial assistance came partially from a Faculty of Science Fellowship and a scholarship from the Mid-Canada Association of Official Analytical Chemists. Drs. Michael Sumner and David Punter also provided financial and logistical support for the research. Other financial incentives were gained by employment opportunities offered by the Departments of Botany and Biology.

I would like to thank my advisor, Dr. Mike Sumner for his guidance and encouragement with all stages of the project. As well, a big thank you is due the other members of my committee, Dr. David Punter, Dr. Bill Remphrey and Dr. Isobel Waters, for all their helpful suggestions and support. Dr. Tom Booth was generous with the use of his computer, slide scanning equipment and software. Lynn Burton, our EM technician, was extremely competent and aided with a number of technical procedures in the laboratory. For answering and solving my many departmental questions and concerns over the years, my sincere thanks goes to Keith Travis, administrative assistant and Mark Elliott, greenhouse technician. To Cindy Ross, what can I say.....heartfelt thanks for her friendship, company and help, both in the field and in the lab. Cheryl Jerome's tenacious, yet open nature in regard to both school and personal life was inspirational at times, and kept me on the right track. Jen Line, Jennifer Mustard and Vera Williams, you have been wonderful friends and schoolmates; I really appreciated being able to vent now and then. And finally, my family, Dennis and Graham.....I thank you for all your patience and support, throughout all the stages of this thesis and the rest of my education. Especially your computer help near the end Dennis.....I couldn't have done it without you.

Table of Contents

List of Figures

List of Tables

List of Abbreviations

AM	amyloplast
c	columella
CS	cross-section
cw	cell wall
DDW	deionized, distilled water
ep	epidermis
ER	endoplasmic reticulum
ex	exine
gcw	generative cell wall
gn	generative nucleus
in	intine
lp	leaf primordium
LS	longitudinal section
m	microspores
M	mitochondrion
ml	middle layer
mmc	microspore mother cells/microsporocytes
n	nucleus
nu	nucleolus
OS	oblique section
p	parietal layer
PAS	periodic acid Schiff's
pg	pollen grains
SEM	scanning electron microscopy
sp	sporogenous tissue/cells
t	tapetum
te	tetrads
TEM	transmission electron microscopy
UV	ultraviolet
v	vacuolate cell
va	vacuole
ve	vesicle
vn	vegetative nucleus

List of Appendices

1.0 INTRODUCTION

1.1 General Introduction to the Dwarf Mistletoes

1.1.1 Distribution and life history

Plant parasitism has arisen at least eleven times over the course of angiosperm evolution. Worldwide, 22 dicot families contain around 4000 parasitic species. All acquire at least some minerals, water and/or carbohydrates from their host, either from aerial or underground parts. Host plant effects can range from slight to fatal, and many are considered noxious weeds. Parasitic plants are believed to have originally been facultative photosynthesizers. A trade-off between chloroplast genome losses and the acquisition of new traits perpetuating the parasitic mode of nutrition has allowed for their continued existence (Yoder 1999).

Parasite relationships are often very host-specific. The dwarf mistletoes (*Arceuthobium* spp.) are dicotyledonous angiosperms, belonging to the family Viscaceae, tribe Arceuthobeae. Eight species in the Old World and 39 in the New represent the genus. All are hemiparasitic on members of either the family Pinaceae or Cupressaceae (Calder 1983, Hawksworth & Wiens 1996), and nearly every coniferous tree species has its own associated species of *Arceuthobium* (Hawksworth & Wiens 1996, Weber 1976).

The distribution of the dwarf mistletoes is limited to the Northern Hemisphere (Figure 1.1), except for a small region in Kenya (Barlow 1983, Hawksworth & Wiens 1996). The greatest diversity of species is in southwestern parts of North America (Wiens 1968). Mexico and California each have 22 and 14 taxa respectively. In North America nearly all species are found in the western parts of the continent (Hawksworth & Wiens 1996). The distribution of *Arceuthobium americanum* Nutt. *ex* Engelm (lodgepole pine dwarf mistletoe, Viscaceae) in North America (Figure 1.2) is similar to that of its primary hosts, *Pinus contorta* Dougl. *ex* Loud. (lodgepole pine, Pinaceae), principally varieties *latifolia* Engelm. *ex* S. Wats. and *murrayana* Engelm. *ex* S. Wats., and *Pinus banksiana* Lamb. (jack pine, Pinaceae) (Baranyay & Safranyik 1970, Hawksworth & Wiens 1996). At present, the most easterly populations are found in Manitoba, along the eastern shore of Lake Winnipeg, although the parasite is known to be capable of spreading further east (French & Baker 1982, Jerome 2001). At least two other infection

centres, which have since been eradicated by fire, have been documented to the east (French & Baker 1982).

Figure 1.1 Distribution of the genus *Arceuthobium*, worldwide (Hawksworth & Wiens 1996, p. 28).

Two species of dwarf mistletoe are found at their eastern and western limits in Manitoba (Figure 1.3). *Arceuthobium americanum* is found in western Canada attacking a few species of pine, whereas *A. pusillum* Peck (eastern dwarf mistletoe, Viscaceae) is found primarily in eastern parts of Canada attacking mainly *Picea glauca* (Moench) Voss (white spruce, Pinaceae) and *P. mariana* (Mill.) BSP (black spruce, Pinaceae). In Manitoba, *Arceuthobium americanum* is parasitic primarily on *Pinus banksiana* (Gilbert 1984, Hawksworth & Wiens 1996). In parts of the province where jack pine is the dominant tree species, dwarf mistletoe can cause serious problems economically, ecologically and aesthetically (French & Baker 1982).

Figure 1.2 North American distribution of *Arceuthobium americanum* (Hawksworth & Wiens 1972, p. 99).

Most dwarf mistletoes, including *Arceuthobium americanum*, have a long life cycle (Figure 1.4). During early spring of the first year, pollen grains are released and

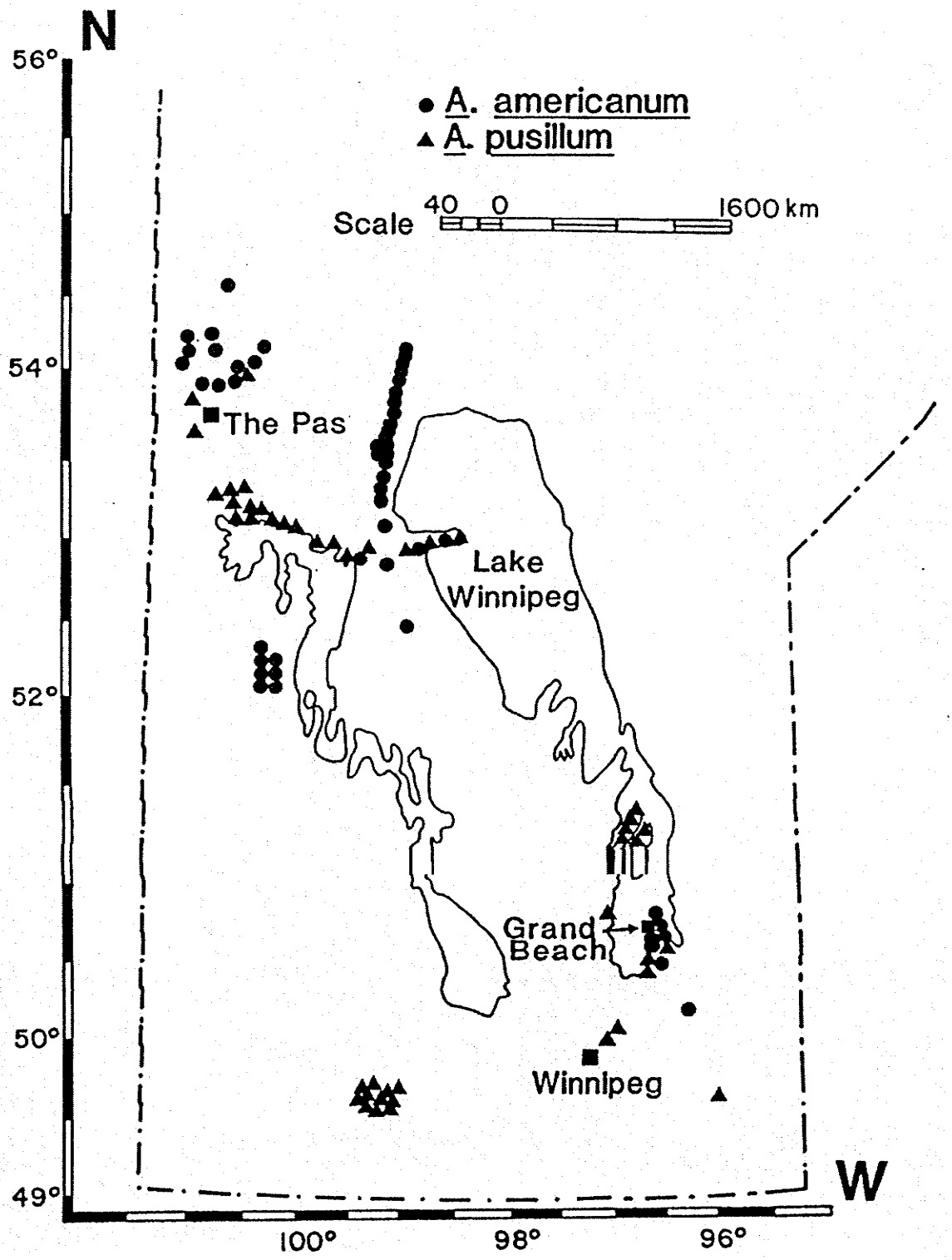

Figure 1.3 Known locations of dwarf mistletoe (*Arceuthobium americanum* and *pusillum*) infections in Manitoba (after Gilbert 1984, p. 4).

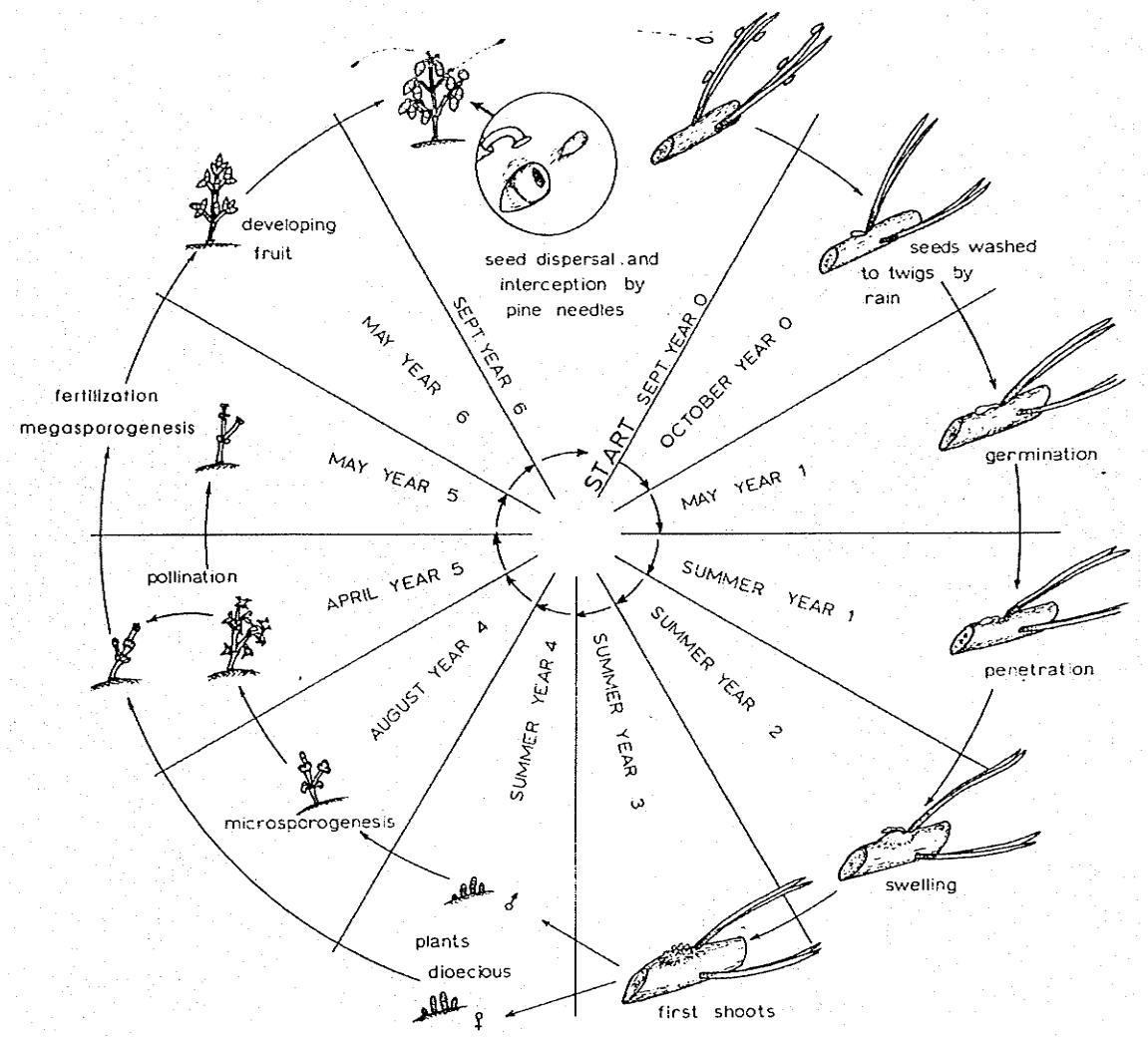

Figure 1.4 Life cycle of *Arceuthobium americanum* (Hawksworth & Wiens 1996, p. 9).

transported by insect vectors (entomophily) (Gilbert 1984, Gilbert & Punter 1990, Gill 1935, Gregor *et al.* 1974, Hawksworth & Wiens 1996, Penfield *et al.* 1976, Stevens & Hawksworth 1970) or wind (anemophily) to the pistillate plants (Baker 1981, Coppola 1989, Gilbert 1984, 1988, Gilbert & Punter 1990, Penfield *et al.* 1976, Player 1979). Once fertilized, the immature fruits overwinter and complete their development late the second summer. Fruits, called pseudoberries, mature in the fall, and embryos surrounded by chlorophyllous endosperm (Hawksworth & Wiens 1996), which are often called 'seeds', along with carpellary viscin (Calder 1983), are explosively discharged in late August or early September (Hawksworth 1961, Hawksworth & Wiens 1996, Punter &

Gilbert 1991). If seeds fall onto the shoot of a suitable host, they adhere via specialized viscin cells, and remain dormant for the winter months (Cohen 1963a).

Spread of dwarf mistletoe is solely via seed (Hawksworth & Wiens 1996, Punter & Gilbert 1991). Wind has been proposed to be a factor in the spread of some species (Hawksworth 1961, Korstian & Long 1922, Kujit 1955), but others disagree and believe the seeds are too heavy to be carried by wind (Gill 1935), although prevailing winds probably aid somewhat in keeping seeds aloft (Kujit 1955). All agree that the primary mechanism of dispersal is via the explosive discharge of seeds (Gill 1935, Gilbert 1988, Hawksworth 1961, Kujit 1955, Punter & Gilbert 1991), although birds (Gilbert 1988, Hawksworth & Geils 1996, Punter & Gilbert 1989) and small mammals (Hawksworth & Geils 1996, Kujit 1955) have also been implicated.

Upon germination the following spring, the radicle emerges and the apex forms a holdfast that penetrates the host periderm (Alosi & Calvin 1984, 1985, Calvin & Wilson 1996, Cohen 1963b). Fusiform swelling of the host tissue at the site of infection is usually evident the next year, but aerial, flowering shoots of mistletoe often do not appear until two to five or even up to eight years later (Calvin & Wilson 1996, Hawksworth & Wiens 1996). The life cycle therefore takes a minimum of three years to be completed and as long as eight years has been recorded (Hawksworth 1961).

1.1.2 Morphology and anatomy of the genus *Arceuthobium*

Members of the genus *Arceuthobium* are small, dioecious herbs, although a few species tend to become woody with age (Wiens 1968, Wilson & Calvin 1996). A single plant consists of aerial shoots connected to a network of cortical strands and vertical sinkers (Figure 1.5) within the coniferous host (Calvin & Wilson 1996, Cohen 1965, Gill 1935, Kujit 1955). That portion of mistletoe within the host is termed the endophytic system (Alosi & Calvin 1984, 1985, Calvin & Wilson 1996, Cohen 1965, Gill 1935, Hawksworth 1961, Kujit 1955). The aerial shoots have reduced scale-like leaves and are somewhat chlorophyllous (Calder 1983, Wilson & Calvin 1996). The genus is so greatly reduced that in most species, the vascular bundles lack phloem tissue or at least sieve tube elements (Wiens 1968, Wilson & Calvin 1996), although at least one species contains a special type of phloem tissue (Calvin *et al.* 1984).

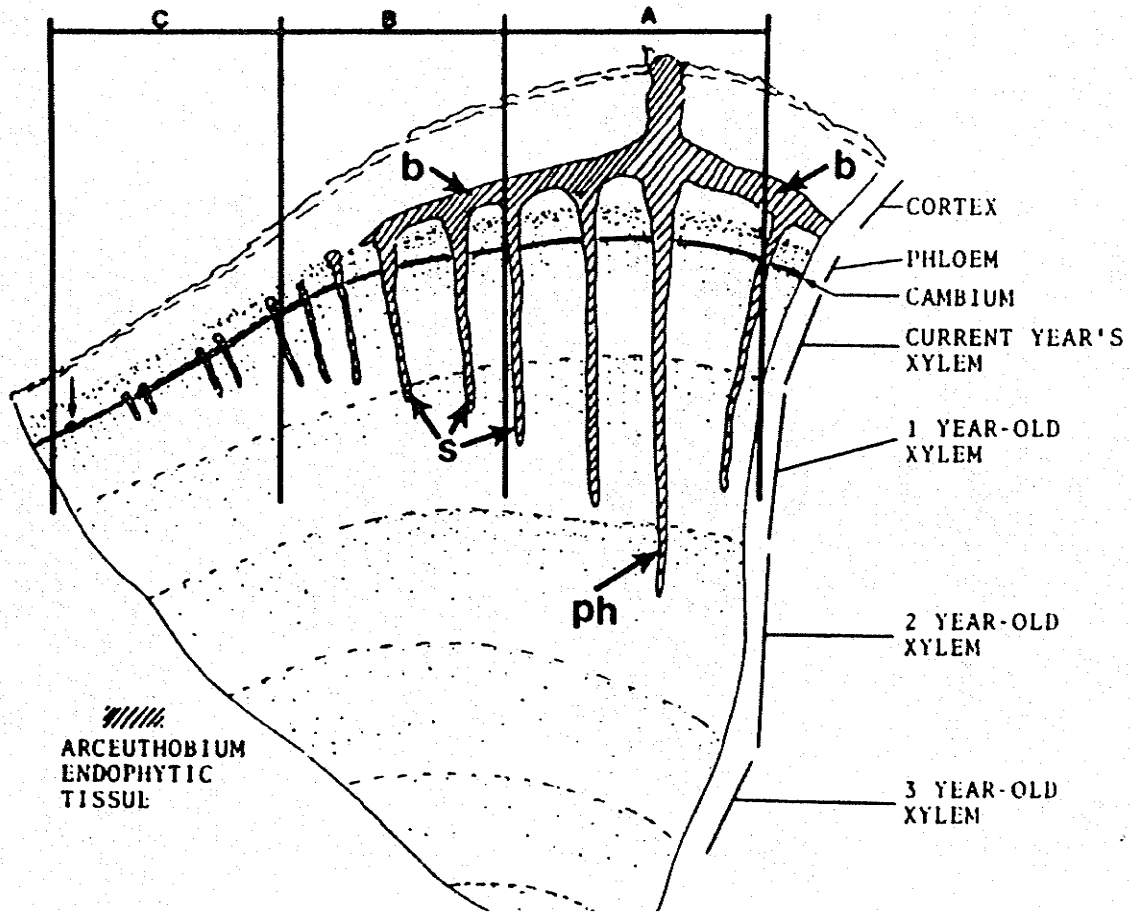

Figure 1.5 Cross-sectional diagram of cortical strands (b), vertical sinkers (s) and the primary haustorium (ph) of an *Arceuthobium* infection within a coniferous host. The region indicated A is the oldest portion of the endophytic system, and C is the youngest (Calvin &Wilson 1996, p. 115).

The parasite induces abnormal growth patterns within the host tree, and this results in the production of dense clumps called witches' brooms (Gill 1935, Hawksworth & Wiens 1996, Kuijt 1955, Mathiasen 1996). Infections may be localized or systemic. Localized infections are confined to the region of initial entry, whereas systemic infections spread and affect entire branches. In the latter case, growth of the parasite within its host is acropetal, basipetal and circumferential. Aerial mistletoe shoots tend to emerge from the host on the previous year's new twig growth, but this is dependent on the type of infection (Alosi & Calvin 1984, Calvin & Wilson 1996). The endophytic system

has also been shown to follow the development of the vascular cambium within the host tree (Calvin & Wilson 1996, Srivastava & Esau 1961).

1.1.3 Staminate development of *Arceuthobium*

Staminate flowers of *Arceuthobium* are typically made up of bright yellow, sessile anthers, about 0.5 mm in diameter, on persistent, olive-green perianth parts (Hawksworth & Wiens 1996, Johnson 1888, Kuijt 1955, Player 1979), sometimes referred to as sepals (Cohen 1968). Male flowers contain a slightly raised nectary in the middle, which excretes an extremely sugary nectar (Penfield *et al.* 1976). Dehiscence of pollen from the anther is via a transverse slit (Gilbert & Punter 1990, Johnson 1888, Player 1979) in the epidermis that develops via fibrous thickenings, thus making the epidermis an exothecium. No endothecium forms (Dowding 1931, Gill 1935).

Each male flower produces about 11,300 pollen grains (Penfield *et al.* 1976), and anthers have an unusual ability to reversibly open and close in response to temperature and humidity changes (Gilbert 1988, Gilbert & Punter 1990). The tapetum is said to be uninucleate and uniseriate (Cohen 1968), but other Viscaceae have bi-or tetranucleate tapetal cells, and sometimes an endothecium (Bhandari & Vohra 1983). The reduction of this plant is also reflected in the lack of vascular tissue going to the anther (Cohen 1968, Johnson 1888, Kuijt 1982).

The first person known to examine microscopically the male and female flowers of *Arceuthobium*, was Hooker, in 1840. He used *Arceuthobium oxycedri* (D.C.) M. Bieb. (juniper dwarf mistletoe, Viscaceae) as the example for his diagrams. His observations were later compared with and discussed by, Johnson's (1888) examination of herbarium and preserved material. Illustrations show the bisporangiate anthers to be round to kidney bean-shaped (Cohen 1968, Dowding 1931) and sessile on perianth segments, with a uniseriate epidermis making up the mature anther wall (Cohen 1968, Johnson 1888, Thoday & Johnson 1930). At dehiscence, the interceding septum between the two microsporangia appeared to break down causing the anther to become unilocular. In these specimens, the epidermis had developed fibrous thickenings (Thoday & Johnson 1930). Illustrations of nearly mature pollen grains were represented only by small

spheres, 1/3000th inch in diameter and yellow-brown in color with a large round vegetative nucleus, and a fusiform generative nucleus (Johnson 1888).

Some authors state that anthers of the genus *Arceuthobium* are monosporangiate (Cohen 1968, Dowding 1931, Gill 1935, Wiens 1968) and others report a bisporangiate condition that becomes unilocular at dehiscence (Johnson 1888, Van Tieghem 1895). Proponents of the monosporangiate anther describe them as ring-like archesporia (Cohen 1968, Wiens 1968). There are conflicting opinions about the monosporangiate origin of the anther. From anatomical studies, Cohen (1968) concluded that the unilocular anther is a predetermined condition in the anther's ontogeny and not derived by a later breakdown of the partition between two thecae. He hypothesized that the sporogenous cells originate as a continuous ring around the central cushion of tissue. Bhandari and Vohra (1983) proposed that development begins with two microsporangia, and the later breakdown of a dividing septum results in a single, horseshoe-shaped archesporium around a central sterile column of tissue, first referred to as the columella by Dowding (1931). She proposed that the septa are actually tapetal extensions of the columella originally dividing the anther into four archesporangia. Although Mauseth (1988) states that all four microsporangia fuse to form one loculus in *Arceuthobium*, this has never been conclusively proven.

The pollen grains themselves are released at the two-celled stage and are echinate, viscaceous, tricolpate and nearly spherical. A thick, spiny exine is layered over a thinner intine (Bhandari & Vohra 1983). Hawksworth and Wiens (1972) observed differences in the heights of spines relative to overall pollen wall thickness and argued that this feature is of taxonomic value for this genus. Parallel to and alternate with the colpae are pseudocolpae. They are shorter grooves that do not extend as far towards the poles as the colpae themselves. In addition, variation in the spacing and placement of papillae and spines in relation to the grooves has been observed, as well as differences in the surface texture of grains of the two species they examined, *A. pusillum* and *A. verticilliflorum* Engelm. (big-fruited dwarf mistletoe, Viscaeae).

Arceuthobium americanum typically flowers from early April to late May, depending on environmental conditions (Gilbert 1984, 1988), although anthesis has been observed

as early as March (Hudson 1966) and as late as July (Gilbert 1984). Aerial shoots of *A. americanum* are perennial and may persist and produce flowers for several years (Dowding 1929). Both the dimerous female flowers and the usually trimerous male flowers are terminal on decussately branched shoots (Cohen 1968, Dowding 1931, Penfield *et al.* 1976). Tetramerous male flowers (Gill 1935, Penfield *et al.* 1976), however are not uncommon, especially at the apex of the shoot, and occasionally dimerous staminate flowers are seen (Cohen 1968, Dowding 1931).

Johnson (1888) observed the pollination and subsequent *in vivo* germination of pollen to occur in late September or early October, for *A. oxycedri,* but fertilization not until the following spring. She commented on the similarity of this reproductive event to the sequence that occurs in the coniferous host. This correlation however, does not hold for all host species parasitized by the family Viscaceae (Hawksworth & Wiens 1996).

Gilbert and Punter (1991) found that 20% sucrose, 0.01% boric acid and 1.5% agar, at 30°C produced the greatest amount of pollen germination for *A. americanum*, but percentages tended to be lower than 30%. Warmer temperatures (up to 30°C) prior to sampling seemed to improve the germinability of pollen and cooler temperatures to cause a decline in the number of pollen tubes produced (Gilbert 1988, Gilbert & Punter 1991). Other than this study, no other work on pollen germination has been published for the genus.

1.2 Thesis Objectives

Arceuthobium species spread solely via seed. If the only mode of dispersal of a parasite is via seed, any interference in the production of seed should reduce its spread. A better understanding of the normal reproductive biology of an organism is the first step. In particular, the development of pollen and pollination mechanisms are of interest, since a decrease in the amount of viable seed produced could facilitate a dwarf mistletoe control program (Gilbert 1984). A disruption in the development of pollen would facilitate a reduction in the number of successful fertilizations. To this end, the identification of a cytoplasmically male sterile line would be a good starting point for further investigations of the causes of inviable pollen (Kaul & Nirmala 1991). As well,

understanding the requirements for *in vitro* pollen germination could also aid in the future study of fertilization events, pollen tube growth and generative cell division.

The ontogeny of an organism can also be applied to taxonomic problems such as morphological evidence of phylogeny (Duvall 2001). Taxonomically, the dwarf mistletoes are considered difficult because of their reduction in size and convergent evolution (Nickrent 1996). Developmental patterns of reproductive organs have been used to clarify family and even generic relationships (Foster & Gifford 1974), as differing developmental pathways can result in mature pollen of unrelated genera appearing morphologically the same. Evolutionary convergence may result in superficial similarities (Duvall 2001, Furness & Rudall 1999), but developmentally, a distinction can still be made.

Anther and subsequently pollen grain development can be broken down into four main stages: microsporogenesis, microgametogenesis, pollen dehiscence and pollen germination. Each of these can also be subdivided into several steps.

The main objective of this study is to describe the overall timing and process of anther and pollen development, including microsporogenesis and microgametogenesis, of *Arceuthobium americanum,* on its host *Pinus banksiana*, using microscopical and cytochemical techniques. Secondary objectives include more detailed transmission and scanning electron microscopy observations on select stages of development, such as the mature pollen grains. As well, the conditions for the *in vitro* germination of mature pollen grains will be further explored.

2.0 LITERATURE REVIEW

2.1 Microsporogenesis of Angiosperms

2.1.1 Stamen initiation

Mature angiosperm anthers are typically tetrasporangiate and found terminally on a filament. This is considered to be a phylogenetically advanced trait (Esau 1965), since primitive stamens are more leaf-like and lack a filament (Bhandari 1984). In this case, sporangia are embedded in an abaxial (Bhandari 1984, Esau 1965) or adaxial surface (Bhandari 1984) between two of three veins (Esau 1965), whereas most tetrasporangiate stamens have a single vascular bundle supplying the anther via the filament. The morphological structure of primitive stamens has greatly influenced acceptance of the hypothesis that stamens are modified, fertile leaves (Greyson 1994, Meyerowitz 1994, Stanley & Linskens 1974). Sterile stamens are seen in many species and when they are consistently produced in the normal scheme of floral development, they are called staminodia (Greyson 1994). They lack the sporogenous or fertile tissues, which produce pollen grains (Bhandari 1984).

Many morphological variations have been observed for stamens. The most common type is free, but varying degrees of coalescence of either the anthers and/or the filaments, to each other or other floral parts also exist. Two of the microsporangia usually fuse forming a single loculus. The two anther loculi then dehisce at maturity, resulting in the release of the pollen grains via lateral, longitudinal slits from the anther (Mauseth 1988, Stanley & Linskens 1974). A good summary of the terminology used in describing mature floral organography may be found in Greyson (1994).

Stamen primordia mostly arise as a mound of undifferentiated cells with a tunica-corpus arrangement, in an acropetal and helical fashion (Greyson 1994), although some species have a whorled pattern of initiation (Esau 1965, Goldberg *et al.* 1993). Acropetal development is defined as centripetal but centrifugal examples are not uncommon (Bhandari 1984, Greyson 1994). Centrifugal initiation occurs when primordia arise below (or outside) previously initiated primordia. This tends to occur more for stamens than for other floral parts (Greyson 1994).

Stamen primordia are usually anti-petalous or anti-sepalous, but in some species such as *Silene* L. (catchfly, Caryophyllaceae), they are axillary to petals and sepals (Esau 1965, Greyson 1994). This has raised the question as to whether or not stamens are stem-like, as in the latter situation, or truly modified leaf-like structures, as in the former (Greyson 1994). It has been proven experimentally, however, that stamen development is not dependent upon the presence of petals or sepals (Goldberg *et al.* 1993).

After the establishment of anther and filament domains, bilaterally symmetrical thecae (microsporangia) develop within the primordium (Goldberg *et a*l. 1993). Anatomically, the initiation of sporogenesis usually begins with the differentiation of four subepidermal regions containing mitotically active cells, although anthers with one (Bhandari 1984), two (Bhandari 1984, Davis 1966, Greyson 1994) or even eight (Bhandari 1984, Davis 1966) microsporangia are known. These groups of cells are termed the archesporial initial cells.

The first periclinal division of a hypodermal, archesporial cell results in an outer primary parietal cell and an inner primary sporogenous cell (Bhandari 1984, Davis 1966, Greyson 1994). The sporogenous cells proliferate via periclinal and anticlinal divisions to produce the microspore mother cells (microsporocytes). Despite some authors stating that only L_2 cells produce gametes (Sussex 1989), they have also been shown to arise from both the first and second tunica layer and the outer corpus, although this varies from species to species (Greyson 1994).

Sporogenous tissue may initially be horseshoe-shaped (Prasad *et al.* 1990) or spherical (Bhandari 1984), but in either case, the cells are closely packed together (Esau 1965). While the anther wall is developing, the sporogenous tissue is usually proliferating by anticlinal and periclinal divisions (Bhandari 1984). The number of divisions has been suggested to be constant at the generic level, but this has never been confirmed (Davis 1966).

2.1.2 Anther wall development

Periclinal divisions of the parietal cells result in the layers which make up the future anther wall. A second periclinal division of the primary parietal cells produces two secondary parietal cell layers, termed the inner and outer secondary parietal layers.

These lie between the sporogenous cells and the epidermis (Davis 1966). Based on whether or not the secondary parietal wall layers undergo a further mitotic division and their eventual differentiation, species can be categorized into one of four patterns of anther wall development (Figure 2.1). Wall type ontogeny is mostly family specific, but this is not always the case (Davis 1966, Bhandari 1984). The four main constituents of an anther wall, regardless of their origin, are from outside to inside, epidermis, endothecium, middle layer(s) and tapetum. These and other parts of the anther vary from species to species.

The epidermis is the original covering of the primordium. It persists in some species but if no additional anticlinal divisions occur, it is sloughed off during anther maturation (Bhandari 1984, Goldberg *et al.* 1993). It gives structure and support to the anther, prevents water loss, yet allows for gas exchange, and is sometimes involved in dehiscence (Goldberg *et al.* 1993).

The endothecium usually develops fibrous thickenings in its cell walls, which function in the dehiscence of the anther (Bhandari 1984, Davis 1966, Goldberg *et al.* 1993), but also gives structure and support to the anther (Goldberg *et al.* 1993). Occasionally, the endothecium may retain the ability to undergo periclinal divisions. This results in a bi- or even multi-layered endothecium, and occurs mostly in more primitive families such as Magnoliaceae (Bhandari 1984).

Middle layers are usually transient since they are not able to divide anticlinally (Davis 1966) and are eventually crushed (Anjaneyulu & Lakshminarayana 1989, Bhandari 1984, Davis 1966, Esau 1965). Persistent middle layers are found in a few genera. This is most likely due to their developing wall thickenings (Hardy *et al.* 2000). The number of middle layers can range from zero to seven, but two to four is the most common (Davis 1966). They also give structure and support to the anther and if persistent, can be involved in dehiscence (Goldberg *et al.* 1993, Hardy *et al.* 2000). In many anthers, a supportive connective joins the anther thecae to each other and to the filament. The vascular bundle supplying nutrients and water to the developing anther runs through the filament from the main body of the plant. A circular cell cluster may

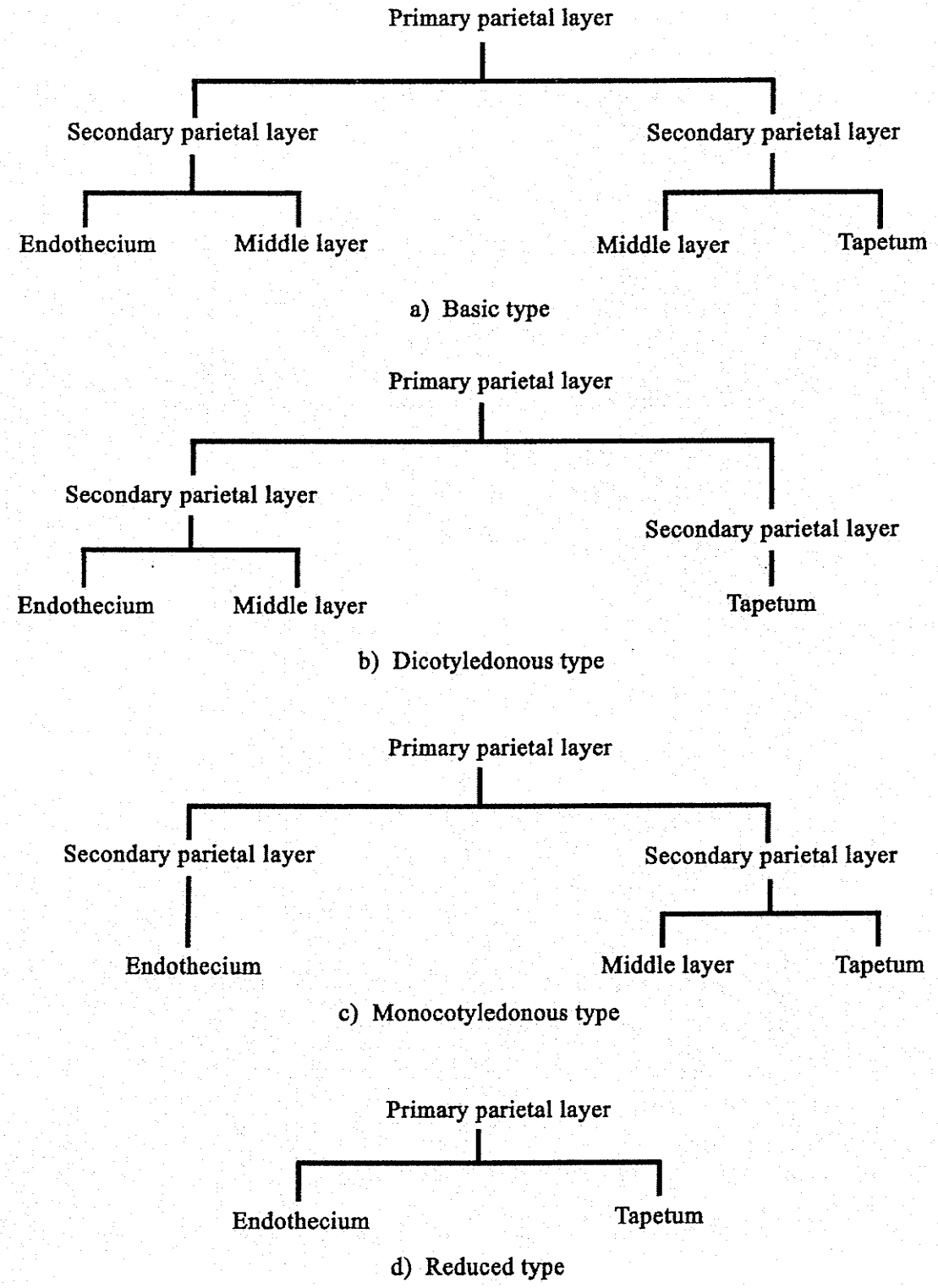

Figure 2.1 The four different types of anther wall ontogeny (after Bhandari 1984, Davis 1966).

also be present and/or a stomium. These are both involved in anther dehiscence (Esau 1965, Goldberg *et al.* 1993).

The innermost wall layer, the tapetum, supplies nutrients and other substances to the reproductive cells (Goldberg *et al.* 1993). It is of physiological and developmental importance (Bedinger 1992, Pacini *et al.* 1985) and will be discussed in more detail in the following section.

Goldberg *et al.* (1993) have determined a complete cell lineage for *Nicotiana tabacum* L. (cultivated tobacco, Solanaceae) anthers (Figure 2.2) based on histological observations. Their analysis points out the contribution of each of the tunica layers, L_1, L_2 and L_3, to the mature anther, as well as the fates of each tissue type. This and other examples illustrate that during anther development, cell division and differentiation occurs at precise times and locations.

2.1.3 The tapetum

Generally the tapetum is a single layer of cells, but bi- and multiseriate conditions are also known for some angiosperms (Bhandari 1984, Davis 1966). Usually tapetal development is completed before that of the microsporocytes, but sometimes tapetal cells undergo mitotic divisions while meiosis of the pollen mother cells is occurring. This results in a two-layered tapetum with diploid and polyploid nuclei surrounding the coenocytic haploid microspores (Bhandari 1984, Hanácková & Piñeyro-López 1997). Davis (1966) also states that there may be a relationship between a multi-layered tapetum and the dicotyledonous type of wall development.

It is common for tapetal cells to undergo mitosis without cytokinesis resulting in bi- (Dwivedi *et al.* 1988) or multinucleate cells (Bedinger 1992, Bhandari 1984, Esau 1965, Greyson 1994, Pacini *et al.* 1985). Polyploidy up to 16*n* has been recorded (Bhandari 1984), or if radial cell walls break down a multinucleate syncitium is produced which is eventually resorbed (Bedinger 1992, Dwivedi *et al.* 1988, Esau 1965, Greyson 1994). The timing and mode of degeneration of the tapetum varies from species to species (Echlin 1971, Furness & Rudall 2001). In *Zea mays* L. (maize, Poaceae), this occurs while the microspores are becoming vacuolate (Bedinger 1992), and in *Lilium longiflorum* L. (Easter lily, Liliaceae) around the time of the first mitotic event (Clément

et al. 1998), but in *Agave fourcroydes* Lemaire (henequén, Agavaceae) it occurs after the first mitosis is complete (Piven *et al.* 2001).

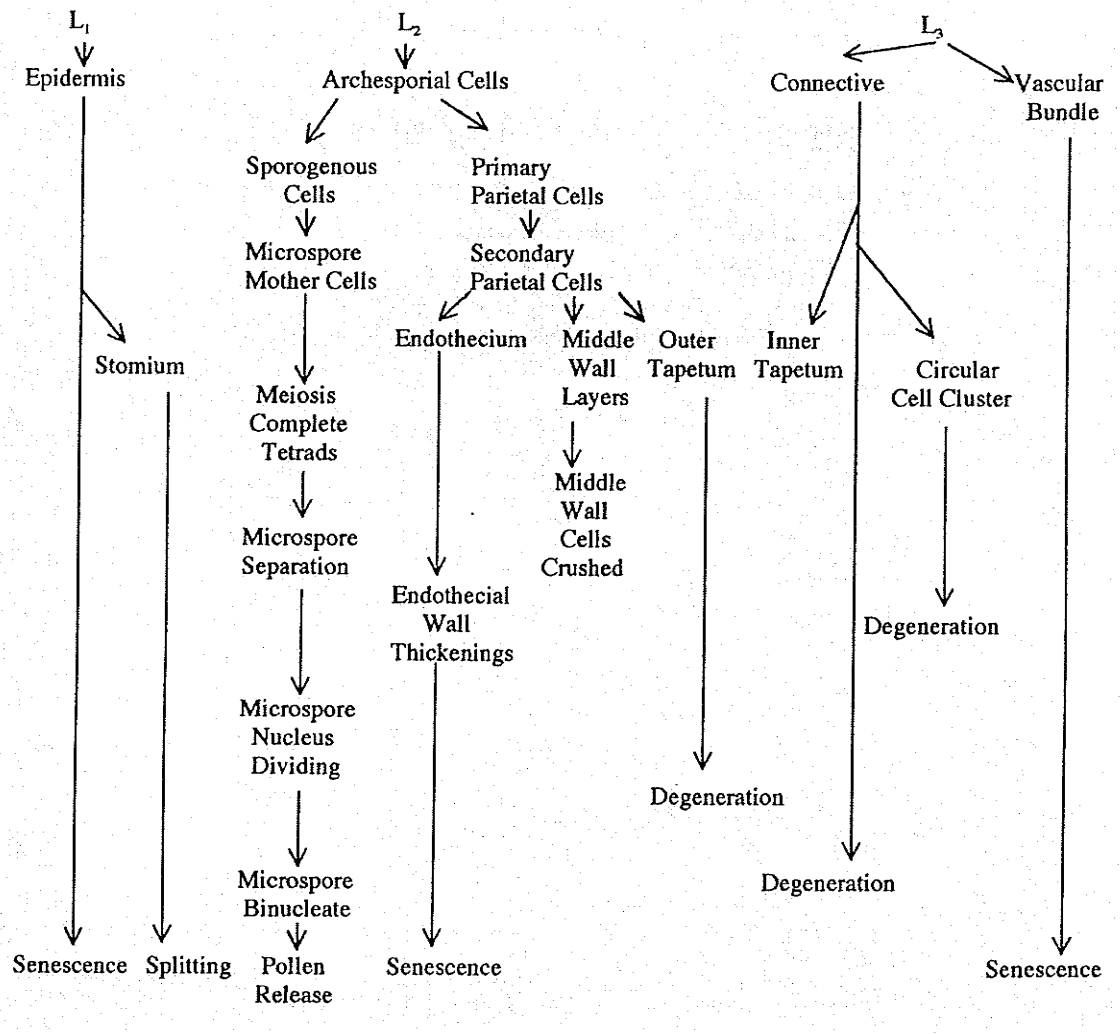

Figure 2.2 Cell lineages and the relative timing of major events that occur during anther differentiation and dehiscence in tobacco (after Goldberg *et al.* 1993).

Tapetal cells can originate from more than one tissue type (Anjaneyulu & Lakshminarayana 1989, Bhandari 1984, Echlin 1971). This is overlooked in many studies since observations are mostly concentrated on the outer anther surface. Although some authors state that there is a continuity of the tapetum with the connective on one side (Prasad *et al.* 1990), this is not always the case. Future cells of the tapetum largely

originate from the secondary parietal layer, but may also originate as connective (Anjaneyulu & Lakshminarayana 1989) or sporogenous tissue (Bhandari 1984, Echlin 1971).

Regardless of their origin, two main types of tapeta have been described. The commonest is the secretory tapetum (Furness & Rudall 2001), also called glandular (Bhandari 1984, Davis 1966, Echlin 1971, Greyson 1994), parietal (Mauseth 1988, Pacini *et al.* 1985) or cellular. It is believed to secrete an electron dense material into the microsporangium (Furness & Rudall 2001, Pacini *et al.* 1985). The origin of this material is not known, although the tapetum has been implicated because in species with this type of tapetum, tapetal cells are rich in endoplasmic reticulum (ER) (Echlin 1971, Greyson 1994, Hanácková & Piñeyro-López 1997). The secretory tapetum of *Zea mays*, for example, contains not only abundant ER, but also ribosomes, mitochondria, dictyosomes and vesicles (Bedinger 1992). The presence of ER, plus dictyosomes and vesicles, suggests these cells are highly synthetic (Greyson 1994).

In accordance with this secretory function, orbicules, also called plaques, Übisch granules or Übisch bodies (Echlin 1971), are often observed on the inner surface of this type of tapetum (Bedinger 1992, Bhandari 1984, Davis 1966, Echlin 1971, Furness & Rudall 2001, Greyson 1994, Pacini *et al.* 1985, Prasad *et al.* 1990). Some authors believe them to contain sporopollenin precursors (Bhandari 1984, Heslop-Harrison 1976), but others disagree (Moore *et al.* 1991). These osmiophilic bodies are generally round and 1-4 μm in diameter with a distinct sporopollenin wall surrounding an inner lipid core (Furness & Rudall 2001). Usually orbicules remain separate, but sometimes they fuse into compound aggregations when released into the microsporangium. They may be released directly into the locule or remain attached to the inner tapetal surface and acquire a sporopollenin-like coating. If the latter, they are released later when the tapetum degenerates. This electron dense material then migrates to and accumulates on the surface of the developing microspores. There is disagreement as to the origin and significance of orbicules, although they do appear to be related to the deposition of exine in species with this type of tapetum (Bhandari 1984). A good discussion of the formation and function of orbicules may be found in a review by Echlin (1971).

Secretory tapetal cells appear to be polarized (Bedinger 1992) both in structure and function, especially in regard to the secretion of various stored substances into the locule (Bhandari 1984, Pacini *et al.* 1985) often via vesicles (Bedinger 1992). Individual cells have most of their cytoplasm on the side towards the locular face and a large vacuole on the opposing side (Clément *et al.* 1998). The occurrence and supply of locular fluid is generally associated with this type of tapetum (Pacini *et al.* 1985), and is assumed to be involved in the supply of nutrients, such as starch or lipids (Bhandari 1984), to the young microsporocytes (Davis 1966, Greyson 1994, Pacini *et al.* 1985). This is referred to as an indirect mode of nutrition (Pacini *et al.* 1985). Tapetal cell walls generally remain intact, but can be digested in some species (Greyson 1994). When this occurs, vesicles are released between tapetal cells and the radial walls are digested (Bhandari 1984). Eventually the cell contents are resorbed and the tapetal cell walls adhere to the middle layer of the anther wall (Greyson 1994).

The second type of tapetum is referred to as amoeboid (Bedinger 1992, Echlin 1971), periplasmodial (Bhandari 1984, Echlin 1971, Greyson 1994), or invasive (Davis 1966, Echlin 1971, Furness & Rudall 2001, Mauseth 1988, Pacini *et al.* 1985). The cells are not polarized (Pacini *et al.* 1985). Tapetal cell walls also break down in this type, but in this case the protoplasts fuse and a coenocytic plasmodium protrudes into the locule (Bhandari 1984, Furness & Rudall 2001, Greyson 1994, Pacini *et al.* 1985). An acetolysis-resistant membrane surrounds this structure. It is called the tapetal membrane (Bhandari 1984, Echlin 1971, Furness & Rudall 2001) or culture sac (Pacini *et al.* 1985). Formation of the tapetal membrane is preceded by a wave of lysis that appears to occur from the tapetal cells inward, anatomically indicated by the presence of multivesiculate bodies (Bhandari 1984). Locular fluid is either absent or greatly reduced and nutrition is therefore referred to as direct in the amoeboid type (Pacini *et al.* 1985), since the tapetum itself envelopes the sporogenous tissue. Some authors have further subdivided this group, depending on when during microspore development the invasive process occurs, but this is not always reliable, since some secretory tapeta also break down at later stages (Bhandari 1984, Greyson 1994, Pacini *et al.* 1985).

A few angiosperm families have intermediate forms of tapeta, but these are not well described in the literature (Pacini *et al.* 1985). It has been suggested that a third category described as invasive nonsyncytial be adopted (Furness & Rudall 2001).

Secretory tapeta tend to predominate more in the Dicotyledonae and amoeboid in the Monocotyledonae, but many families remain uninvestigated (Davis 1966, Furness & Rudall 2001, Pacini *et al.* 1985). A better correlation seems to be with dry or wet habitat type. Species with the secretory type tend to be found in dry habitats and those with periplasmodial in wetter locations (Pacini *et al.* 1985), although some aquatic genera such as *Callitriche truncata* Guss. (short-leaved water-starwort, Callitrichaceae) seem to have the former type of tapetum (Osborn *et al.* 2001).

Whether secretory or amoeboid, from cytological studies, the tapetum is known to be essential for the production of fertile pollen (Bhandari 1984, Bhojwani & Bhatnagar 1988). This has been recently confirmed by molecular studies using mutants (Cigan *et al.* 2001), and morphological irregularities in tapetal cells have been observed in male sterile species prior to pollen abortion (Bedinger 1992). Any factor that upsets the balance between the tapetum and the sporogenous tissue usually results in pollen degeneration. This is referred to as cytoplasmic male sterility (Bhandari 1984, Bhojwani & Bhatnagar 1988, Knox 1984). It has generally been accepted that the tapetum supplies nutrients to the developing microgametophytes and then undergoes apoptosis (Bedinger 1992, Bhandari 1984, Davis 1966, Esau 1965, Greyson 1994, Pacini *et al.* 1985), although the interdependency of the two cell types appears to go beyond simply the supply of nutrients (Bedinger 1992).

Another important function of the tapetum is the production of callase (β-1,3-glucanase). During development, the microsporocytes and the resultant tetrads of microspores come to be surrounded by a callose-containing wall (Pacini *et al.* 1986). Callose is a β-1,3-polyglucan made up of β-D glucopyranose residues (Stanley & Linskens 1974). It accumulates around each microsporocyte just before meiosis (Bhandari 1984) and is secreted by the microsporocytes themselves (Hanácková & Piñeyro-López 1997). The tapetum later produces callase to release the haploid

microspores from their relatively impervious callose-rich wall (Bedinger 1992, Bhandari 1984, Bhojwani & Bhatnagar 1988).

Eventually, the sporogenous cells become spherical and separated from one another (Bedinger 1992), and the layered callose (Bhandari 1984) or pollen mother cell wall (Esau 1965) is deposited. This is the first partition between the future microspores (Bedinger 1992, Esau 1965) and is deposited between the plasmalemma and the original cellulose cell wall. It is unclear whether the monomers are synthesized in the ER or dictyosomes, but the wall itself appears to be assembled by the plasma membrane. It has an outer more electron dense and an inner less electron dense zone (Osborn *et al.* 2001). The occurrence of callose is nearly universal, although a few species that release compound grains do not appear to produce it (Bhandari 1984).

Initially, microsporocytes and tapetal cells may be interconnected with each other via plasmodesmata, later replaced by cytomictic channels (Bedinger 1992, Bhandari 1984, Knox 1984, Pacini *et al.* 1986, Stanley & Linskens 1974) between the microsporocytes or tapetal cells separately (Hanácková & Piñeyro-López 1997, Stanley & Linskens 1974). These connections are a possible conduit for nutrients, but if they are lost in later stages (Bhandari 1984, Greyson 1994, Pacini *et al.* 1985) the subsequent pathway is uncertain. Later, when microsporocytes become encased in the relatively impermeable, thick, callose-rich wall, channels would allow for the intercellular movement of solutes (Bhandari 1984, Stanley & Linskens 1974). In some species, cytomictic channels are usually sealed off by the conclusion of meiosis I (Pacini *et al.* 1986). After microspore separation, nutrients may be absorbed by the developing microgametophytes via pores or gaps in the exine (Pacini *et al.* 1985). Even though microsporocytes appear isolated from the tapetum and one another (Bedinger 1992, Bhandari 1984, Pacini *et al.* 1985), some communication must be occurring since there is often a high degree of synchronization of meiotic events (Bhandari 1984, Stanley & Linskens 1974).

Other macromolecules such as lipids are also excreted by the tapetum. The first abundance of lipids occurs during callose dissolution, when lipidic sporopollenin precursors are secreted by the tapetum (Piffanelli *et al.* 1998). After exine formation and the first mitotic division are complete, a second lipidic secretion by the tapetum usually

occurs. This material has been called pollenkitt, tryphine and pollencoat. Some authors reserve the term pollencoat to mean a combination of the first two substances (Greyson 1994), although others use the terms interchangeably (Bhandari 1984, Knox 1984, Stanley & Linskens 1974). More specific definitions describe tryphine as being a complex mixture of hydrophobic and hydrophilic substances often containing degenerated organelles, whereas classic pollenkitt is oily (Bhandari 1984, Echlin 1971, Pacini *et al.* 1985). Dickinson *et al.* (2000) use the term pollenkitt to refer to coatings formed from complete tapetal degeneration, and those formed by only partial degeneration, which therefore often contain intact organelles, are referred to as tryphine.

Whichever the term, this lipidic material coats the surface of all angiosperm pollen grains (Heslop-Harrison 1976, Pacini *et al.* 1985), and is especially abundant in entomophilous grains, where it may make up 10-15% of the total pollen mass (Piffanelli *et al.* 1998). Once lysis of the tapetum has occurred, more of these osmiophilic/lipidic compounds are released into the locule and seem to be attracted to the surface of the maturing pollen grains (Knox 1984, Hanácková & Piñeyro-López 1997). There is also evidence that this material can traverse the callose wall (Piffanelli *et al.* 1998). The mechanism of coat formation is uncertain, but it has been suggested that physical forces are the primary mode (Dickinson *et al.* 2000). Except for apertures, pollenkitt is deposited relatively evenly over the entire grain. This suggests an attraction mechanism rather than a mechanical or capillary action. Proteinaceous portions are found more within the bacular spaces, while lipids are primarily found on the surface (Heslop-Harrison 1976). With maturity, a fairly homogeneous membranous layer becomes apparent over lipidic areas, resembling a phospholipid monolayer (Piffanelli *et al.* 1998).

Functions of pollenkitt include the adhesion of grains to each other (Dickinson *et al.* 2000, Knox 1984, Stanley & Linskens 1974), vectors (Dickinson *et al.* 2000) and stigmas (Dickinson *et al.* 2000, Piffanelli *et al.* 1998). The retardation of water loss from grains (Bedinger 1992, Dickinson *et al.* 2000, Knox 1984, Piffanelli *et al.* 1998), protection from bacterial pathogens, and solar radiation (Dickinson *et al.* 2000, Piffanelli *et al.* 1998) are other functions, since grains are usually pigmented (Stanley & Linskens 1974). Some of these pigmented substances are carotenoids and flavonoids (Knox 1984, Stanley

& Linskens 1974). Many of the compounds are volatile and could serve as olfactory cues to animal pollinators (Bedinger 1992, Dickinson *et al.* 2000, Knox 1984, Moore *et al.* 1991, Piffanelli *et al.* 1998). Hygroscopic processes facilitate hydration of the grain in preparation for germination (Piffanelli *et al.* 1998, Taylor & Hepler 1997). As well, this semi-solid coat contains embedded recognition proteins involved in compatibility responses (Dickinson *et al.* 2000, Piffanelli *et al.* 1998), whereas other embedded fibrillar proteins are believed to help anchor the bulk of the lipidic material to the grain (Piffanelli *et al.* 1998).

The source of pollenkitt from within the tapetal cells has also been investigated. After the first mitosis, elaioplasts and cytoplasmic lipid bodies begin to accumulate. Plastids have been observed to dedifferentiate and lose their thylakoid membranes, and any starch grains present gradually disappear and are replaced by osmiophilic droplets (Piffanelli *et al.* 1998). Smooth ER and plastids are believed to be synthesizing this material (Clément *et al.* 1998). Lipids within the tapetal cytoplasm are probably produced by the ER as are associated proteins. Indeed, some of the proteins have been found to be encoded for by genes only expressed in the tapetum (Piffanelli *et al.* 1998).

In addition to nutrients, β-1,3-glucans, sporopollenin, lipids, pollenkitt and recognition proteins, both types of tapeta may produce carbohydrates, other enzymes (Bhandari 1984, Greyson 1994, Pacini *et al.* 1985), crystals (Bhandari 1984, Hardy *et al.* 2000), and viscin threads (Pacini *et al.* 1985) or their precursors, although this area needs further research.

2.1.4 Microsporocyte meiosis

The primary sporogenous cells become the pollen mother cells or microsporocytes and undergo meiosis to produce haploid microspores (Bedinger 1992, Esau 1965). The meiotic trigger is unknown but can be affected by environmental factors such as temperature. The duration of meiosis ranges from 24 hours to three months and may also be altered by ploidy level (Bhandari 1984). DNA is replicated during a pre-meiotic S-phase and when the content is calculated per cell, drops sharply when meiosis is concluded. RNA synthesis, however, occurs just before or during early prophase I (Stanley & Linskens 1974).

The callosic wall not only retains the four cells in a tetrad, but also later isolates the microspores chemically and mechanically from each other and surrounding somatic tissue (Bhandari 1984). Rodríguez-García and Majewska-Sawka (1992), however, have evidence that some substances, such as cerium perhydroxide and cerous ions, may pass through the callose walls. These walls are also known to protect the developing microspores from dehydration. Mogami *et al.* (2002) recently isolated a pollen specific protein localized in the callosic wall, which may be involved in tolerance to desiccation. At the very least the callose wall is a selective barrier providing a degree of autonomy to the developing microspores (Bhandari 1984).

Microsporocyte cytokinesis may be successive or simultaneous (Bhandari 1984, Bhojwani & Bhatnagar 1988, Davis 1966, Esau 1965) and it is at this time that the tapetum attains its maximal development (Esau 1965). The successive process is believed to be the more primitive trait (Davis 1966), but this is uncertain (Bhandari 1984).

Successive cytokinesis occurs when each meiotic division is immediately followed by the formation of walls (Bhandari 1984, Esau 1965), resulting in dyads and then tetrads of nuclei. Wall formation is by the usual centrifugal growth of cell plates (Bhandari 1984) followed by callose deposition on either side of the plate (Bhojwani & Bhatnagar 1988). This is particularly common in monocotyledons (Davis 1966, Esau 1965) such as *Zea* (Bhandari 1984). The second division of the dyad may or may not be synchronous (Bhojwani & Bhatnagar 1988).

The simultaneous process delays cytokinesis until meiosis is complete and walls form via concurrent centripetal furrowing (Bhandari 1984, Bhojwani & Bhatnagar 1988, Esau 1965). After meiosis I the two nuclei of the resultant binucleate cell synchronously complete the meiotic event. Callose deposition occurs after the second meiotic division (Bhojwani & Bhatnagar 1988). Dicots mostly exhibit simultaneous cytokinesis (Davis 1966, Esau 1965). *Nicotiana* (Bhandari 1984), *Cudraniajavanensis* Trec. (mai luang, Moraceae) (Dwivedi *et al.* 1988) and *Karwinskia parvifolia* Rose (coyotillo, Rhamnaceae) (Hanácková & Piñeyro-López 1997), for example, exhibit simultaneous

cytokinesis in which the deposition of callose around each individual microspore occurs in a centripetal fashion.

A few families produce partial or ephemeral cell plates, followed by furrowing (Bhandari 1984, Davis 1966, Esau 1965). Genera such as *Magnolia* L. (magnolia, Magnoliaceae) (Brown & Lemmon 1992a) and *Laurelia* Juss. (laurel, Monimiaceae) exhibit these variations (Bhandari 1984). These are sometimes referred to as an intermediate type (Davis 1966), but some authors also class them as subcategories of simultaneous cytokinesis (Bhandari 1984).

The arrangement of tetrads (Figure 2.3) is generally a species characteristic (Davis 1966, Esau 1965, Knox 1984). If the second meiotic event is perpendicular to the first, then radially symmetrical arrangements of nuclei result (Stanley & Linskens 1974).

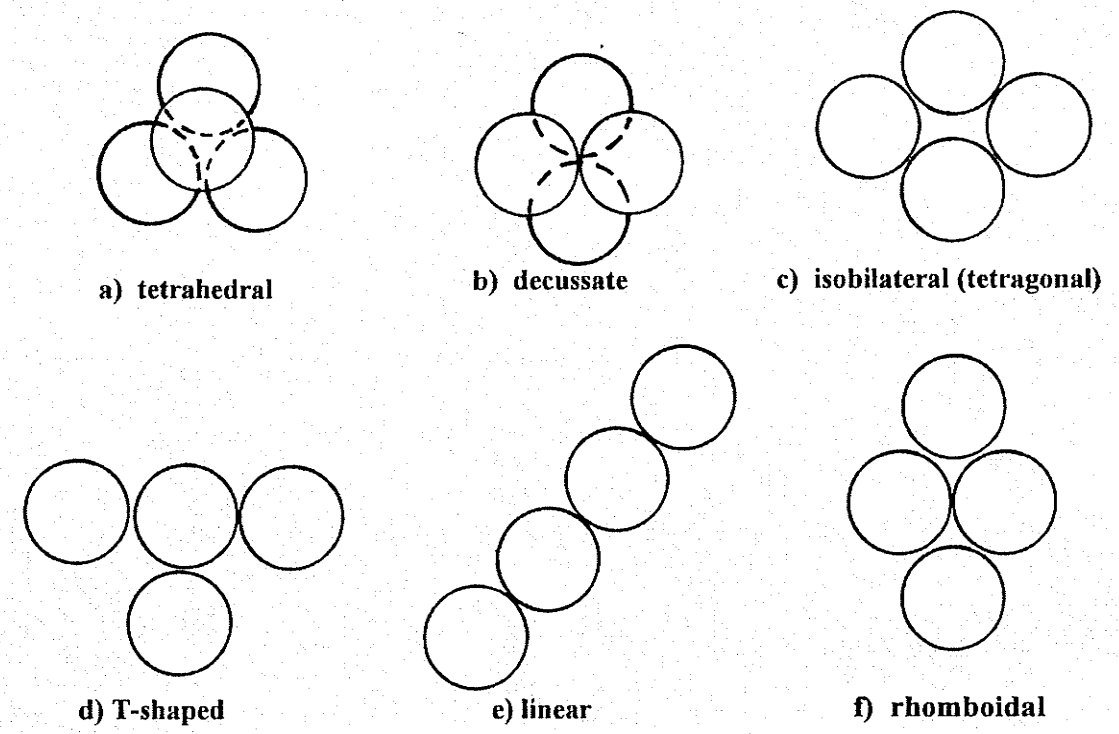

Figure 2.3 Different types of tetrad arrangements produced by angiosperms (after Davis 1966, Dwivedi *et al.* 1988, Khan *et al.* 1991, West 1971).

Differing orientations of spindles will produce other arrangements even within the same anther. Tetrads of *Cyphomandra betacea* (Cav.) Sendtn. (tree tomato, Solanaceae) are

tetrahedral or isobilateral (Prasad *et al.* 1990), those of *Nelumbo lutea* Willd. (American lotus-lily, Nelumbonaceae) tetrahedral or tetragonal (Kreunen & Osborn 1999), whereas *Cudrania* are mainly tetrahedral, but also decussate and isobilateral (Dwivedi *et al.* 1988). Other possible tetrad arrangements are T-shaped (Piven *et al.* 2001), linear (Davis 1966, Khan *et al.* 1991, West 1971) or rhomboidal (Khan *et al.* 1991). All four male cells are normally functional, but exceptions do exist (Knox 1984). Members of the Cyperaceae, for example, have a degeneration of three of the microspores, and only one develops into a functional pollen grain called a pseudomonad, cryptotetrad or transformed microspore mother cell (Brown & Lemmon 2000, Dunbar 1973, Ranganath & Nagashree 2000).

During microsporogenesis, organelle populations within the microspore mother cells have been observed to follow specific patterns in several dicot species (Kudlicka & Rodkiewicz 1990, Rodkiewicz *et al.* 1989, 1992). Changes in the number and orientation of nuclear pores, ribosomes, nucleoli, mitochondria and plastids have been observed (Bhandari 1984). Organelle movements are the most fascinating of these changes.

Plastids, mitochondria, vesicles and sometimes dictyosomes, are the organelles most often observed to aggregate and desegregate. One or two cycles can occur, a first in prophase I and/or a second from prophase II to telophase II. Large proportions of the plastids in *Nymphaea* L. (water lily, Nymphaeaceae) are also believed to be actively dividing during prophase I (Bhandari 1984, Rodkiewicz *et al.* 1992).

Plastids and mitochondria in the microsporocytes of *Nymphaea* aggregate to one side of the nucleus and then later scatter (Rodkiewicz *et al.* 1989). Both *Nymphaea* and *Impatiens* L. (jewelweed, Balsamineaceae) organelles may also aggregate at the poles of the diploid nucleus during prophase I and then move to an equatorial position during metaphase I and remain there until the end of telophase II (Rodkiewicz *et al.* 1992). Equatorial aggregations later become partitioned into four parts, one around each of the four resulting haploid nuclei (Rodkiewicz *et al.* 1989, 1992). The tetrads are still completely encased in callose at this stage.

The equatorial aggregations are layered in *Nymphaea* and *Impatiens*. Two outer layers are composed of plastids and an inner one of mitochondria. The inner layer also

produces a partial transient cell plate, positive for callose, which disappears before the second meiotic division. Rodkiewicz *et al.* (1992) considered this as evidence of repressed cytokinesis I, as both these genera exhibit simultaneous cytokinesis. An alternate suggestion is that layers of aggregated organelles may ensure an equal proportioning of organelles to daughter cells as well as preventing premature fusion of nuclei (Kudlicka & Rodkiewicz 1990).

2.2 Microgametogenesis of Angiosperms

2.2.1 Microspore maturation

Meiosis of the microsporocytes results in tetrads of haploid microspores (Davis 1966, Knox 1984, Moore *et al.* 1991) held together by a callose wall, but microspores are usually released from one another and disperse as separate pollen grains (Davis 1966, Knox 1984) also called monads (Knox 1984, Stanley & Linskens 1974). In a few families, individual microspores are not liberated and the pollen grains develop and dehisce as tetrads (Hermann & Palser 2000). Partial dissolution of the complex callose envelope occurs in both *Annona glabra* L. (pond apple, Annonaceae) and *Annona montana* Macfad. (mountain soursop, Annonaceae) resulting in the release of pollen in tetrads. Ontogenetically, sporopollenin is deposited over the remnants of the cellulose-callose layers and later in development the endexine of each grain becomes fused (Tsou & Fu 2002). In some cases, the release of tetrads has been interpreted as meaning microgametophyte development proceeds rapidly. *Callitriche truncata* is such a case, as anthers containing tetrahedrally arranged tetrads, free microspores and mature grains are frequent (Osborn *et al.* 2001). Other genera are known to release mature pollen grains in groups such as dyads, massulae or pollinia (Davis 1966, Knox 1984, Moore *et al.* 1991, Pacini *et al.* 1985). Families in which pollen is released in clumps tend to have the glandular type of tapetum (Pacini *et al.* 1985).

If released, the order of events following the release of the microspores may vary. Depending on this order, some authors have broken down microgametogenesis into three major classes. The first of these is the most common and is referred to as the Normal Type (Stanley & Linskens 1974). Immediately after release from the tetrad, the microspores increase in size (Bedinger 1992, Knox 1984, Stanley & Linskens 1974). The

production of numerous small vacuoles, which eventually coalesce into a single large vacuole, is believed to aid in the cell's enlargement (Bedinger 1992, Knox 1984). Often a nuclear migration from the center of the cell to its periphery also occurs. This is partially a result of the cytoplasm being pushed to one side of the spore by the large vacuole (Bedinger 1992), but microtubules are also believed to be involved (Brown & Lemmon 1991a, b). This nuclear migration to the periphery has been observed in *Karwinskia* (Hanácková & Piñeyro-López 1997), *Zea* (Bedinger 1992), and *Phalaenopsis* Blume (moth orchid, Orchidaceae) (Brown & Lemmon 1991c, 1992b). Chemical or electrical gradients have also been suggested (Stanley & Linskens 1974). Exine deposition and microspore mitosis occur after these changes are complete.

The Cyperaceae and Juncaeae exhibit the Juncus Type of gametogenesis. This type of development is characterized by microspore mitosis occurring before an increase in size of the microspore. As well, the initiation of the exine occurs before vacuolization of the microspore. An increase in the size of the pollen grain may still happen after division of the generative nucleus (Knox 1984, Stanley & Linskens 1974).

A third type is referred to as the Triglochin Type, since *Triglochin* L. (arrowgrass, Juncaginaceae), and other aquatic genera, including *Potamogeton* L. (pondweed, Potamogetonaceae), *Ruppia* L. (wigeongrass, Ruppiaceae), *Najas* L. (naiad, Najadaceae), and *Ceratophyllum* L. (coontail, Ceratophyllaceae), all exhibit this type of development. After release from the tetrad the young microspores may grow slightly, but vacuolation and the main increase in size mostly occurs after microspore mitosis. Some exine deposition is observed early, but most of the deposition occurs later (Knox 1984, Stanley & Linskens 1974). Whatever the type of pollen maturation, once the intine and exine are complete pollen grains generally dehydrate (Bedinger 1992, Knox 1984) and the vacuole is resorbed (Knox 1984).

The microspore provides a surface template system, which determines exine patterning (Bhandari 1984, Knox 1984, Moore *et al.* 1991). This template is referred to as the primexine (Bedinger 1992, Bhandari 1984, Knox 1984) or glycocalyx (Bedinger 1992). Primexine is of a microfibrillar nature in a polysaccharide matrix (Heslop-Harrison 1976). More recent data on *Lilium* suggests that the tapetum also contributes to

the primexine (Aouali *et al.* 2001). There is circumstantial support for its function as a template in that a primexine cannot be detected in species that lack an exine (Knox 1984).

Soon after (Piffanelli *et al.* 1998) or sometimes during meiosis (Hanácková & Piñeyro-López 1997), while the microspores are still encased in their callose wall, a homogeneous cellulose matrix forms between the callosic wall and the plasmalemma of each microspore (Pacini *et al.* 1986, Piffanelli *et al.* 1998). It first appears as a narrow halo of cellulose, which gradually increases in thickness. Once grains enlarge the primexine and cellulose layers are stretched and thinned out, but this is not always noticeable because of the concurrent thickening of the exine (Moore *et al.* 1991). In some species primexine remnants appear as a fibrillar intine along with fragmented lamellae, positive for acidic polysaccharides (Osborn *et al.* 2001).

Other evidence for the primexine's role in exine patterning is that the presence of ER just beneath the microspore cell membrane has been correlated with the future location of apertures in the mature grain. Wherever there is an underlying plate of ER in the microspore cytoplasm, no primexine is laid down. These discontinuities of the primexine are the sites where apertures will eventually be located (Knox 1984, Moore *et al.* 1991, Stanley & Linskens 1974). Sometimes this is related to the three dimensional arrangement of the microspores within the tetrad (Knox 1984). A template of future patterning of the exine has also been detected on the inner surface of the enclosing callose for some species (Bhandari 1984, Stanley & Linskens 1974).

Since there appears to be a relationship between the location of ER within the microspore and the patterning of the microspore's surface (Dickinson 1976), the haploid genotype itself seems to be directing deposition. However, there must be at least some involvement of the sporophytic genotype, since it is supplying the precursors for the exine wall (Knox 1984, Pacini *et al.* 1985, Stanley & Linskens 1974). As well, segments of ER are sometimes in place before the microsporocyte has undergone meiosis (Dickinson 1976, Moore *et al.* 1991), although there is some disagreement between authors on this point (Knox 1984, Moore *et al.* 1991, Pacini *et al.* 1985). Dickinson (1976) discusses the establishment of exine pattern in some detail.

Once the individual pollen walls, sometimes called sporoderm, begin to develop around each microspore (Esau 1965), the callose layer begins to disappear in a centripetal fashion (Bhandari 1984). Sporoderm is made up of an outer exine and an inner intine layer (Esau 1965). Intine is of a primarily polysaccharide nature and exine consists mainly of a lipid-like material called sporopollenin characterized by a high degree of resistance to degradation (Knox 1984, Moore *et al.* 1991, Southworth 1986, Stanley & Linskens 1974, West 1971). Development of the exine is a product of both the tapetal cells as well as the microspores (Bedinger 1992, Knox 1984, Pacini *et al.* 1985, Stanley & Linskens 1974), as exine patterning has been observed on microspores before their release from callose (Nitta *et al.* 1997), and mutations affecting exine development (Taylor *et al.* 1998) can cause partial or complete male sterility (Piffanelli *et al.* 1998).

The intine is made up of acidic polysaccharides (Knox 1984) or a mixture of polysaccharides and polyuronides (Esau 1965). Intine thickening is dependent on a viable microspore and generally occurs soon after release (Heslop-Harrison 1976), although intine has also been reported to be laid down after the sporopollenin (Stanley & Linskens 1974). Specific carbohydrates that have been shown to be present include cellulose (Ferguson *et al.* 1998), callose, hemicelluloses and pectins (Esau 1965, Knox 1984, Stanley & Linskens 1974). Enzymes have been detected within inclusions, often concentrated in the thickened intine regions below apertures (Heslop-Harrison 1976). Bedinger (1992) states that intine deposition does not occur until after the first microspore mitosis in maize, but for many other species occurs while microspores are still encased in callose (Hanácková & Piñeyro-López 1997). Intine formation can also occur in waves. Evidence of this is seen as concentric laminations (Stanley & Linskens 1974) or lamellae (Knox 1984). Intine secretion, by the microspore itself, begins first in the aperture regions and then spreads to the rest of the maturing grain (Knox 1984, Hanácková & Piñeyro-López 1997).

2.2.2 Exine development

The exine of mature pollen grains is composed largely of sporopollenin (Bedinger 1992, Heslop-Harrison 1971, Knox 1984, Taylor & Hepler 1997), although special staining methods have also revealed a small amount of cellulose and some enzymes

(Knox 1984, Stanley & Linskens 1974). For most species, the presence of exine is necessary for viable pollen. Its remarkable ability to resist degradation (Heslop-Harrison 1976), coupled with a species level uniqueness of patterning, has made palynological studies possible (Moore *et al.* 1991, Stanley & Linskens 1974, West 1971). Precursors initially have a lignin reaction (Stanley & Linskens 1974) and are hypothesized to be transported as monomers (Bhandari 1984, Stanley & Linskens 1974) from the tapetum to the young exine via orbicules (Bhandari 1984, Knox 1984, Moore *et al.* 1991, Prasad *et al.* 1990). Sporopollenin is one of the most chemically resistant biological substances known, but is not completely impermeable (Knox 1984). It was thought to be composed of polymerized carotenoids (Bedinger 1992, Bhandari 1984, Knox 1984, Moore *et al.* 1991, Stanley & Linskens 1974, West 1971) or terpenes (Stanley & Linskens 1974), however recent data indicates it is not (Bedinger 1992). Chemical analysis has shown that sporopollenin is made up of long chain fatty acids (Guilford *et al.* 1988), phenyl propanoids and oxygenated aromatic rings (Piffanelli *et al.* 1998), although the exact chemical composition of sporopollenin remains elusive.

Exine structure and hence its development, can be quite simple or complex depending on the species (Knox 1984, West 1971). There is an abundance of terminology used to describe the exine (Figure 2.4). Terms such as ektexine and endexine are based on staining characteristics of the outer and inner layers of mature exine, but when misused or mixed with new terms can be quite confusing (Knox 1984). Often the terms used reflect whether the grain was being examined for taxonomic, morphological or developmental reasons (Stanley & Linskens 1974). An alternate system of naming layers using nexine and sexine is used by some authors. It is based less on the differential staining characteristics of the layers and more on morphological characters of the exine (Knox 1984, Moore *et al.* 1991, Stanley & Linskens 1974). The two sets of terminology are often used interchangeably depending on the point of view, and other naming systems have been developed (Moore *et al.* 1991, Stanley & Linskens 1974).

The beginning of endexine development is simultaneous with callose dissolution. The primexine has not thinned yet, but it also is not laid down evenly in all areas.

Interporal areas thicken evenly, but are not homogenous (Stanley & Linskens 1974). The outermost exine is often stratified into a foot layer, columellae and tectum, but any of these layers may be absent (Knox 1984, West 1971). Typically, columns of granular

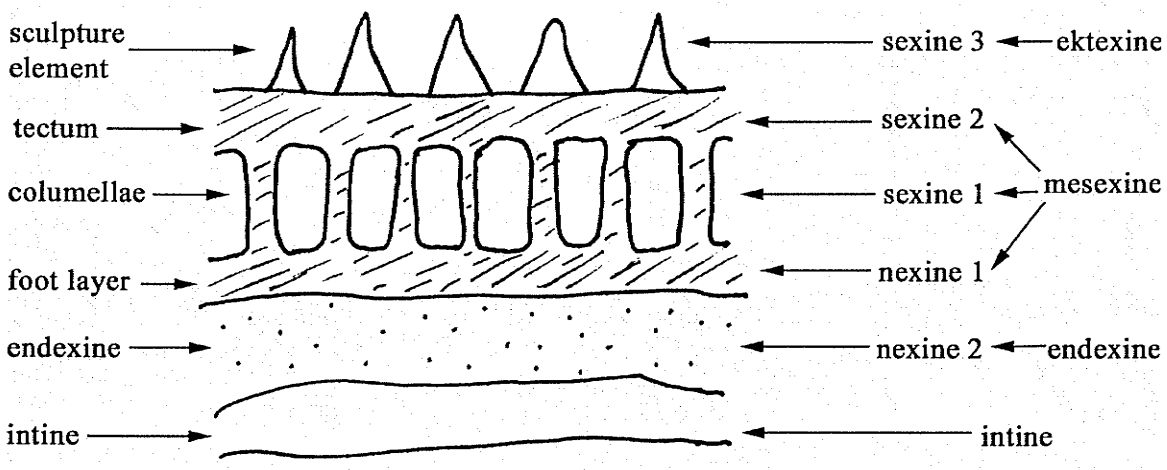

Figure 2.4 Pollen wall layer terminology based on structural, staining or morphological characteristics (after Knox 1984, Moore *et al.* 1991, Stanley & Linskens 1974, West 1971).

material called probacula (Knox 1984, Stanley & Linskens 1974) or procolumella (Moore *et al.* 1991) are deposited over the surface of the primexine (Stanley & Linskens 1974). They are composed of lipoprotein (Knox 1984, Moore *et al.* 1991). These may also extend upward and interconnect in a roof-like manner, leaving chambers beneath. Later these roofed areas will be referred to as the tectum, and the pillars as the baculae, but these terms are reserved for after the deposition of sporopollenin (Knox 1984), Stanley & Linskens 1974). Moore *et al.* (1991) state that rods, which are supporting the tectum, should be called columellae and the term baculum should be reserved for a rod not supporting anything. Knox (1984) agrees that rods covered by a roof are columellae but when no tectum is present should be called pili (singular pilum), and in both situations may be referred to as baculae. Exine accumulation continues until a complete coating is established and normally extends over the baculae, but is discontinuous over pore sites (Knox 1984, Stanley & Linskens 1974). Orbicules may also contribute to the outer exine

at this stage of development (Knox 1984, Moore *et al.* 1991, Pacini *et al.* 1985, Prasad *et al.* 1990).

If probaculae are absent, deposition is in irregular masses (Stanley & Linskens 1974). At maturity the exine of *Karwinskia*, for example, is of a granular, noncolumellar nature (Hanácková & Piñeyro-López 1997). The inner exine forms via the apposition of lamellae with sporopollenin deposition on the distal surfaces. The ektexine is a coarse reticulum whereas the endexine has a variable homogenous to lamellar appearance, from the distal to proximal surface. Other electron microscope studies have also found endexine to be laminate and ektexine amorphous to granular in nature (Knox 1984, Moore *et al.* 1991). When Southworth (1986) did exine extractions followed by SEM, she observed a granular substructure interconnected in a lattice. The outer exine surface also had a layer of fibrillar material on it, and the proximal intine surface had plasma membrane invaginations containing microspore cytoplasm. In contrast, most angiosperms have a columellate, stratified exine (Davis 1966). Developmental descriptions of noncolumellar exines are rare (Hanácková & Piñeyro-López 1997).

2.2.3 Microspore mitosis

Some time after meiosis, a precisely located (Knox 1984), but asymmetric, mitotic division results in two cells within the microspore (Bedinger 1992, Knox 1984). Synchronous division is said to occur only when microspores remain in tetrads and retain cytoplasmic connections (Knox 1984), but also occurs in anthers with separate microspores. Mitosis may happen only a few hours or many months after the meiotic division (Knox 1984, Stanley & Linskens 1974), and terminates the microspore stage. The mitotic event begins the bicellular microgametophyte stage, which by definition, is referred to as pollen, although a second mitotic event by the generative cell has yet to occur (Knox 1984, Stanley & Linskens 1974). Tricellular pollen is released by members of the Asteraceae, Brassicaceae and Poaceae (Knox 1984).

The products of the first mitotic division are referred to as the generative and vegetative cells (Knox 1984, Stanley & Linskens 1974, Tanaka 1997). The differing fate of these two cells is reflected in their structural composition and metabolic activities (Tanaka 1997). The nucleus of the vegetative cell tends to be round in shape (Baltz *et al.*

1999), have decondensed chromatin (Okada & Toriyama 2001), be larger than and possess more (Bedinger 1992, Stanley & Linskens 1974) and denser nuclear pores (Straatman *et al.* 2000, Tanaka 1997), than the generative cell. The latter cell is usually smaller, lenticular or spindle-like in shape (Baltz *et al.* 1999, Stanley & Linskens 1974), and possesses denser chromatin (Okada & Toriyama 2001). As well, the smaller generative cell is often at a point furthest from the aperture (Bedinger 1992, Stanley & Linskens 1974). This could ensure the vegetative cell entering the pollen tube first upon germination (Knox 1984), but exceptions are known (Bannikova & Khvedynich 1977, Saito *et al.* 2000). In all cases, mitosis results in a small generative cell contained within the larger vegetative cell (Osborn *et al.* 2001). The histone (Tanaka *et al.* 1998), DNA (González-Melendi *et al.* 2000), and RNA content do not appear to be the same in both nuclei (Stanley & Linskens 1974) and this may partially account for the differences in appearance of the two nuclei, particularly their staining properties (Tanaka 1997).

Cellular polarity of the microspore seems to be established before the asymmetric mitotic event. Developmentally, a cytological change within the uninucleate microspore, displacing the nucleus to one pole, appears to involve microtubules. This also results in a distinctly polar distribution of organelles prior to mitosis (Tanaka 1997). The spindle apparatus is commonly cone-shaped, with the broadest end located closer to the future generative pole rather than biacuminate. Chromosomes destined to become the vegetative nucleus have also been observed to move at a slower rate than those moving towards the generative pole do (Brumfield 1941). A similar asymmetric spindle, perpendicular to the plasma membrane, coordinates the division in *Phalaenopsis* (Brown & Lemmon 1992b). Formation of an unusual hemispherical cell plate between the two resulting nuclei at the generative pole completes the mitotic event (Brown & Lemmon 1991a).

Experiments involving microtubule-perturbing drugs show that the differentiation of the generative cell is dependent on this asymmetric cell division, whereas the development of the vegetative cell is not. A symmetric mitotic division occurs when the microtubular apparatus is disrupted. Both the resultant nuclei resemble the vegetative nucleus in many of the previously mentioned traits, functionally and structurally. Plastids

seem to be excluded from that pole fated to be the generative (Tanaka 1997) in most species, but there are a few reports of generative cells containing mitochondria and plastids (Russell & Cass 1981, Saito *et al.* 2000).

2.2.4 Mature angiosperm pollen

Cytochemical and ultrastructural studies show that during their maturation, pollen grains tend to accumulate either polysaccharides or lipids (Piffanelli *et al.* 1998). Starch grains and lipid bodies, also called spherosomes, are believed to be utilized as the initial source of energy for germinating grains. A switchover to a heterotrophic mode of nutrition from the stylar tissues is believed to occur later (Southworth 1996, Stanley & Linskens 1974). Although some species, such as *Zea*, contain high amounts of both types of storage substances, grains generally tend to accumulate an abundance of one type of macromolecule (Bedinger 1992, Piffanelli *et al.* 1998, Stanley & Linskens 1974). This allows for pollen to be classified as either an oily or starchy type of grain, although both types may also contain storage proteins. Some oily grains have a temporary accumulation of starch grains, which rapidly disappear once lipid production begins. As well, during microgametogenesis starch may be stored once or twice. In some species, starch is deposited in young microspores, then hydrolyzed, and a second deposition occurs later during the bicellular pollen stage. If only one starch deposition event occurs, it is during the latter stage (Pacini 1996).

The fat and starch content has been correlated with dispersal mechanism. Fatty grains such as those of *Taraxacum officinale* G.H. Weber *ex* Wiggers (common dandelion, Asteraceae) tend to be dispersed by bees, and those high in carbohydrate, like *Typha elephantina* Roxb. (elephant's grass, Typhaceae) by wind (Piffanelli *et al.* 1998). Other chemical analyses done include the percent ash, fiber, proteins, free amino acids, nucleic acids, organic acids, sterols and individual mineral content on a dry weight basis. Values usually vary with species, but may change depending on environmental conditions during development (Stanley & Linskens 1974). Nutritive storage materials are found only in the vegetative cell (Piffanelli *et al.* 1998).

The water content of mature pollen varies from 6 - 60% (Taylor & Hepler 1997). This variable dehydration status has been correlated with the longevity of pollen viability,

but also seems to be related to the location and type of carbohydrate reserve in developing and mature grains. Generally, pollen that is not dehydrated when dispersed does not remain viable for long. This is the case for both *Zea mays* and *Cucurbita pepo* L. (marrow, Cucurbitaceae). *Lavatera arborea* L. (tree mallow, Malvaceae), however, appears to be tolerant to desiccation. Pacini (1996) postulates that this resistance may be related to the presence of cytoplasmic polysaccharides, but it could also be influenced by the occurrence of soluble sugars, such as sucrose. Further ecological evidence of this relationship is that xeric species, such as cacti, have only cytoplasmic carbohydrates. Other evidence is that polysaccharides within the pollen of *Parietaria judaica* L. (pellitory of the wall, Urticaceae) are found within starch grains in the spring and autumn, but cytoplasmically during the summer when it is drier. Species that have cleistogamous flowers may also have two types of pollen, with starch grains in the cleistogamous flowers and soluble, cytoplasmic carbohydrates in the chasmogamous. Speranza *et al.* (1997) tested mature pollen grains from 13 angiosperms for soluble and insoluble carbohydrates and used this as a basis to classify them into one of three classes; 1) pollen slightly dehydrated at anthesis or 2) pollen dehydrated at anthesis, types a and b. Type one pollen tends to be large and has a low soluble sugar content, but abundant starch. Examples include *Cucurbita pepo*, *Zea mays* and *Lolium perenne* L. (perennial rye grass, Poaceae). An abundance of soluble sugars, especially sucrose, was correlated with little or no starch content. Type 2a tends to be small to medium in size and long-lived. *Malus domestica* Baumg. (domestic apple, Rosaceae), *Ricinus communis* L. (castor bean, Euphorbiaceae) and *Typha latifolia* (broadleaf cattail, Typhaceae) are of this type. The third category, 2b, is represented by *Lilium*, *Magnolia* and *Passiflora caerulea* L. (blue passionflower, Passifloraceae). These species exhibit an intermediate status in regard to both soluble sugar and starch content. Pollen grain size is quite variable from small to large. The authors hypothesized sucrose molecules protect dehisced grains from desiccation and may also have a role in pollen tube metabolism during germination.

Amyloplasts may contain one or more starch grains, but insoluble polysaccharides have also been located via the Schiff's reaction and cytodensitometry of cytoplasmic vesicles. Species such as *Cucurbita pepo* contain insoluble carbohydrate, such as starch

grains, only within amyloplasts whereas *Lavatera arborea* also has insoluble carbohydrates within cytoplasmic vesicles. Both species are not dehydrated at dehiscence (Pacini 1996).

Pollen has also been classified by the type of aperture (Knox 1984, Moore *et al.* 1991, West 1971). The two main types of apertures are distinguished by shape (Esau 1965, Knox 1984, Moore *et al.* 1991). Pores or pori in pollen grains are isodiametric depressions, which if elongate, have rounded ends. Grains with pori are referred to as porate pollen. Furrows or colpi are long with pointed ends and the pollen is described as colpate. If both types of depressions are found making up an aperture, the term used is colporate (Moore *et al.* 1991). Pori are thought to be the more advanced trait (Knox 1984, Moore *et al.* 1991). The number of apertures on a single grain can vary from none to many, and they may not all be of the same type (Esau 1965, Knox 1984). *Nelumbo lutea* for example, produces mainly tricolpate, but also monosulcate and diaperturate grains (Kreunen & Osborn 1999). Even within one anther not all pollen grains will necessarily have the same number of apertures (Ressayre *et al.* 2002).

Inaperturate pollen has no obvious aperture. There are two main types: omniaperturate and functionally monoaperturate. A pollen tube can potentially emerge from anywhere on the surface of the grain in the former type, whereas a single thickened region of the intine, sometimes called an oncus, exists beneath a superficially uniform layer of exine, indicating the site of the aperture, in the latter. Surface examination of grains via SEM alone is often insufficient to determine into which category a grain falls. Transmission electron microscopy of sectioned material is often necessary to fully describe mature grains (Furness & Rudall 1999) with reference to aperture type.

Moore *et al.* (1991) describe a classification system which takes character, position and number of apertures into consideration, although they mention that there are some unusual types which do not fit into their scheme. Another problem arises when pollen is classified solely on the basis of aperture orientation, using the terms sulcate and colpate. Sulcate is defined as the vertical axis of apertures being parallel to the equatorial region of the grain; in this instance colpate means a grain has perpendicular apertures (Knox 1984). Simpler types include *Cudrania* which has three pores and is therefore triporate

(Dwivedi *et al.* 1988), *Potamogeton* which has no apertures and hence inaperturate (Moore *et al.* 1991), or *Amphibolis* C. Agardh. (seagrass, Cymodoceaceae) which has no exine or apertures, and is called omniaperturate (Moore *et al.* 1991). The type of pollen most commonly produced by dicots is tricolporate (Knox 1984), consisting of three apertures made up of both pori and colpi (Moore *et al.* 1991).

Pollen size (Stanley & Linskens 1974) and shape (Moore *et al.* 1991) are fairly constant within species, but vary between species. Dimensions from 5 – 200 μm are known (Stanley & Linskens 1974), but most grains range from 15 - 45 μm in diameter (Moore *et al.* 1991, Stanley & Linskens 1974). Pollen grains are relatively spherical, but other shapes such as elongate and filiform are also known (Knox 1984). The weight and volume of grains have been measured (Stanley & Linskens 1974), but these parameters need to be used with care since they can be affected by the age of the grain and/or hydration state (Moore *et al.* 1991). Size has been correlated with a number of other variables. Temperature (Omori & Ohba 1996), pollen viability (Kelly *et al.* 2002), mode of pollination, ploidy level, genetic and nutrient status of the parent plant, season of flowering, or anther position within the flower have all been found to have an effect on pollen size (Stanley & Linskens 1974).

The ornamentation of the mature pollen grain can be quite elaborate. Exine sculpturing can be described in sectional or surface views (Moore *et al.* 1991) and the variations possible seem almost endless. The outer exine may be ornamented into spines, depressions or other markings (Knox 1984, Stanley & Linskens 1974). The two basic types of exine are tectate and pilate (Knox 1984), but sectional views often reveal how a similar external appearance may actually obscure differences in internal patterning (Moore *et al.* 1991) or layering (Furness & Rudall 1999). Spaces within the exine may be called cavae, micropores or microchannels, depending on their size, shape and location (Knox 1984). The role of exine patterning is speculative, but grain size and wall patterns are known to be remarkably consistent for a species (Knox 1984, Moore *et al.* 1991, Stanley & Linskens 1974). Exine thickness is variable, even to being completely absent in some species (Furness & Rudall 1999, Knox 1984), and is known to affect the hydration status of mature grains and in their longevity once released. There are four

species of *Callitriche* with pollen known to lack or have a reduced exine layer. The pollen wall of mature *Callitriche truncata* grains produces hydrated grains with a thickened intine and no exine. These grains are dispersed under water for a hypohydrophilous mode of pollination (Osborn *et al.* 2001).

The exine is thinner (Knox 1984, Moore *et al.* 1991) or absent (Knox 1984) in the apertural region of most grains, and the underlying intine is usually thicker (Esau 1965, Furness & Rudall 1999, Knox 1984, Moore *et al.* 1991). The thickened intine has been shown to contain high levels of enzymes (Knox 1984, Stanley & Linskens 1974), and since it is located outside the microspore plasmalemma, these enzymes are extracellular and have been hypothesized to function in pollen tube initiation or compatibility recognition (Knox 1984). Some apertures have a cap-like exine operculum with a fine reticulate substance between it and the intine epidermis (Hanácková & Piñeyro-López 1997). This reticulate material has been called Zwischenkörper, the Z-layer (Knox 1984) and interstitial bodies (Rowley 1976). The intine typically protrudes through this type of aperture with Zwischenkörper occluding the gap in the exine. An additional electron-dense layer has also been observed between the Zwischenkörper and the plasma membrane in some species (Hanácková & Piñeyro-López 1997). Infolding, shutters or plates of the exine may seal apertures without opercula, which open upon hydration of the grain (Heslop-Harrison 1976). Other grains may be covered with a lipid or mucilage seal (Knox 1984).

Pollen pigmentation can range from white to gray, green to blue, or yellow to red. Carotenoids, terpenes or xanthophylls may be present (Stanley & Linskens 1974), but most commonly flavonoids and/or their derivatives are found (Taylor & Hepler 1997). Color has been hypothesized to have evolved as an attractant for pollinators, especially insects, or possibly act as a screen against ultraviolet radiation. The carotenoids in particular have been shown to exert some control over carbohydrate metabolism and to affect pollen germination (Stanley & Linskens 1974). Whatever the role pigments play, they must be essential to pollen development, since sterile pollen often has little or no pigmentation (Taylor & Hepler 1997).

Shape and size, combined with exine sculpturing and aperture orientation, are used to identify pollen grains to at least family or genus, and in many instances to species (Knox 1984, Moore *et al.* 1991, Stanley & Linskens 1974). Dichotomous keys, using descriptions of exine sculpturing, type and number of apertures, as well as overall shape and size of grains, facilitate this identification (Moore *et al.* 1991).

2.2.5 The male germ unit

Generative cell mitosis occurs after germination for two-celled pollen grains (Knox 1984, Southworth 1996, Stanley & Linskens 1974). The timing of generative cell division is genetically determined (Southworth 1996). A special spatial problem exists if division occurs within the pollen tube (Stanley & Linskens 1974). Mitosis is typical except the cell plate is oriented longitudinally or slightly oblique to the pollen tube axis (Southworth 1996). Cytoplasmic microtubules appear key in helping this process move along normally (Derksen *et al.* 2002, Moscatelli *et al.* 1996, Stanley & Linskens 1974). The vegetative nucleus is usually observed distal to the generative (and ultimately the two sperm nuclei) in the elongating pollen tube (Bedinger 1992, Derksen *et al.* 2002). In contrast, artificially germinated *Camellia sasanqua* Thunb. (Sasanqua camellia, Thecaceae) pollen was reported to have the vegetative nucleus behind the generative within the growing pollen tube. Cytoplasm surrounded the elliptical generative nucleus, but division into the two sperm cells was not observed (Mathew 1978).

Although most families release bicellular pollen, some are tricellular and contain one vegetative nucleus and two sperm cells (Baltz *et al.* 1999). Collectively these three cells making up the microgametophyte are called the male germ unit (McConchie *et al.* 1985). Despite transient physical contact, they remain close to one another during pollen growth (Derksen *et al.* 2002). Their membranes closely parallel one another and cellular extensions from the generative cell around the vegetative nucleus are often observed (Southworth 1996). Three-dimensional reconstructions of the trinucleate pollen of *Plumbago zeylanica* L. (white leadwort, Plumbaginaceae) (Russell 1984, Russell & Cass 1981, Russell *et al.* 1996) and *Brassica campestris* L. (field mustard, Brassicaceae) (McConchie *et al.* 1985) show clearly that the vegetative nucleus and two sperm cells are interconnected.

The vegetative nucleus is usually larger and more centrally located. It tends to be lobed at maturity (McConchie *et al.* 1985), and contain many organelles (Knox 1984). It is sometimes described as being a nurse cell for the generative and/or sperm cells, although physical evidence of nutrient transfer does not exist (Southworth 1996). Immediately after microspore mitosis, the generative nucleus is spherical, but soon becomes ellipsoidal and eventually spindle-shaped (Saito *et al.* 2000, Southworth 1996). This is believed to occur via a microtubule network. There are conflicting opinions as to whether or not actin microfilaments are present. Sperm cell cytoskeletons arise from that of the generative and like the generative, are entirely contained within the vegetative cell's membrane (Southworth 1996). Sperm cells contain oval to elongate highly condensed nuclei (Baltz *et al.* 1999, Saito *et al.* 2000), and occasionally vacuoles and mitochondria have been observed, presumably trapped, within sperm nuclei (Southworth 1996). Usually generative cells and sperm cells have a limited range of cytoplasmic organelles (Knox 1984, Southworth 1996). Organelles seen in sperm cells include mitochondria, ribosomes, plastids, ER, dictyosomes, vesicles and polysomes (Mogensen & Rusche 2000, Southworth 1996). Sperm cells have long been thought to be isomorphic, but recent evidence has shown that dimorphism does occur, in organelle content, (Russell 1984, Saito *et al.* 2000), shape (Mogensen & Rusche 2000, Saito *et al.* 2000) and volume (Tian *et al.* 2001).

Sperm cells of *Triticum* L. (wheat, Poaceae) have been described as going through four stages of development; naked, walled, cytoplasm increasing and mature. These were correlated with organelle, membrane and wall changes. Other differences between sperm cells that have been noted include whether or not a tailed structure is present and how they are attached to the vegetative cell (Knox 1984). Morphologically dissimilar sperm cells have been observed for three-celled species such as *Plumbago zeylanica* in that the two sperm cells were quite divergent in terms of the types and numbers of organelles found within them (Russell *et al.* 1996, Southworth 1996). Sperm cell dimorphism has implications for preferential fertilization and paternal inheritance mechanisms (Southworth 1996).

Maternal inheritance of organelles containing DNA occurs for the majority of angiosperms (Sodmergen *et al.* 2002). Both mitochondria and plastids are commonly found within egg cells, but not always in sperm cells. The paternal inheritance of mitochondria is more common that the paternal inheritance of plastids. Sperm cell dimorphism reported for a few tricellular species such as *Secale cereale* L. (rye, Poaceae) (Mogensen & Rusche 2000) and *Plumbago zeylanica* (Russell *et al.* 1996) is responsible for the presence of mitochondria within the sperm cell destined to fuse with the egg cell.

Potential biparental inheritance via pollen plastid DNA was evaluated for 235 species in 80 families, using an epifluorescent technique (Corriveau & Coleman 1988). This cytological method detects DNA aggregates in the cytoplasm of generative or sperm cells within pollen grains or tubes. In 18% of the species examined, cytoplasmic DNA was observed in the male reproductive cells, and based on size, was assumed to be of plastid origin. There was a high degree of correlation between this cytological data and the genetic evidence found in the literature, but agreement was especially true for studies employing ultrastructural methodology. This shows that paternal inheritance occurs more often than previously thought (Southworth 1996).

The mode of transmission of plastid DNA, whether maternal or biparental, is usually, but not always, consistent within a family (Corriveau & Coleman 1988), but is constant within a genus. There is still a possibility of male plastid elimination at a later stage via normal developmental processes, or a mechanism such as the exclusion of sperm cell cytoplasm (Southworth 1996) during or after the fertilization event. A 97% reduction in the amount of mitochondrial DNA within male reproductive cells of *Hordeum vulgare* L. (barley, Poaceae) during pollen development has also been documented, and suggested as a method by which paternal inheritance is inhibited (Sodmergen *et al.* 2002). This would help explain the small number of discrepancies noticed, when cytological and genetic evidence is compared (Corriveau & Coleman 1988). Overall, the primary mode of plastid inheritance is via the maternal parent (Southworth 1996).

2.3 Pollen Germination

2.3.1 Nutritional and environmental requirements

There is considerable variability in the germination requirements of pollen of different genera. Generally, tricellular pollen does not germinate as easily as bicellular (Knox 1984), but many other factors are also involved. The most commonly included components of media for *in vitro* germination of pollen include minerals (especially boron and calcium), sugars, and growth hormones, such as auxins (Stanley 1971, Taylor & Hepler 1997). Sucrose concentration and pH affect germination of fresh pollen (Kopp *et al.* 2002) as well as environmental factors such as temperature, irradiation, moisture, osmotic pressure and the partial pressures of oxygen and carbon dioxide (Stanley 1971). Some authors have found that the addition of vitamins to media stimulates germination somewhat (Piven *et al.* 2001). Other biotic variables such as pollen maturity, size, time since dehiscence (Tejaswini 2002), mycorrhizal infection, and soil phosphorus availability (Poulton *et al.* 2001) may also influence germination. Grain density is often not controlled for, but is known to affect pollen tube growth of many species (Chen *et al.* 2000, Kopp *et al.* 2002).

The optimum temperature for pollen germination is known to vary by species (Stanley & Linskens 1974), but preferences of individual genotypes within a population have not been examined extensively. Some evidence for an environmental influence on the maintenance of genetic variability in pollen performance has been obtained in pollination studies where temperature was varied. For example, when pollen of five genotypes of *Betula pendula* Roth (silver birch, Betulaceae) was germinated *in vitro* at five temperatures there was considerable variation in the length of pollen tubes. The rank order of genotypes based on pollen germination and pollen tube length was dependent on the prevailing temperature. Despite this variability, the optimum germination temperature for most of the genotypes was 30°C. There was no pollen germination at 10°C, and the length of tubes was considerably shorter at both 15°C and 35°C than at 22°C or 30°C (Pasonen *et al.* 2000). Although gametophytic selection and pollen competition has the potential to decrease genetic variability, environmental interactions are one mechanism of circumventing this loss of genetic variation.

Pollen grain size was found to be positively correlated with percent germination for both *Dianthus caryophyllus* L. (pink carnation, Caryophyllaceae) and *D. chinensis* L. (Chinese pink, Caryophyllaceae), but was negatively correlated with pollen tube length. When grains were compared over three size classes; small, medium and large; the medium category always had a higher germination rate. Smaller grains, however, tended to have longer pollen tube lengths. The larger grains showed the highest germination response when cultured in the presence of a fungal pathogen filtrate. It was therefore hypothesized that pollen size polymorphism is a survival strategy. Smaller grains would produce longer, more vigorous tubes and be more successful at fertilization under optimal conditions, whereas larger grains would be able to survive and germinate under adverse conditions (Tejaswini 2002).

Flavonols have been found to restore the germinability of pollen from flavonol deficient *Petunia hybrida* Vilm. (garden petunia, Solanaceae) plants. These plants are usually conditionally male fertile. Kaempferol and quercetin are the major flavonols in normal *Petunia* pollen, and their effectiveness at restoring germinability in conditionally male fertile pollen is both concentration dependent and saturable (Xu *et al.* 1997). Differences in cell walls were observed in the tips of pollen tubes from flavonol deficient plants (Derksen *et al.* 1999). It was hypothesized that flavonols are incorporated into the pollen tube cell wall, but was refuted experimentally (Xu *et al.* 1997). The actual site of flavonol activity is unknown.

Ethylene is not correlated with *in vivo* pollen tube growth in *Nicotiana tabacum*. It is however, synthesized *de novo* during pollen tube penetration into the style, but is not believed to be essential for tube growth (De Martinis *et al.* 2002). Ethylene precursors were found to stimulate pollen germination and tube growth in five plant species; *Amelanchier sinica* Chun (asian serviceberry, Rosaceae), *Cercis chinensis* Bunge (Chinese redbud, Fabaceae), *Prunus triloba* Lindl. (flowering almond, Rosaceae), *Sophora japonica* L. (Japanese pagoda tree, Fabaceae) and *Cucumis sativus* L. (cucumber, Cucurbitaceae). The addition of ethylene glycol-bis(β-aminoethyl ether)-*N,N,N',N'*-tetraacetic acid, phenothiazine or lithium chloride caused a decrease in stimulated germination, whereas inositol 1,4,5-triphosphate further increased the

stimulative effect. When cytosolic Ca^{+2} concentrations were measured they were positively correlated with an increase in pollen germination. A messenger system involving Ca^{+2}, calmodulin and inositol phospholipids was proposed as a possible mechanism (Song *et al.* 1998).

Pollen tube growth rates were measured and compared for *Ornithogalum virens* Lindl. (star of Bethlehem, Hyacinthaceae) cultured using solid and liquid media. Those germinated in liquid media always had growth rates twice as fast as those on a solid medium. As well, the rates from both media were found to oscillate between faster and slower periods. This pulsatory growth mode is believed to be related to fluctuations of extracellular Ca^{+2} in pollen tube cell walls (Stepka *et al.* 2000).

Clones of *Viola tricolor* L. (heartsease, Violaceae) were propagated under differing conditions of soil phosphorus and pH and their pollen performance evaluated. Sporophytic traits and pollen tube growth rate were both positively correlated with high soil pH. Soil phosphorus content, however, showed a variable response, although the rank order of donors was not changed with regard to the rate of pollen tube growth. Genotype therefore has a stronger influence on pollen tube growth rate than soil phosphorus, but variation in environmental parameters may be one mechanism of maintaining the genetic diversity of pollen (Lankinen 2000).

Oxygen gradients have been proposed as another of the factors influencing pollen germination. Pollen germination rate was stimulated by increased oxygen tension for *Brassica rapa* L. (turnip, Brassicaceae) and *Nicotiana alata* Link & Otto (jasmine tobacco, Solanaceae), but was inhibited for *Pieris japonica* D. Don *ex* G. Don (Japanese andromeda, Ericaceae). However, *Lilium formosanum* Wallace (Formosa lily, Liliaceae) pollen germination rates did not appear to be affected by a change in the oxygen tension, either positively or negatively. When these and four other species were tested experimentally, a variety of tropic responses were observed, which did not appear to be correlated with phylogeny. *L. formosanum*, *P. japonica* and *Andromeda glaucophylla* Link (bog rosemary, Ericaceae) demonstrated negative oxytropism, and *N. alata* a positive oxytropic response, whereas *B. rapa*, *Convallaria majalis* L. (lily of the valley, Convallariaceae), *Eccremocarpus scaber* Ruíz & Pav. (Chilean glory vine, Bignoniaceae)

and *Fritillaria meleagris* L. (Guinea hen flower, Liliaceae) exhibited a random pollen tube directionality with regard to an oxygen gradient (Blasiak *et al.* 2001).

A variation seen in the number and size of apertures, as well as exine wall thickness may be related to germination requirements. Large, numerous apertures and thinner walls allow a greater surface area for interaction with the stigmatic surface. Sometimes grains with this morphology extend their tubes more rapidly than grains with fewer or smaller apertures (Stanley & Linskens 1974). In a small number of species pollen is released without an aperture and is able to synthesize one *de novo* at a site adjacent to the stigmatic surface (Knox 1984).

Since pollen normally germinates within hours or days of anthesis, long term dormancy of grains is not necessary. Storage oil bodies are enclosed in extensive ER and other intracellular membranes. The level of some oily substances rises until after division of the generative cell and then sharply declines once germination occurs. Oil bodies have been observed to be rapidly converted into vesicles, which migrate to and fuse with the tip of a growing pollen tube. An alternate function for oil bodies might therefore be a ready source of membrane lipids, to facilitate the dramatic increase in surface area during pollen germination. An extensive endomembrane network is one of the characteristics of the vegetative cell, which is thought to have a role in pollen germination and subsequent pollen tube elongation (Piffanelli *et al.* 1998).

2.3.2 Pollen tubes

When a pollen grain germinates, a pollen tube emerges from an aperture and increases in length by apical growth (Esau 1965, Knox 1984, Stanley & Linskens 1974) also referred to as tip growth (Bedinger 1992, Knox 1984, Laitiainen *et al.* 2002, Stanley & Linskens 1974). If a grain has multiple apertures, usually only one tube elongates (Stanley & Linskens 1974), but some genera have occasionally been observed to be polysiphonous (Khan *et al.* 1991). Germination is coincident with a rehydration of the pollen grain and may occur on a stigma or artificial media (Bedinger 1992, Taylor & Hepler 1997).

The uptake of water causes the intine to become gel-like within an aperture, and when an operculum is present, this will cause it to lift off and allow the pollen tube to

extrude from the grain (Heslop-Harrison 1976, Knox 1984). Tube extension may occur minutes or months after a grain lands on a suitable substrate (Stanley & Linskens 1974). If released as a bicellular grain, the two nuclei move into the protrusion via a microtubule cytoskeletal network (Laitiainen *et al.* 2002), and the second mitotic division occurs within the growing pollen tube, (Bedinger 1992, Knox 1984, Stanley & Linskens 1974). In tricellular grains, all three, the two sperm cells and the vegetative nucleus, usually move into the pollen tube (Knox 1984), although in some three-celled genera, only the two sperm cells enter the pollen tube (Bannikova & Khvedynich 1977). Oscillations of Ca^{+2}, K^{+}, H^{+} and Cl^{-} ions are correlated with pulses of elongation and may be involved in the driving force (Zonia *et al.* 2001).

As the tube elongates, the pollen cytoplasm and nuclei remain close to the tip (Bedinger 1992, Knox 1984) and older parts of the tube are sealed off behind by plugs containing callose (Esau 1965, Knox 1984) and cellulose (Ferguson *et al.* 1998). Tube elongation can occur at a remarkable rate. *Zea* tube growth *in vivo* has been measured as fast as 1 $cm \cdot h^{-1}$ and the nuclei transported within the tip may move as much as 30 cm in 24 hours (Bedinger 1992), but *in vitro* growth rates are usually slower than those *in vivo* (Derksen *et al.* 2002). Growth sometimes occurs in discrete pulses alternating with stationary phases (Zonia *et al.* 2001). There is evidence that faster growing pollen tubes produce more vigorous offspring (Knox 1984).

3.0 METHODS

3.1 Study Site

3.1.1 Geographical location

Initially, three jack pine trees with actively growing male *Arceuthobium americanum* infections were selected from the Belair Provincial Forest, Disease Management Area, which is 9.2 kilometers north of the Grand Beach turnoff on provincial highway #59, 75 km north of Winnipeg, Manitoba (Figure 3.1). Similarly aged trees with brooms at comparable heights were chosen to try and minimize growth variation. The approximate locations of each tree relative to one another are shown on the detailed map. Samples from each tree are designated by abbreviated location names: KD, RD and DL. Ten additional *A. americanum* infected jack pine trees were later selected for the pollen germination experiments. These are simply numbered as #1-#10 on the same site map.

3.1.2 Sample collection

Whole shoots of dwarf mistletoe were collected for developmental anatomy from the three primary trees in the Belair Provincial Forest and put directly into glass vials of fixative at regular intervals from May 1996 to April 1999. Later in the lab, samples were dissected into shoot tips or individual buds. Sampling was done every 3-7 days during the warmer months and at monthly or bimonthly intervals once daytime temperatures dropped below 0°C. Two primary fixatives were used at each sampling: 3% glutaraldehyde and Karnovsky's (Appendix 8.1.1), both in 0.025 M potassium phosphate buffer, pH 6.8 (Appendix 8.1.2). Primary fixation was at ambient temperature for the initial two hours followed by vacuum aspiration to aid fixative penetration. Continued primary fixation was at 2-4°C at least overnight or until further tissue processing.

Mature pollen for germination experiments was taken directly from dehiscing anthers on each of the ten brooms, in the spring of 1998, and placed onto one of two agar media (Appendix 8.1.3) in sterile Petri dishes. The method of application changed depending on weather conditions (Table 3.1). The same ten brooms were sampled four times each at weekly intervals from the beginning of anthesis, until the staminate mistletoe flowers began to abscise from shoots. Two replicate samples were taken for

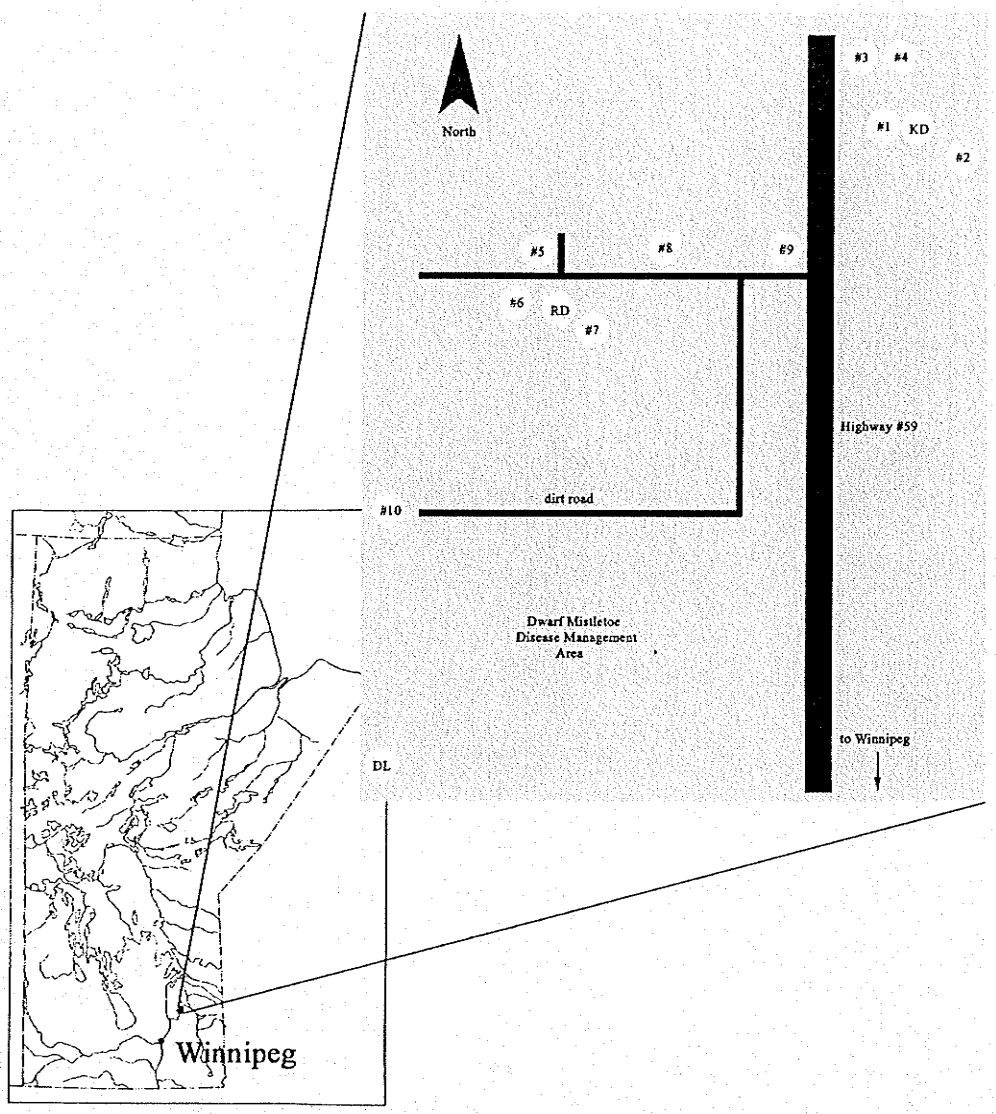

Figure 3.1 Location of the study site at the Dwarf Mistletoe Disease Management Area, Belair Provincial Forest, Manitoba and the positions of the infected trees relative to one another, which were sampled for developmental anatomy (KD, RD, DL) and pollen germination (#1-10), at the Dwarf Mistletoe Disease Management Area. The maps are not to scale.

each treatment and broom combination for the first three samplings, and three replicates each for the May 11 sampling. Inoculated dishes were kept at ambient temperature in the dark, until placed into incubators in the laboratory.

Table 3.1 Sampling dates, numbers of replicates, grains counted per treatment, and the methods used for the application of fresh *Arceuthobium americanum* pollen grains to the agar germination media in the field, in 1998.

Sampling date	Application method	Reps per treatment	Grains counted/plate	Total grains counted
20-Apr	in field, brush with alcohol between	2	300	600
27-Apr	in field, brush with no alcohol between	2	300	600
04-May	shoots air-dried 36 hrs, brush, no alcohol	2	300	600
11-May	48 hrs in closed vials, brush, no alcohol	3	100	300
18-May	no dehiscing flowers found	0	0	0

Mature pollen was also collected for scanning electron microscopy (SEM) images. In the field on April 16, 2001, the contents of dehiscing anthers from dwarf mistletoe flowers on the DL tree were squeezed into 5 mL glass vials containing either Karnovsky's fixative or 3% glutaraldehyde (Appendix 8.1.1) in 0.025 M potassium phosphate buffer, pH 6.8 (Appendix 8.1.2). The initial two hours of fixation were at ambient temperature, and then samples were placed into a 2-4°C refrigerator overnight until further processing.

3.2 Developmental Anatomy

3.2.1 Light microscopy

Shoot tips and lateral buds were dissected, using a Wild Heerbrugg stereoscopic microscope, from the bulk of stem tissue and placed back into the same fixative for at least 24 hours before embedding. Some were separated into individual buds and others left as terminal shoot tips with three attached buds, a terminal and the next two lower laterals. Tissues were then washed three times in 0.025 M potassium phosphate buffer (Appendix 8.1.2) each change for 15 minutes. All tissue processing steps were conducted at room temperature, unless otherwise noted. Post-fixation was with 2% osmium tetroxide, in the same buffer, at 2-4°C for two hours in a refrigerator. This was followed by three 15 minute washes with Millipore-filtered (0.2 μm pore size), deionized, distilled water (DDW) and a serial dehydration with an ethyl alcohol series: 50%, 70%, 90%, 95% for 20 minutes each, and three changes of 100% ethanol for 10 minutes each. An absolute ethanol:propylene oxide (1:1) solution for 10 minutes, followed by three changes of 100% propylene oxide for 10 minutes each, accommodated the transition to Spurr resin (Appendix 8.1.4). Subsequent Spurr:propylene oxide ratios of 1:1 and 3:1

were allowed to infiltrate the samples for at least four hours or overnight on a Fisher Roto-Rack rotator. Three 100% Spurr resin changes on the rotator completed the infiltration. These were left for 24 hours each. The tissues were embedded in the final Spurr change in 44 mL aluminum pans to facilitate their later orientation for sectioning. Polymerization of the resin was achieved by placing the pans in a 65-70°C oven overnight.

For sectioning, the plastic discs were removed from the aluminum pans, and small pieces of plastic containing the embedded tissue were cut out using a jeweler's saw. These were mounted on flat-topped plastic stubs in the desired orientation with Lepage's epoxy. After drying overnight, the stubs were trimmed down to the desired tissue area using a Reichert-Jung TM60 pyramitome, a Dremel 332 grinder and razor blades.

Initially, 1.0-3.0 μm sections were cut using glass knives equipped with a water trough on either a Reichert OM U2 or a Sorvall JB-4 microtome and mounted on gelatin-coated slides (Appendix 8.1.6) using a glass microprobe. Sections were floated on droplets of Millipore-filtered DDW and dried a Fisher slide warmer set to 75°C. Sections were stained with crystal violet (Appendix 8.1.5) for initial observation at the light level. Selected slides were later stained with differential stains (Table 3.2, Appendix 8.1.5) in order to characterize the general cytochemistry. A Nikon Optiphot compound microscope, equipped with a 50 watt high pressure mercury lamp and an episcopic fluorescence attachment, was used to generate specific wavelengths of light. Blue light (495 nm) was obtained with a 410-485 nm excitation filter coupled with a 515W barrier filter, and ultraviolet (UV) light (365 nm) with a 330-380 nm excitation filter coupled with a 420K barrier filter. Photography was done on the same microscope equipped with a Nikon AFX automatic exposure meter and a Nikon FX-35 camera back loaded with 35 mm color slide film, either bulk-rolled Kodak 64T Ektachrome or commercially bought Kodak 400 ASA Ektachrome professional. Color slide images were digitized using a Polaroid Sprint Scan/35 LE scanner and digital plates made using Adobe Photoshop 6.0. Color photographic plates were printed on glossy ink jet photographic paper with an Epson Stylus Color 900 ink jet printer. Drawings were done with the aid of a camera lucida on a Leitz-Wetzlar compound microscope.

Table 3.2 Cytochemical stains (Appendix 8.1.5) and the types of macromolecules they differentially stain using specific colors of light (O'Brien & McCully 1981).

Stain	Page	Macromolecule stained	Light	Positive reaction
aniline blue	6.97	β-1,3-glucans, callose	UV	yellow fluorescence
aniline blue black	6.90	hydrolytic proteins healthy cells	white	dark blue to black light blue cytosol
calcofluor white M2R	6.97	β-1,4-glucans, cellulose or hemicellulose	UV	blue florescence
periodic acid Schiff's	6.83 6.90	insoluble polysaccharides with vicinal 1,2-glycol groups, hemicellulose, pectins, starch	white	dark pink to purple
sudan black B	6.84	lipids	white	blue-black to black

In order to minimize individual variation, aerial shoots from one infection (DL tree) in 1996 were primarily used for developmental observations. The timing and sequence of key phenological events was confirmed by and compared to the other two infections (KD and RD trees), and samples collected in the other two years (1997 and 1998).

3.2.2 Transmission electron microscopy

Which samples were selected for transmission electron microscopy (TEM) was determined by observations made at the light level. Specific stubs were trimmed down further using a double-edged razor blade and ultrathin gold sections (100 nm) were cut using a Diatome diamond knife on a Reichert-Jung Ultracut microtome. Sections were mounted on uncoated 75/300 mesh copper grids and stained for 20 and 10 minutes with uranyl acetate and lead citrate, respectively (Appendix 8.1.5). The grids were washed three times with boiled, cooled DDW after each staining step and allowed to air dry before observation.

Initially, only the original samples were sectioned, but later, additional samples were processed and embedded specifically for TEM. An alternate potassium-ferricyanide method enhances membrane visibility in the electron microscope (Hepler 1981). Mature buds were fixed in cacodylate-buffered glutaraldehyde (Appendix 8.1.1) for two hours at room temperature and then placed in a 2-4°C refridgerator overnight. All subsequent

steps were done at room temperature unless otherwise noted. Samples were next washed with cacodylate buffer (Appendix 8.1.2) three times for ten minutes each wash and then post-fixed in osmium tetroxide-potassium ferricyanide (Appendix 8.1.1) for four hours in the refrigerator. Each sample was then thoroughly washed with DDW five times for ten minutes each. An additional three water washes were done with the vials on the rotator for 3-5 minutes, to ensure all fixative was removed. *En bloc* staining was done by submersing each sample in an aqueous solution of 0.5% uranyl acetate (Appendix 8.1.5) for 5.5 hours in the refridgerator. Samples were washed three times with DDW again for 20 minutes each, and then dehydrated with an ethanol series; 30%, 50%, 70%, 90%, 95% for 20 minutes at each step. Processing was stopped at the 30% step, and samples stored in the refridgerator overnight and continued the following day. Dehydration was completed by three changes of 100% ethanol for ten minutes each. The samples were split into three groups from this point on, and embedded in three different plastics (Appendix 8.1.4). The first group was embedded in Spurr resin as previously described. The second group was embedded in LR White acrylic resin and the third in an ultra-low viscosity resin. The latter two sets were immersed in a 1:1 mixture of plastic:ethanol for 30 minutes on the rotator, and then a 3:1 (plastic:ethanol) overnight. Three changes of 100% plastic for eight hours each completed the infiltration. Polymerization of both of these resins was achieved by placing the pans in a 60°C oven for 24 hours. Ultrathin sections were cut of these samples as previously described and grids stained for ten minutes with lead citrate (Appendix 8.1.5), then rinsed three times with boiled, cooled DDW, and allowed to air dry before observation.

TEM observations were done using a Hitachi H-7000 electron microscope at an accelerating voltage of 75 kV, and with an objective aperture of 40 μm. Images were recorded onto 3 $^{1}/_{4}$" x 4" Kodak electron microscope film (Estar thick base #4489) and later printed on medium weight, glossy Ilford multigrade IV RC deluxe photographic paper. Enlargements were made using a Simmon-Omega point source enlarger. Prints were digitized using a UMAX Astra 3450 flatbed scanner and imported into Adobe Photoshop 6.0 for photographic plate construction. Black and white printouts were done with glossy ink jet photographic paper and an Epson Stylus Color 900 ink jet printer.

3.2.3 Scanning electron microscopy

The content of vials of pollen fixed in Karnovsky's or glutaraldehyde were transferred to 1.5 mL Eppendorf tubes together with rinses of each using extra phosphate buffer. Tubes were centrifuged in an IEC Micromax centrifuge for five minutes at 15,000 rpm, and with care not to disturb the pellet, the supernatant of each was discarded. The contents of one sample were then recombined into a single Eppendorf tube, again rinsing with buffer. Tubes were allowed to sit for ten minutes and centrifuged as above. This process of centrifugation and supernatant removal was repeated for the following dehydration series, using an adaptation of techniques described by Hayat (1978), Lynch and Webster (1975) and Nickerson *et al.* (1970). Each step lasted ten minutes at room temperature, except where otherwise indicated.

Fixative
Potassium phosphate buffer washes x 3
2% OsO_4 in phosphate buffer, pH 6.8 (two hours in a 2-4°C refrigerator)
Distilled water washes x 3
Ethyl alcohol 10%, 20%, 30%, 40%, 50%, 70%, 90%, 95%, 100% x 3

Samples were stored in a 2-4°C refrigerator overnight at the 70% ethanol stage and processing continued the following day. In order to compare six different fixation protocols (Table 3.3), OsO_4 was not used for some of the samples. Two additional samples of pollen, collected the same day as the fixed samples, were allowed to air dry for a week, and simply rinsed and centrifuged in either 100% acetone or ethanol.

After the last centrifugation, samples were resuspended in 100% ethyl alcohol (one in 100% acetone) and vacuum filtered using 47 mm diameter filters (Sartorius-membranfilter GMBH), with a 0.45 μm pore size), in a Buchner funnel. The Eppendorf tubes were rinsed with additional solvent and filtered to recover as many pollen grains as possible from each sample. The filter papers were placed into sterile disposable petri dishes and allowed to air dry overnight in a desiccator.

The following day, aluminum SEM stubs were prepared by cleaning them with 100% acetone in a Mettler Electronics ultrasonic cleaner for ten minutes. Using clean forceps, stubs were removed from the acetone, blown dry with filtered air and placed in a holder. Double-sided sticky tabs were then applied to each stub. Using clean forceps,

each stub was picked up and placed, sticky side down, on one of the pollen containing filter papers. For each stub, this was done in at least three locations on a filter paper. Stubs were then replaced in the holder and the entire holder was put back into the dessicator overnight at room temperature.

Table 3.3 Six fixative combinations used in the processing of whole, mature *Arceuthobium americanum* pollen grains for scanning electron microscopy.

Primary Fixative	Secondary Fixative
Karnovsky's	osmium tetroxide
Karnovsky's	none
glutaraldehyde	osmium tetroxide
glutaraldehyde	none
air dried	100% acetone
air dried	100% ethanol

In the SEM lab, stubs were placed under vacuum (~4 bars), and coated with gold-palladium (100-200 nm thick), using argon gas as a carrier in an S150B Edwards Sputter Coater. Samples were viewed immediately on a Cambridge Instruments Stereoscan 120 scanning electron microscope at an accelerating voltage of 20 kV, and selected images saved via a Kontron electronik IBAS Image Analyzer. Scanned images were transferred to a PC-formatted 100 zip disk as *.gif files and plates made using Adobe Photoshop 6.0. Printing of images was done as previously described.

Observation of scanning electron microscopy images showed that air dried samples which had only one rinse of either 100% alcohol (Figure 3.2) or acetone (Figure 3.3) were not as clean as any of the other protocols. Debris on the surface of the grains was quite common. These two samples also had a higher frequency of collapsed grains (not shown) and large clumps of grains were often seen. The collapse of grains fixed by air drying and either 100% ethanol or acetone is probably due to the lack of a gradual dehydration. Neither of these solvents removed the material holding grains together thus the observation that grains tended to be found in clumps. Karnovsky-fixed pollen also tended to be found in groups (Figure 3.4), with extracellular material connecting individual grains, but debris was less of a problem. Both sets of samples post-fixed with

osmium tetroxide exhibited charging problems while in the SEM, and occasionally specimens exploded while under the electron beam and/or exhibited swellings (Figure 3.5). Samples fixed with osmium tetroxide may have had irregular deposition of the heavy metal, and this could account for the charging problems exhibited by these samples while in the SEM. Other types of cells were a frequent occurrence in these samples (Figure 3.6). Cells other than pollen grains were also seen in TEM samples; and these cells had an intact nucleus and numerous starch grains (Figure 3.7).

Figure 3.2 Scanning electron micrograph of a group of mature pollen grains air-dried and rinsed in 100% ethanol. Numerous pieces of extraneous debris (small white arrows) were present on and between the grains.. Scale bar 20 μm.

Figure 3.3 Scanning electron micrograph of a mature pollen grain air-dried and rinsed in 100% acetone. Numerous pieces of extraneous debris (small white arrows) were present on the grains. Scale bar 10 μm.

Figure 3.4 Scanning electron micrograph of mature pollen grains fixed in 3% glutaraldehyde and 2% osmium tetroxide showing spines (small white arrows) and swellings (large black arrowhead) on the grains which appeared while grains were being observed. Scale bar 20 μm.

Figure 3.5 Scanning electron micrograph of a group of mature pollen grains fixed only in Karnovsky's fixative showing extraneous material (small white arrows) holding grains together. Scale bar 20 μm.

Figure 3.6 Scanning electron micrograph of other cells commonly seen with the Karnovsky fixed, ethanol dehydrated pollen grains. Scale bar 20 μm.

Figure 3.7 Transmission electron micrograph of other cells commonly seen with the Karnovsky fixed, ethanol dehydrated pollen grains. These uninucleate (medium black arrow) cells contained numerous starch grains (large white arrowheads). Scale bar 3 μm.

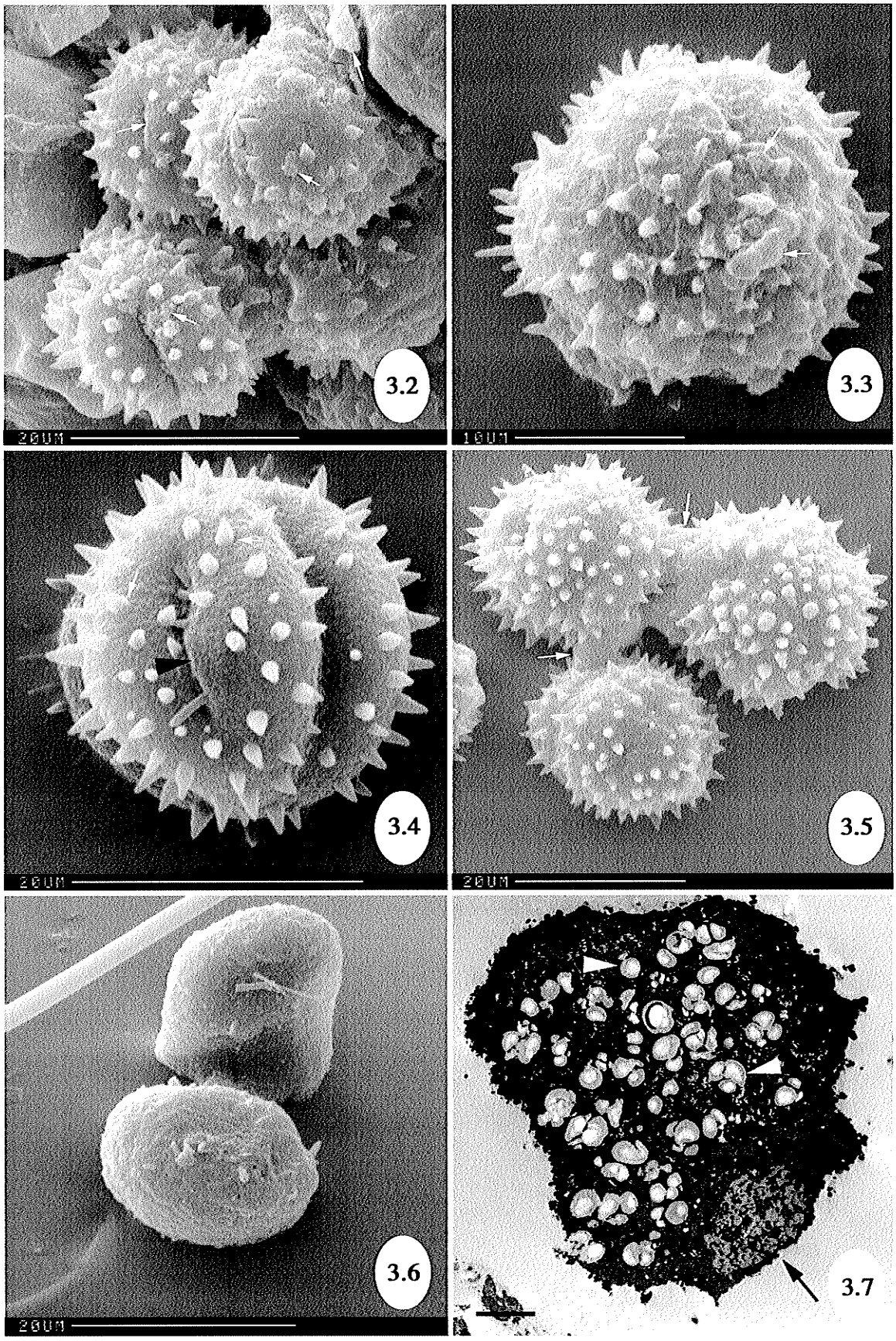
3.2
20UM
3.3
10UM
3.4
20UM
3.5
20UM
3.6
20UM
3.7

3.3 Pollen Germination

3.3.1 Environmental conditions and media

Pollen germination media contained either 15 or 20% sucrose in an aqueous, semi-solid medium (Appendix 8.1.3). Dishes were incubated at either 20 or 30°C in the dark. Percent germination and pollen tube length were determined after 48 hours, and the criterion of germination is if a pollen tube is at least as long as the diameter of the grain (Gilbert & Punter 1991). If observations could not be done immediately samples were removed from the incubator and held in a 2-4°C refrigerator pending analysis.

Measurements were done using an Olympus SZH stereoscopic microscope. Pollen grains were stained by pipetting three drops of basic toluidine blue O (Appendix 8.1.5) onto the edge of the agar surface. Three mL of tap water was quickly added and each dish swirled for 30 seconds to circulate the stain. The stain was then poured off and the dish inverted over a paper towel for a few minutes to allow it to drip. Dishes were recovered and stored in the refrigerator pending observation. Staining of grains was improved by allowing dishes to sit for at least 30 minutes at room temperature. Pollen grains were stained dark green to blue on a pale blue background. Contaminating fungal hyphae were easily distinguished from pollen tubes of germinated grains, as the former took on a dark blue color, whereas pollen tubes remained an opaque white. Fungal spores mostly did not stain.

3.3.2 Measurements and analysis

Three hundred grains were counted on each of two dishes for the first three sampling dates and 100 on each of three dishes for the last sampling date. Counts were averaged and reported as mean percent germination. The length of the pollen tube was measured for all germinated grains, using an eyepiece reticle. These optical units were later converted to μm by calibration of the optical scale with a micrometer slide.

4.0 RESULTS & DISCUSSION--DEVELOPMENTAL ANATOMY

4.1 Microsporogenesis

4.1.1 Stamen initiation and development of the microsporocytes

Once anthesis and the dehiscence of pollen finishes in the spring, staminate flowers abscise, and the vegetative meristem (Figure 4.1) reverts almost immediately to the production of flowers for the next season. The vegetative meristem is dome shaped, and has a tunica-corpus arrangement (Figure 4.2) with leaf primordia overarching the shoot apex. Shoot tips with developing inflorescences consist of a single terminal bud with two lateral buds just below in an opposite arrangement (Figure 4.3). Taller stems also possess additional sets of buds below these laterals, and if present are decussate to the first set of laterals.

Conversion to a floral meristem is indicated by the alteration of the apex to a flattened shape (Figure 4.4). In 1996, the production of perianth segments overarching the meristematic tissue, is observed in late May. By early June, these further elongate and in longitudinal-section (LS) a space within the floral bud is apparent above the stamen primordia (Figure 4.5). A cross-sectional (CS) view (Figure 4.7), however, shows the three stamen primordia to be quite closely fitted together. At this time, anticlinal (Figure 4.6) and periclinal (Figure 4.8) divisions, of the parietal and protodermal cells respectively, still occur. These divisions eventually result in a uniseriate outer epidermis and a primary parietal cell layer surrounding a cluster of hypodermal sporogenous cells (Figure 4.9) by late June. The sporogenous cells stand out from the surrounding tissues because of their lack of a large vacuole, darker staining cytoplasm and large nuclei with prominent nucleoli (Figure 4.6).

Continued mitotic divisions result in a single region of sporogenous cells (Figure 4.10), and appear as a horseshoe or oval shape, depending on the plane of section. In early July, the sporogenous tissue is covered by three cell layers on the adaxial side of the anther. From inside to outside, these are the tapetum, middle layer and epidermis. A well-developed nectary is also present in the center of the floral axis by this time. At this stage of development, other cell types are also present. Vacuolate cells are fairly common, especially within the tapetum and epidermis (Figure 4.11), as well as cells filled

with crystals of phenolic or tannin-like compounds. Still others have heavy depositions of lignin-like compounds around their periphery (Figure 4.12).

In samples collected in July and August terminal and lateral buds are not always at the same stage of development. Often the lower laterals lag behind the development of the terminal bud. Vegetative growth and development, however, appears to be continual as evidenced by observations in early August, of axillary buds further down the stem containing leaf primordia and a vegetative apical meristem. These buds continue to grow into the fall and will presumably produce the following year's staminate flowers (Figure 4.13).

Meanwhile in more distal flowers proliferation of the reproductive tissue continues (Figure 4.14). The epidermis, middle layer and tapetum are all uniseriate on the adaxial surface of the anther, but two and sometimes three cell layers thick in areas towards the base of the anther's connection to the perianth. The sporogenous cells are tightly fitted together with prominent nucleoli and well-defined cell walls, and in longitudinal section are polygonal in shape (Figure 4.15). In a cross-sectional view of the anther however, these cells are elongate (Figure 4.16). They continue to divide well into August and contain starch grains as well as vacuoles with lignified regions at this time. The highly active nature of both the tapetal and sporogenous cells is demonstrated by their intense protein staining ability, evidence of abundant enzymatic activity (Figure 4.17).

When mitotic divisions of the sporogenous cells cease, anthers are at their maximal size. The eventual three-dimensional shape of the microsporangium can be described as a cup shape lying on its side surrounding a central region of sterile, parenchymatous cells called the columella. There has been some disagreement between authors on this point, but has probably arisen because two dimensionally, the shape of the locule can appear to be a horseshoe or an oval shape, depending on the plane of section (Figure 4.13). Dowding (1931) also noticed variation in the extent of the columella. Her drawings show it as a central pillar within the anther surrounded by a ring of sporogenous tissue, but also extending from the center to one or both extremities of the mature anther, thereby dividing the anther locule in half. This is consistent with that observed in serial sections through an entire anther.

The early sequence of development is similar to that observed in *Phoradendron* Nutt. (American mistletoe, Viscaceae). The first indication of the development of archesporial tissues in *Phoradendron* is the elongation of a few hypodermal cells. Periclinal divisions of a hypodermal initial, resulting in an inner primary sporogenous cell and an outer primary parietal cell, follow. Continued divisions of the sporogenous cells produce a proliferation of the future microsporocytes. Other periclinal divisions of the outer cells result in several layers around the sporogenous cells (Billings 1932). The sporogenous tissue of a more closely related species, *Arceuthobium minutissiumum* (Indian dwarf mistletoe, Viscaceae), also originates as a single horseshoe shaped region around a central columella. Bhandari and Nanda (1968) described a young anther as consisting of an epithecium, one middle layer and a uniseriate tapetum surrounding the microspores. This is remarkably similar to that observed in *A. americanum*, although the layer which they refer to as the epithecium appears to be the epidermis with wall thickenings, and is more correctly called an exothecium. The use of the term epithecium is most likely a translation error or the authors created their own term.

I agree with the developmental argument presented by Johnson (1888) of the perianth-anther nature of *Arceuthobium americanum* staminate flowers. Anatomically, the leaf-like perianth segments develop first (Figure 4.4) followed by the initiation of anther primordia at the floral apex (Figure 4.5), and not on the surface of the perianth. The anther itself originates laterally as a multicellular outgrowth of the floral apex, separate from the associated perianth segment, and the two later fuse via intercalary growth. This evidence convinced Johnson (1888) of the fused nature of the perianth-anther, rather than foliar stamens of one phyllome.

Floral abnormalities are also evidence for the independence of these two floral structures. Most male flowers of *A. americanum* are trimerous (Figures 4.58, 4.59), but it was not uncommon to see terminal flowers with four perianth segments (Figure 4.60), and occasionally these had only three anthers instead of four. Two of the anthers would be in their usual sessile location on the surface of their associated perianth segment, and the third would be located partially in the gap between the two opposite perianth segments. Rarely, dimerous flowers were also seen, and in this case, the perianth

segments were larger than usual and more rounded, as though two normally shaped perianth segments of a tetramerous flower had merged during their development. Johnson (1888) also occasionally observed staminate flowers with only two anthers, but three perianth segments. She described the anthers as being positioned opposite one another, meaning if one is centrally located on a perianth segment, the other would have to be in the space between the opposing two perianth leaves, as observed for the abnormal tetramerous flowers. This does not, however, indicate a recent anatomical change, as macroscopic remains of *Arceuthobium* have been recovered from Miocene deposits. Male flowers in these samples were three or four parted, and each perianth segment bore a unilocular, sessile anther (Lancucka-Srodoniowa 1980).

4.1.2 Microsporocyte and anther wall development

Once mitotic divisions have ceased in mid-August, the sporogenous cells are referred to as the microsporocytes or microspore mother cells. At this stage, a vacuolate epidermis surrounds the smaller, flattened cells of the middle layer, which in turn surrounds a uninucleate tapetum and the sporogenous tissue. Morphological changes in the tapetum are becoming apparent, such as the presence of large vacuoles within the tapetal cells (Figure 4.18). Tapetal cytoplasm, however, is dense and TEM examination shows these cells to be quite organelle-rich, even those with large central vacuoles. In addition to intact nuclei, stacks of ER, mitochondria and vesicles are very common (Figure 4.19). Also quite commonly seen are vacuolated cells in all of the outer anther tissues (Figure 4.20). Many of these cells contain crystalline phenolics (Figure 4.21).

At the onset of prophase I of meiosis, a slight plasmolysis of the microspore mother cells is observed (Figure 4.22). Intercellular spaces develop between the individual microsporocytes and between them and the anther wall as the locule expands (Figure 4.23). Adjacent microspore mother cells, however, still retain some contact with one another. Large nucleoli are commonly observed within cells, suggesting they are synthetically active (Figure 4.24). Cell walls still persist between individual cells, but microsporocytes have cytomictic channels (Figure 4.25) of varying sizes in their walls (Figure 4.26). Some of these channels, for example, are large enough for mitochondria to pass between individual cells, as well as other cytoplasmic materials (Figure 4.27).

Lilium, for example, has channels as large as 2 μm (Bhojwani & Bhatnagar 1988). Pollen mother cells of *Acorus* L. (sweet flag, Araceae) also have cytomictic channels, and there is evidence of organelles passing through them (Duvall 2001). Bhojwani and Bhatnagar (1988) propose that cytomictic channels promote synchronous meiosis of the microsporocytes. *Catananche caerulea* L. (Cupid's dart, Asteraceae), however, does not have synchronous meiosis despite the occurrence of cytomictic channels, which persist until metaphase (Blackmore & Barnes 1988).

A slight separation of the tapetum from the inner surface of the middle layer also begins to appear (Figure 4.28). Cells of the middle layer are becoming crushed but still contain intact nuclei and cell walls at this time. TEM also reveals cytomictic channels in the cell walls between individual tapetal cells. When TEM sections are observed, two types of tapetal cells are seen (Figure 4.18) at the light level. It is possible that these are tapetal cells in differing states of preservation, but there is no plasmolysis of the protoplast and intact organelles are present within the condensed cytoplasm (Figure 4.19). As well, not all tapetal cells are affected. It has been suggested that 'degeneration of the tapetum' is not the best way to describe tapetal change since this is really programmed cell death. Santos *et al* (2003) propose instead that, 'senescence of the tapetum', would be a more accurate description.

Observations on August 22 show the microsporocytes have become quite oval (Figure 4.29), and a thick cell wall positive for callose (Figure 4.31) has developed. Intercellular spaces have also further increased between individual cells as they become more spherical. As meiosis proceeds, plasmolysis of the microsporocytes becomes more pronounced and the periplasmic space and intercellular spaces between cells continue to enlarge (Figure 4.30). The periplasmic spaces appear to be entirely void of cytoplasmic materials. A central columella is present with connections to the anther wall by cells which appear to be tapetal in origin (Figure 4.29). This agrees with the suggestion of Dowding (1931), although she proposes tapetal extensions dividing the anther into four sporangia, and I have only seen divisions into two.

Vacuolated cells in the anther wall are still present (Figure 4.35), but less common than previously (Figure 4.29). Perhaps they have released their contents into the locule,

as one of the important functions of the tapetum is supplying nutrients to the developing sporogenous tissue (Bhjowani & Bhatnagar 1988). Despite being crushed, cells of the middle layer still have intact cell walls and nuclei (Figure 4.35). Cytoplasmic channels between microsporocytes persist (Figure 4.36) although the cell walls have thickened considerably (Figure 4.37). Other species, such as *Iris pallida* Lam. (European iris, Iridaceae), have also been observed to possess cytomictic channels just before meiosis (Lippi *et al.* 1994).

The large periplasmic space between the intine and microspore plasmalemma can be interpreted to be a plasmolysis artifact. This could be due to a pH or osmotic change within the anther. Changes in the composition of *Lilium* anther locular fluid were related to developmental stage (Clément *et al.* 1998), and in *Petunia hybrida*, a drop in pH was noted at early meiotic stages (Izhar & Frankel 1971). Since the same pH and osmolarity of buffer fixative were used for all stages, any changes within tissues could cause variable preservation of cells. In *Callitriche truncata* this seems to be more pronounced in tetrads than in either free microspores or mature grains (Osborn *et al.* 2001), whereas in *Arceuthobium americanum* the microsporocyte stage is more affected. The poor preservation of particular stages may be because they are pH or osmotically sensitive and a slight plasmoloysis of the protoplast during fixation results in this phenomenon.

By late August meiosis has concluded and tetrads of microspores are found (Figure 4.32) surrounded by callose-rich walls (Figure 4.38, 4.39). Cytokinesis appears to be simultaneous, as no evidence of dyads is seen. Prophase I is followed quickly by the appearance of tetrahedrally arranged tetrads, and an infurrowing of the new cell wall (Figure 4.32). This arrangement of microspores also suggests that cytokinesis is simultaneous. The meiotic event could occur quite rapidly as observed by Cohen (1968). In this study, anthers of *Arceuthobium americanum* with degenerated contents are first observed at this stage. Most have a complete epidermis and middle layer surrounding some tapetal tissues and an otherwise empty locule (Figure 4.33). Others have a partially crushed middle layer and some remnant microsporocytes with thickened cell walls (Figure 4.34), evidence that development was arrested at a later stage of development.

Observation of an anther with degenerated contents is not necessarily evidence of a cytoplasmically male sterile plant. Temperature, osmolarity, pH and the timing of fixation can all affect the preservation of tissues. Improperly fixed samples would show varying degrees of tissue degeneration (O'Brien & McCully 1981). Additionally, the micrographs used in this study are all from a single tree. Assuming a single infection, all samples would have the same genotype, so one would suppose all to be either sterile or fertile. There are some instances, however, of fertile genotypes producing cytoplasmically sterile anthers under adverse environmental conditions (Suzuki *et al.* 2001). It is also common for cytoplasmic male sterility problems to exhibit themselves around the time of the meiotic event (Kaul & Nirmala 1991).

The timing of meiosis was not identical for all three years sampled and could be due to a difference in weather conditions. Temperature in particular can have dramatic effects on developmental processes. In *Mangifera* L. (mango, Anacardiaceae) the duration of microsporgenesis decreases as ambient temperature increases (Issarakraisila & Considine 1994), but heat stress induces male sterility in *Phaseolus vulgaris* L. (snap bean, Fabaceae). The first indication was an alteration in the normal distribution pattern of stacks of ER in tapetal cells (Suzuki *et al.* 2001). Temperature is also known to influence pollen development in more closely related species. When male flowers of *Phoradendron* collected in the fall and winter were compared with those collected in the spring, many abnormalities, and on occasion, complete abortion of the sporogenous tissue was observed. Billings (1932) proposed that either unfavorable temperatures or poor nutrition was responsible. .

In another study, water stress caused abnormal development and ultimately the abortion of pollen grains in normally fertile plants of *Triticum aestivum* L. (wheat, Poaceae). The earliest effects were detected at the time of meiosis (Lalonde *et al.* 1997). Photoperiod also affects microsporogenesis in *Oryza sativa* L. (common rice, Poaceae). In particular, abnormal tapetal development is believed to be the ultimate cause of male sterility (Jin-Hui *et al.* 1994).

By the last week in August the callose wall has disappeared and the resultant microspores with prominent nucleoli have separated (Figure 4.40). Initially, those from

the same tetrad remain in close proximity and have some remains of their thickened callose walls. As these walls break down the microspores become quite vacuolate (Figure 4.41). A fairly thin sporopollenin wall is now apparent around each microspore (Figure 4.42) and tapetal cells are now full of small vacuoles.

The source of callase and sporopollenin has long been proposed to be the tapetum (Bhojwani & Bhatnagar 1988). Vacuoles appearing within tapetal cells could be an indicator of synthetic activity at this time. As well, stacks of ER observed in tapetal cells are also evidence of their synthetic activity in *A. americanum* (Figure 4.19). The tapetum of *Catananche caerulea* releases finely beaded material presumed to be sporopollenin precursors (Barnes & Blackmore 1988).

Near the end of August is also when anthers of *A. americanum* with degenerated contents are first noticed (Figure 4.33, 4.34). Some of the wall layers are usually still intact, but the sporogenous tissues have been lost. These could be anthers of cytoplasmically male sterile plants, or just poorly preserved samples. Simply observing the anatomical loss of tissues is not proof of sterility. This is however, a common time period for sterile anthers to become evident (Kaul & Nirmala 1991). It is possible for the same genotype to exhibit sterile and fertile anthers, since environmental factors such as photoperiod and temperature can induce male sterility (Bhojwani & Bhatnagar 1988).

Degeneration of the fertile tissue occurred at the dyad or tetrad stage in a male sterile variety of *Iris pallida*. The researchers believed that morphological variation in the tapetum, was related to an altered physiological function (Lippi *et al.* 1994). Male sterile mutants of *Arabidopsis thaliana* L. (mouse-ear cress, Brassicaceae) also showed changes from normal microsporogenesis during microsporocyte meiosis. An early dissolution of callose by callase, released by stacks of rough ER in the tapetum, was hypothesized to be responsible. Normally, the callose layer remains until meiosis is complete and tetrads have formed (Fei & Sawhney 1999). Another study of the same species found pollen abortion occurred after microspore release. The tapetum in these anthers appeared normal. The sterility defect was related to the deficient activity of adenine phosphoribosyltransferase, and probably cytokinin metabolism (Mascarhenas 1989).

Other evidence of the importance of the tapetum in normal development is that male sterile mutants of *Zea mays* were found to produce an abnormal five layered anther wall. A fourth periclinal division of the secondary parietal layer resulted in a biseriate tapetum that did not differentiate normally. Shortly after this event the pollen mother cells became encased in a callose wall, but failed to undergo meiosis, and subsequently aborted (Chaubal *et al.* 2000). This finding supports a role for the tapetum early in the developmental process.

An abnormal tapetum is not always the cause however of male sterility. There are vulnerabilities throughout the developmental process. Male sterility both in *Hordeum vulgare* and *Pisum sativum* L. (garden pea, Fabaceae), for example, is caused by several different nuclear or cytoplasmic genes, each differing in the stage of development it affects. Either viable pollen fails to develop, or if viable, is not released. In all cases, the ultimate consequence is the same, namely a structurally or functionally male sterile plant (Kaul & Nirmala 1991).

Anther wall development in *Arceuthobium americanum* appears to be a variation of the reduced type of anther wall ontogeny (Bhandari 1984, Davis 1966). Cohen (1968) essentially described this process but did not name it as such. Mitotic divisions of the hypodermal archesporial cells result in a primary parietal layer surrounding a single region of sporogenous tissue within each anther (Figure 4.5). A second mitotic event by the primary parietal cell layer produces an outer ephemeral middle layer and an inner layer that develops directly into the tapetum (Figure 4.10).

The middle layer is gradually crushed as the sporogenous cells continue to proliferate via mitotic divisions (Figure 4.14, 4.21). While microsporocytes are enclosed in their callose-rich wall, nuclei within the cells comprising the middle layer are still evident pressed against the inner surface of the epidermis (Figure 4.30), but by the time meiosis occurs, the middle layer of cells is almost completely crushed. This is common in many anthers, although the timing of the degeneration of the middle layer(s) may differ. *Diospyros choroxylon* Roxb. (East Indian ebony, Ebenaceae) and *D. virginiana* L. (common persimmon, Ebenaceae), for example, both have two middle layers which are only beginning to be crushed by the time meiosis of the microspore mother cells occurs.

Eventually these ephemeral layers appear to be completely absorbed (Anjaneyulu & Lakshminarayana 1989), as do those of *Arceuthobium americanum.*

The epidermis develops thickenings and dehisce via a transverse slit to dehisce pollen. It therefore should be called an exothecium (Dowding 1931, Gill 1935, Thoday & Johnson 1930). An endothecium, which normally functions in anther dehiscence, is lacking in *A. americanum.* This agrees with reports for other species in this genus (Bhandari & Nanda 1968, Cohen 1968, Dowding 1931, Johnson 1888, Thoday & Johnson 1930).

4.2 Microgametogenesis

4.2.1 Microspore maturation

After separation, microspores contain nuclei with prominent nucleoli (Figure 4.40), and as they mature appear to dehydrate and become more cytoplasmically dense as well as less vacuolate (Figure 4.42). The most noticeable change however, is their rapid increase in size from approximately 9 μm just after separation (Figure 4.40), to 20 - 25 μm in diameter at the time of the first mitosis (Figure 4.43). This occurs in late August or early September. An increase in size of the uninucleate microspores before mitosis has also been reported in other genera. This has been observed for example in *Agave fourcroydes* and *A. angustifolia* Haw. (Caribbean agave, Agavaceae) (Piven *et al.* 2001).

TEM examination of a uninucleate microspore in a median cross section demonstrates the difference between the true colpae and the pseudocolpae. The intine is thicker beneath each of the three apertures (Figure 4.50), but is uniform under the pseudocolpae. Above apertures the exine thins considerably, and remains a constant thickness elsewhere on the surface of the grain. A differing density within both the intine and exine reveals their layered nature (Figure 4.51).

The tapetum has begun to degenerate and extraneous material, presumably from this secretory tapetum, is seen between grains within the locule (Figure 4.43). On the inner surface of the tapetum many orbicules (Figure 4.52) and other more amorphous tapetal extrusions (Figure 4.53) are present. Both contain small tubular pieces, as well as larger, osmiophilic material. High magnification examination reveals that some of this larger material has a crystalline protein structure (Figure 4.54).

Orbicules and tubular structures are observed in other genera as well. In *Iris pallida*, many orbicules were seen on the locular surface of the tapetal cells at the free microspore stage (Lippi *et al.* 1994). During the uninucleate microspore stage of *Vigna vexillata* (L.) A. Rich. (wild mung bean, Fabaceae), Pérez-Muñoz *et al.* (1993) observed abundant tubules of smooth ER and patches of microtubules beneath apertures, as well as other membranous structures they called multimembrane inclusions. They proposed the smooth ER and microtubules could be involved in the synthesis and transport of the primexine, but suggested the multimembrane inclusions were either chemical fixation artifacts or participated in the development of the exine. The tapetum is believed to be the source of sporopollenin precursors that polymerize to produce the acetolysis resistant exine (Bhjowani & Bhatnagar 1988).

Initially after mitosis, both nuclei are centrally located, and round in sectional views, in this case, spherical three-dimensionally (Figure 4.43). A fairly central cell wall is present between the two nuclei, and the outer wall of the young binucleate grain has thickened considerably. This is unusual. Typically, in most other genera, the generative cell is not centrally located after mitosis. In *Gentiana macrophylla* Bertol. (long-leaf gentian, Gentianaceae), for example, the smaller generative cell is at first closely associated with the wall of the young microgametophyte. The generative cell only later moves into the central region within the vegetative cell (Huijuan & Yaozhi 1994).

A day or two later, morphological changes are seen in the two nuclei (Figure 4.44). The vegetative nucleus becomes slightly elongate in shape, whereas the generative nucleus now has a complete cell wall around it, and is contained completely within the vegetative cell. Both nuclei, however, tend to remain centrally located, although occasionally generative cell walls are seen close to the wall of the developing microgametophyte at this stage.

Organelle segregation before mitosis is an important mechanism of controlling inheritance patterns in angiosperms (Mogensen & Rusche 2000, Southworth 1996). Although mitochondria and plastids have been observed within sperm cells, typically they are not organelle-rich, and if organelles are present, they are not necessarily inherited. Often the cytoplasm and its contents are excluded from contact with the egg

cell at the time of syngamy (Southworth 1996). The transmission of plastids during syngamy still does not guarantee their inheritance, as they are not always expressed in the zygote (Russell & Cass 1981).

Tapetal material is still observable at the periphery of the anther locule and is interspersed throughout the locule itself, although it no longer has a cellular appearance. This is often the time when secretory tapeta degenerate. Programmed cell death of the tapetum is finished by the time pollen is mature in *Oryza sativa*. Morphological signs of apoptosis are cytoplasmic shrinkage, membrane blebbing and vacuolation of cells (Ku *et al.* 2003).

Floral buds with encompassing perianth segments are still completely closed (Figure 4.45) in mid-September, as is the last remaining layer of the anther wall, the epidermis (Figure 4.46). The young pollen grains walls are composed of a spiny exine and a thick underlying intine (Figure 4.47), at this time. In some anthers the generative cell has also undergone a small enlargement and shape change. The generative nucleus is still round, but cytoplasmic extensions of the generative cell are quite obvious in many microgametophytes (Figure 4.48). The vegetative nucleus is fairly elongate and the two nuclei are in close proximity near the centre of pollen grains which also contain many starch grains (Figure 4.49). This is the stage at which pollen grains within the male floral buds overwinter in *Arceuthobium americanum*, at least for the Belair population in Manitoba.

When TEM sections of mature grains are examined, a somewhat electron opaque material is observed covering the surface of the grain (Figure 4.55). This is probably pollenkitt. As well, in apertural regions, small tubular structures are seen at the level of the intine occluding the apertural gap and just above the external surface of the aperture itself. Both of these materials are likely to be tapetal in origin. The tubular structures are quite similar in size and appearance to those seen in orbicules (Figure 4.52) and tapetal extrusions (Figure 4.53) at the uninucleate microspore stage of development. Starch grains seen at the light level (Figure 4.49) are found within amyloplasts in TEM sections (Figure 4.55).

The choice of chemical fixation regime can have a profound effect on the preservation of some components. Glutaraldehyde plus a combination of potassium ferricyanide and osmium tetroxide seems to effect better fixation than glutaraldehyde and osmium tetroxide alone (Hepler 1981). Santos *et al.* (2003) believed their observation of lipidic pollenkitt precursors originating from plastids and ER in tapetal cells of *Ilex paraguariensis* St.-Hil. (Paraguay tea, Aquifoliaceae) was due to the use of this chemical fixation scheme. A potassium ferricyanide/osmium tetroxide fixative was used for those samples of *A. americanum* in which the small tubular structures and a thick coating of pollenkitt over the grain's surface were observed (Figure 4.55). These components were not always present on samples fixed in glutaraldehyde/osmium tetroxide alone.

4.2.2 Mature pollen

Mature pollen grains are present within the anther's locule by mid-September the year previous to anthesis (Figure 4.45). Floral buds remain closed and the microgametophytes overwinter as bicellular grains. Weather conditions and particularily ambient temperatures are the most likely cue for anthesis the following spring (Hawksworth & Wiens 1996). If temperatures fall below 0°C, and then rise above a certain threshold, a physiological trigger could initiate flowering. Indeed in the fall of 1998, some open male flowers, were observed on October 30 (personal observation). This was after a period of below 0°C temperatures followed by much warmer weather conditions.

In early May 1996, anthesis of *A. americanum* was observed at the Belair, Manitoba location. Not all flowers open at once. Anthesis and the release of pollen occurs generally over a three to four week period (Dowding 1931). Indeed while some male flowers were releasing pollen, other unopened floral buds containing mature pollen grains were observed (Figure 4.56). Mature pollen of *Arceuthobium americanum* is released at the two-celled stage of development (Figure 4.57, 4.62). The vegetative cell possesses a more elongate nucleus and also completely encloses the generative cell which has a more spherical nucleus.

The spherical shape of the generative nucleus is quite different from that reported for other angiosperms. Typically, the generative nucleus is described as being lenticular or

cup-shaped and that of the vegetative cell being more rounded (Bhojwani & Bhatnagar 1988, Brown & Lemmon 1992b). The cellular nature of the generative is more apparent in TEM views (Figure 4.66) where its cell wall can be clearly seen. The generative nucleus tends to be more spherical in shape (Figure 4.67), but has cytoplasmic extensions that make it appear slightly lenticular with the light microscope (Figure 4.66) Both mitochondria and plastids, as amyloplasts, were observed within generative cell cytoplasm (not shown). This has implications for cytoplasmic male inheritance patterns, as sperm cells often do not contain any DNA other than in the haploid nucleus (Bhjowani & Bhatnagar 1988).

The micro-morphology of whole grains (Figure 4.61) is consistent with descriptions of other species of *Arceuthobium* (Hawksworth & Wiens 1972). Samples fixed only in buffered glutaraldehyde show the best preservation of intact grains (Figure 4.63), with a minimum of debris on the surface of the grains and on the stub as a whole. Overall grain shape is spherical, with the equatorial dimension being slightly larger (<1 μm) than the polar diameter, but varies from grain to grain. Equatorial grain diameters measured on ten SEM images range from 16.4 - 22.8 μm with a mean of 19.4 ± 2.0 μm.

Spines range in height from 1.4 - 2.6 μm, with a mean of 1.7 ± 0.3 μm, and are distributed over the surface of the grains. Their width at the base is 0.8 - 1.4 μm, with a mean of 1.1 ± 0.2 μm (n = 15). Colpi running from pole to pole occasionally contain spines as well. The base of spines have a distinct rim to them, but the surface of the exine elsewhere is textured, much like rounded tiles tightly fitted together (Figure 4.64), which appear as short papillae in LS (Figure 4.68).

The six colpi are equidistant from one another around the circumference of the grain, and the three longer ones alternate with the three shorter ones (Figure 4.65). TEM observation of a median CS (Figure 4.66) shows two types of colpi to be present. The longer ones are true colpae, and have a thinner exine layer underlain with a thick intine plug, indicating they are the true apertures. The shorter colpi or pseudocolpae, as they are named by Hawksworth and Wiens (1972), have thicknesses of exine and intine similar to the rest of the grain, as seen in cross-sectional view. These are not true colpae.

Oblique sections through the longer grooves reveal differences in the thickness and types of exine and intine layers present throughout the length of a colpus (Figure 4.67).

Karnovsky-fixed SEM samples frequently contain clumps of pollen grains (Figure 3.5). These cells have extracellular material on their surface and also between individual grains connecting them. As well, a second type of cell without spines is seen fairly often in these samples (Figure 3.6). These cells have a diameter of about 15 μm and were slightly smaller than the mature grains. TEM sections of intact anthers at the same stage of development also contain cells without spines of around this size (Figure 3.7). These cells possess intact nuclei and abundant starch grains.

Debris observed on the surface of grains fixed with Karnovsky's could be pollenkitt or tryphine. Both substances are commonly found on the surface of mature grains (Greyson 1994), but are readily lost during regular processing regimes when loose pollen is used. The use of intact anthers containing mature pollen is best for the preservation of these materials (Heslop-Harrison 1976). The greater frequency of observation of groups of grains may also have been due to the preservation of pollenkitt, as it is known to aid in the adherence and therefore dispersal of grains of some species (Dickinson *et al.* 2000). Since *Arceuthobium americanum* is known to be partially entomophilous (Gilbert 1988, Player 1979, Wiens 1968) the presence of a persistent pollen coat is not surprising. The attraction of and adherence to insects for dispersal are possible functions of this material on the surface of grains. This observation is consistent with the fixation regime used, as the addition of para-formaldehyde to the Karnovsky's fixative may have preserved these lipid deposits better than glutaraldehyde alone. Although both are aldehydes, para-formaldehyde is a smaller molecule and is believed to penetrate and therefore effect fixation quicker than glutaraldehyde alone (Karnovsky 1965, O'Brien & McCully 1981).

The second type of cells could be pollen grains that became arrested in their development. This could have happened after the release of microspores from tetrads, but before the first mitotic event, as they are slightly smaller than mature grains, contain starch grains and are unicellular. Another possibility is that they are remnant tapetal cells. They tended to be located around the periphery of the anther locule where other degenerate remains of the tapetum are located.

The SEM images from fresh grains fixed only in 3% phosphate-buffered glutaraldehyde were the best for showing overall grain shape as well as surface details. The echinate nature of the grains of *Arceuthobium* is well-known (Gill 1935, Hawksworth & Wiens 1972) but few SEM examinations of grains have been made. The presence of spines in both colpae and pseudocolpae is similar to that observed in *A. pusillum* (Hawksworth & Wiens 1972). As well, spine bases in *A. americanum* appear to be distinct and vertical like those observed in *A. pusillum* rather than spreading, as in *A. verticilliflorum*.

The ratio of spine height:pollen wall thickness varies depending on where it is measured, as wall thickness varies with proximity to the colpae, but spine height is relatively constant. The mean ratio of spine height:pollen wall thickness for *Arceuthobium americanum* in non-apertural areas was calculated to be 2.7 (n = 10). This value (ratio = 1.2) is quite different from that determined by Hawksworth and Wiens (1972). Although they did not mention what was included in measuring wall thickness, exine alone, or both intine and exine. This value is, however, similar (ratio = 3) to that found for *A. tsugense* (Rosend.) G. N. Jones (hemlock dwarf mistletoe, Viscaceae) but differs from that they calculated for *A. verticilliflorum* (ratio = 0.67). This information has the potential to be of taxonomic importance (Hawksworth & Wiens 1996), but consistency between measurements would be very important.

Other pollen characters can also be used for taxonomic studies. Exine structure for example, distinguishes the Viscaceae from the Eremolepidaceae despite some similarities. In particular, the echinate sculpturing of *Arceuthobium* resembles that of the parasitic Eremolepidaceae (Feuer & Kuijt 1978). A more detailed concurrent SEM and TEM study and comparison of mature pollen for each species of *Arceuthobium* is therefore likely to be of taxonomic value for this genus (Hawksworth & Wiens 1972).

Androecial developmental patterns were used by Bernhard and Endress (1999) to help define systematic relationships in the Flacourtiaceae, and results were largely in agreement with morphological and molecular evidence. In floral developmental terms, species of dwarf mistletoe may be divided into direct and indirect flowering groups. Those that exhibit direct flowering undergo uninterrupted floral development from

initiation to anthesis, whereas there is an intervening dormant period for species with the indirect mode of flowering. *Arceuthobium americanum* exhibits the indirect mode of flowering; that is, floral initiation occurs during the previous growing season, but anthesis does not occur until the following spring (Cohen 1968, Dowding 1931, Hawksworth & Wiens 1996, Wiens 1968). Mostly those *Arceuthobium* species with a direct mode of floral development, flower in the fall, although some intermediates also exist (Wiens 1968). Differences may be environmentally related. During the dry season, some species flower continually, and others have several flowering periods throughout the year, but the timing of meiosis is unknown for many species (Hawksworth & Wiens 1996).

Dwarf mistletoe is one of the first angiosperms to begin anthesis in those parts of Manitoba where it is found (Baker 1981, Gilbert 1988). Retaining an entomophilous pollen dispersal mechanism may be related to the timing of flowering. Early spring anthesis may have evolved as an adaptation to avoid competition for pollinators with summer-flowering species in areas where species overlap in their distribution (Wiens 1968). *A. americanum* is also wind pollinated (Gilbert 1988, Player 1979), so perhaps this avoids interspecies pollen competition by an early anthesis. It releases pollen several weeks before its jack pine host (personal observation). The presence of both lipid bodies and starch in mature grains would also be evidence of the dual pollen dispersal mechanisms for *A. americanum,* as starchy grains tend to be wind-dispersed, whereas lipidic grains are more typical of bee or fly dispersal (Dafni 1992).

A generalist pollination mechanism is employed by several *Salix* species. This combination of wind and insect vectors has been termed ambophily and would be favored in environments with unpredictable insect populations. This generalist strategy has been suggested to be the ancestral state, and would be favored by natural selection in some instances (Karrenberg *et al.* 2002), especially those with unpredictable spring weather conditions. Wyatt (1998) believes that many pollination mechanisms are less specialized than has been proposed. This implies that a generalized pollination strategy may be more common than previously thought. The combination of entomophilous and anemophilous characters (Hawksworth & Wiens 1996) exhibited by *Arceuthobium americanum* implies a generalist approach to pollination, and is probably a necessary approach for an early

flowering species. In temperate regions it may be cold at the time of anthesis, so therefore no insect pollinators would be present, and wind pollination could be more important those years.

The indirect mode of flowering may be related to this as well. In order to enable early flowering, prior floral development may be an adaptation to environmental extremes, such as temperature. Spring-flowering species of *Arceuthobium* with indirect staminate development tend to have more northerly distributions (Wiens 1968), whereas those species with direct development and/or fall flowering times tend to be found at more southerly latitudes (Hawksworth & Wiens 1996). Fall flowering has been observed to occur in *A. americanum* in Manitoba. September 1998 was unseasonably cool with temperatures reaching and remaining below 0°C for several days. During an equally unseasonably warm period later that fall, ambient air temperatures rose to >20°C, male mistletoe flowers opened and the anthers dehisced pollen (personal observation).

In the case of *A. americanum*, microsporocyte meiosis may occur in the fall (Cohen 1968, Hawksworth & Wiens 1996, Wiens 1968), although Dowding (1931) observed this in late July. Cohen (1968) believed meiotic cytokinesis to be simultaneous within a single anther, but he was only able to locate early figures of prophase I. He interpreted this as meaning meiosis occurs quite rapidly, but the phenological details have not been observed anatomically. The timing of floral events is as yet unconfirmed. An additional disparate feature of *A. americanum* is the meiotic asynchrony between the male and female plants. Although microspore mother cells appear to complete meiosis prior to the winter months, the meiotic division of the megasporocytes does not occur until the following spring, after anthesis (Hudson 1966, Wiens 1968).

Even though pollination occurs, the timing of fertilization has frequently been found to be delayed for members of the genus *Arceuthobium* (Hudson 1966). For example, *A. oxycedri* pollination occurs in late September or early October, but fertilization not until the following spring (Johnson 1888). A similar, albeit not shorter delay has also been observed in *A. americanum*. Pollination occurs in early spring, but fertilization a month or so later when female development is complete (Hudson 1966). This may be a host-induced influence, possibly via a hormonal mechanism since a delay in fertilization is a

phenomenon common to coniferous genera (Hawksworth & Wiens 1996). This correlation between host and parasite however, does not hold for all host species parasitized by the Viscaceae (Johnson 1888).

Figure 4.1 Light micrograph of a vegetative shoot tip (LS) showing two leaf primordia (lp) overarching the shoot apical meristem (medium black arrow) containing meristematic cells (*). Area in the box is enlarged in Figure 4.2. Crystal violet. Scale bar 45 μm.

Figure 4.2 Light micrograph of a vegetative shoot apical meristem (LS) showing a leaf primordiim (lp) overarching the meristematic cells (*) enveloped by a uniseriate epidermis (ep). Crystal violet. Scale bar 10 μm.

Figure 4.3 Line drawing of a shoot tip (LS) showing the orientation of terminal (large black arrowhead) and two lateral (medium black arrows) buds. Scale bar 250 μm.

Figure 4.4 Light micrograph of a shoot tip (LS) showing the initiated perianth (small black arrows) overarching the meristematic tissue (*). Crystal violet. Scale bar 55 μm.

Figure 4.5 Light micrograph of a floral bud (LS) showing two perianth segments (small arrows) above two stamen primordia (large black arrowheads), each with a single region of sporogenous cells (sp), surrounded by a uniseriate primary parietal cell layer (p) and outer epidermis (ep). Area in the box is enlarged in Figure 4.6. Crystal violet. Scale bar 45 μm.

Figure 4.6 Light micrograph of a stamen primordium (LS) showing the sporogenous cells (sp) with prominent nucleoli (small black arrows), single layered primary parietal layer (p) and anther epidermis (ep). An anticlinal division (large black arrowhead) is occurring in the primary parietal cell layer. Crystal violet. Scale bar 10 μm.

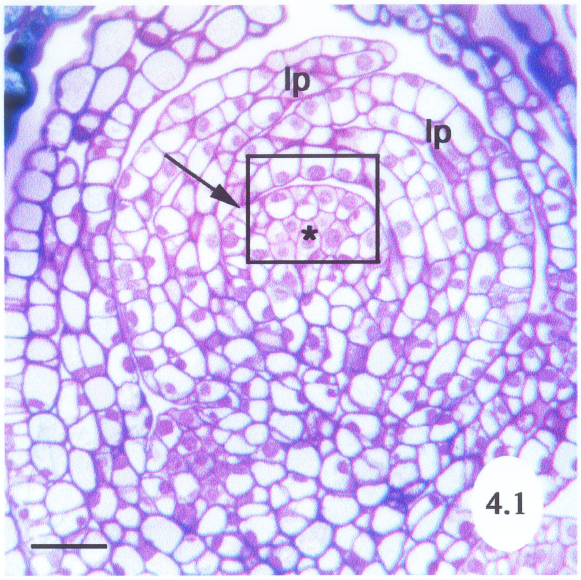
lp
lp
*
4.1

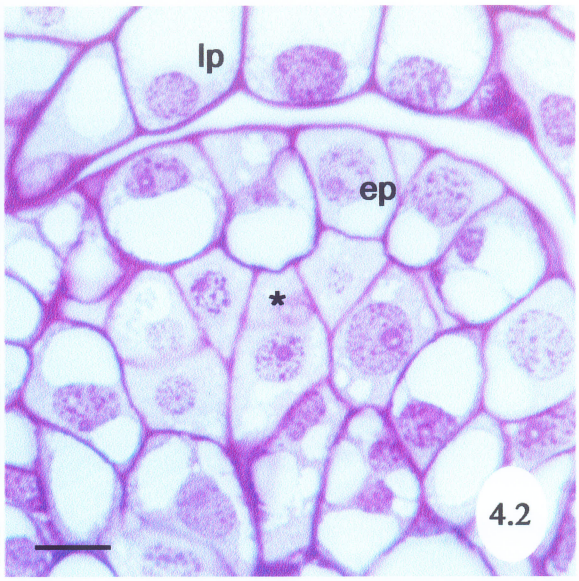
lp
ep
*
4.2

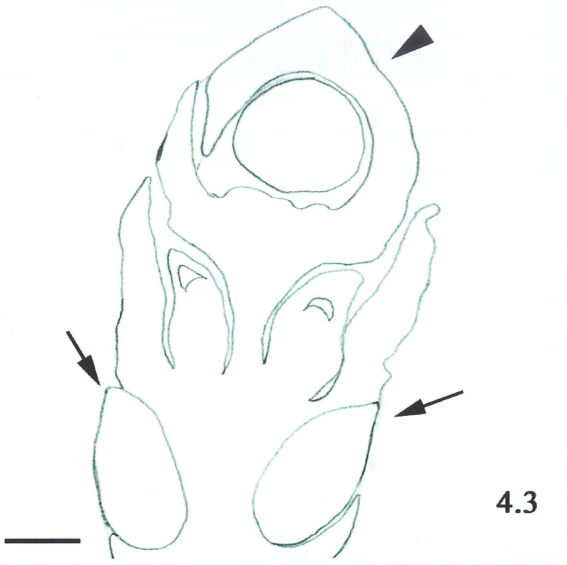
4.3

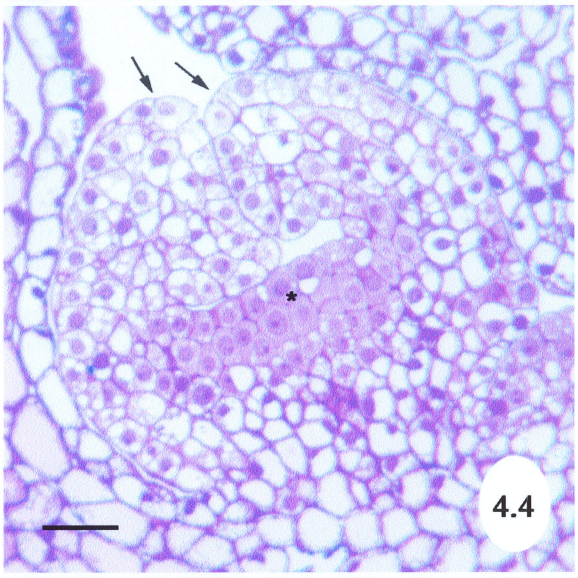
*
4.4

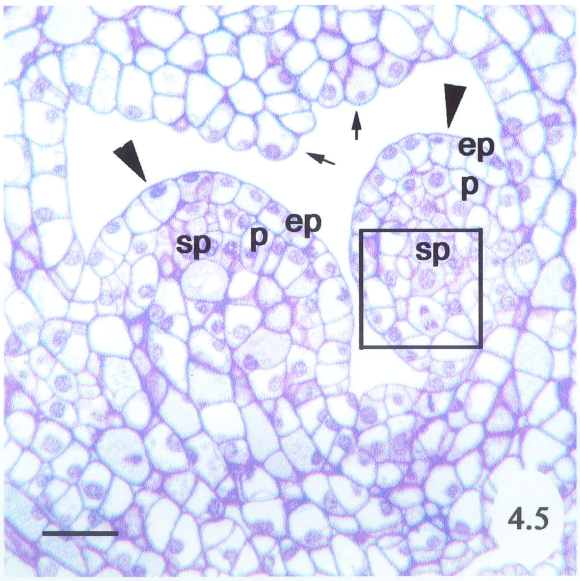
ep
p
sp
p
ep
sp
4.5

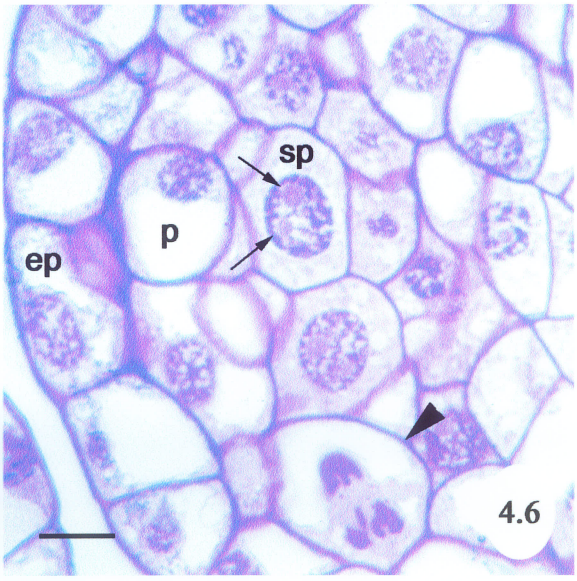
sp
p
ep
4.6

Figure 4.7 Light micrograph of a floral bud (CS) showing the three stamen primordia (large black arrowheads). The single-layered primary parietal layer (p) and epidermis (ep) are visible. Area in the box is enlarged in Figure 4.8. Crystal violet. Scale bar 40 μm.

Figure 4.8 Light micrograph of the three stamen primordia (CS) showing the single-layered primary parietal layer (p) and epidermis (ep), which has a periclinal division (medium black arrow) occurring. Crystal violet. Scale bar 12 μm.

Figure 4.9 Light micrograph of a shoot tip (LS) showing two stamen primordia (large black arrowheads) each with a uniseriate primary parietal layer (p) and epidermis (ep). Also visible is the overarching perianth (small black arrow). A horseshoe of sporogenous (sp) cells is apparent in one anther and two groups of sporogenous cells (medium black arrows) in the other. Crystal violet. Scale bar 45 μm.

Figure 4.10 Light micrograph of a shoot tip (LS) showing the epidermis (ep), middle layer (ml) and tapetal layer (t) surrounding a horseshoe of sporogenous cells (sp) in two anthers. The floral nectary (large black arrowhead) and perianth segments (small arrow) are also in view. Area in the box is enlarged in Figure 4.11. Crystal violet. Scale bar 62 μm.

Figure 4.11 Light micrograph of an anther (LS) showing the tapetum (t) surrounding a horseshoe of sporogenous cells (sp). Vacuolate cells (v) and cells containing phenolics (medium white arrows) are also present. Crystal violet. Scale bar 12 μm.

Figure 4.12 Light micrograph of an anther (LS) with vacuolate cells containing thick deposits of lignin-like compounds (large black arrowhead). Crystal violet. Scale bar 5 μm.

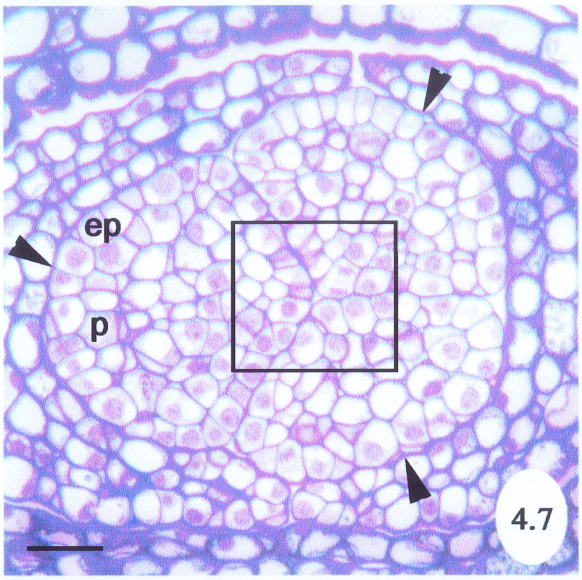
ep
p
4.7

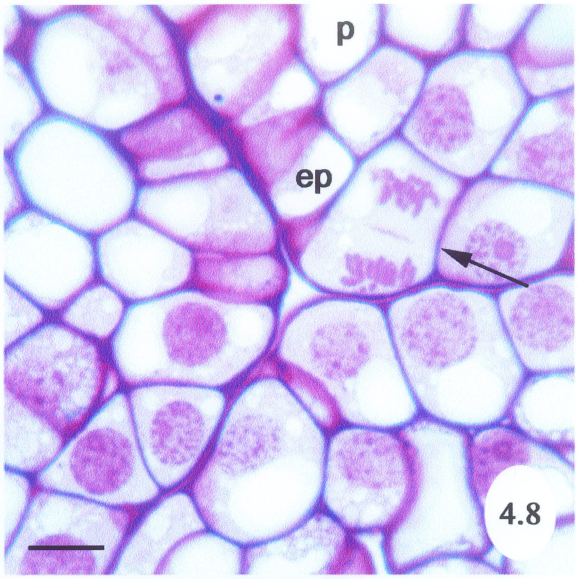
p
ep
4.8

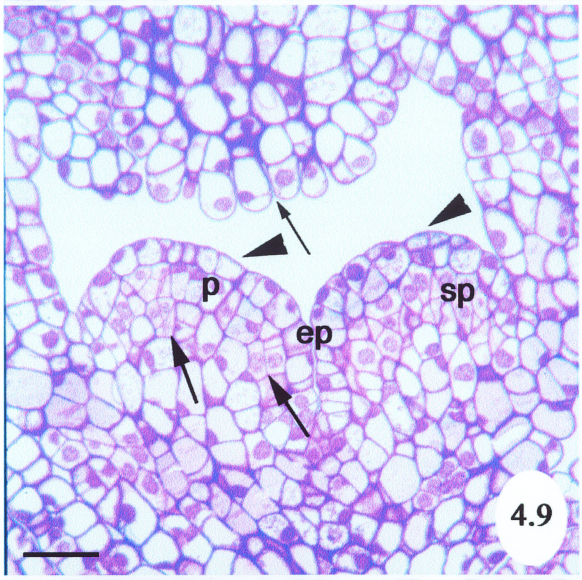
p
sp
ep
4.9

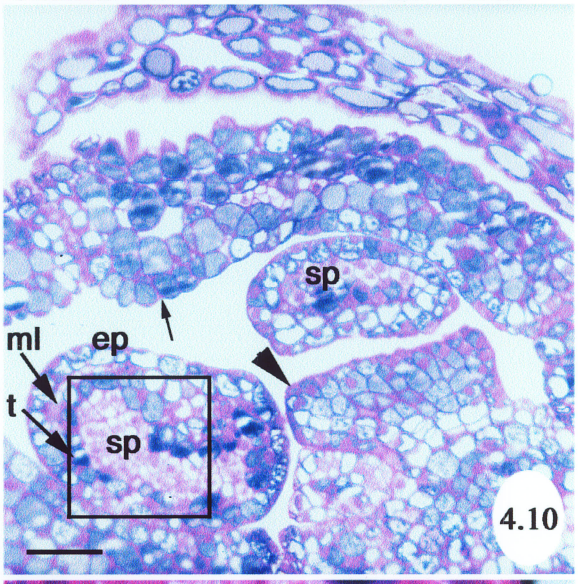
sp
ml
ep
t
sp
4.10

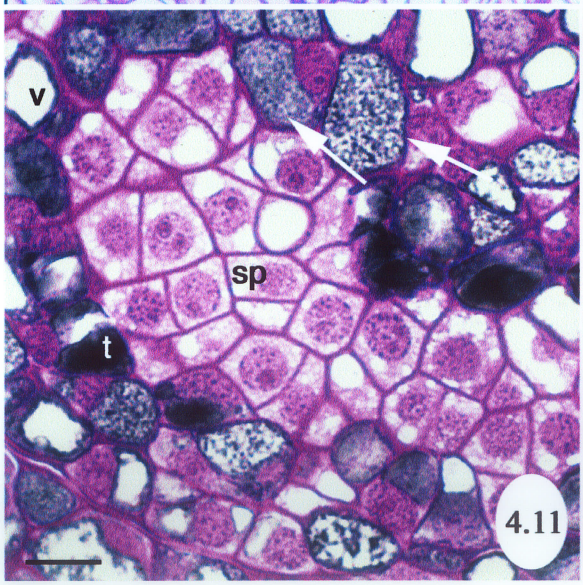
v
sp
t
4.11

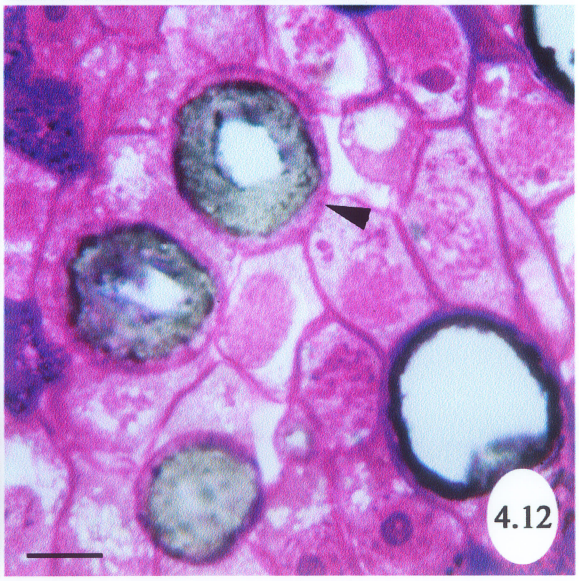
4.12

Figure 4.13 Light micrograph of a shoot tip (LS). The sporogenous tissue (sp) within the two anthers appears as one (large black arrowhead) or two regions (small black arrows) because of their differing planes of section. A lateral bud (medium black arrow) and vegetative meristem (*) are seen below. Crystal violet. Scale bar 300 μm.

Figure 4.14 Light micrograph of a floral bud (LS) showing two anthers sectioned at differing depths. The anther at the top left is sectioned only to the level of the epidermis (ep). The anther at the bottom right shows the tapetum (t), middle layer (ml) and epidermis (ep) surrounding the sporogenous cells (sp). Perianth segments (medium black arrows) are also visible. Area in the box is enlarged in Figure 4.15. Crystal violet. Scale bar 45 μm.

Figure 4.15 Light micrograph of an anther (LS) showing the tapetum (t), middle layer (ml) and epidermis (ep) at the top left of the sporogenous cells (sp) which contain prominent nucleoli (medium black arrow). Crystal violet. Scale bar 10 μm.

Figure 4.16 Light micrograph of sporogenous cells (CS), some of which are elongate (medium black arrows). Vacuolate cells (large arrowhead) are also present. Crystal violet. Scale bar 15 μm.

Figure 4.17 Light micrograph of a floral bud (LS). A well-developed columella (c) separates the two regions of sporogenous cells (sp) surrounded by the tapetum (t), middle layer (ml) and epidermis (ep). Aniline blue black/PAS. Scale bar 45 μm.

Figure 4.18 Transmission electron micrograph of an anther (LS) showing two vacuolate tapetal cells with intact cell walls (cw), a large central vacuole (va), vesicles (ve), mitochondria (M), endoplasmic reticulum (ER) and a nucleus (n). The nucleus of one middle layer (ml) cell is also in view. Area in the box is enlarged in Figure 4.19. Uranyl acetate/lead citrate. Scale bar 298 nm.

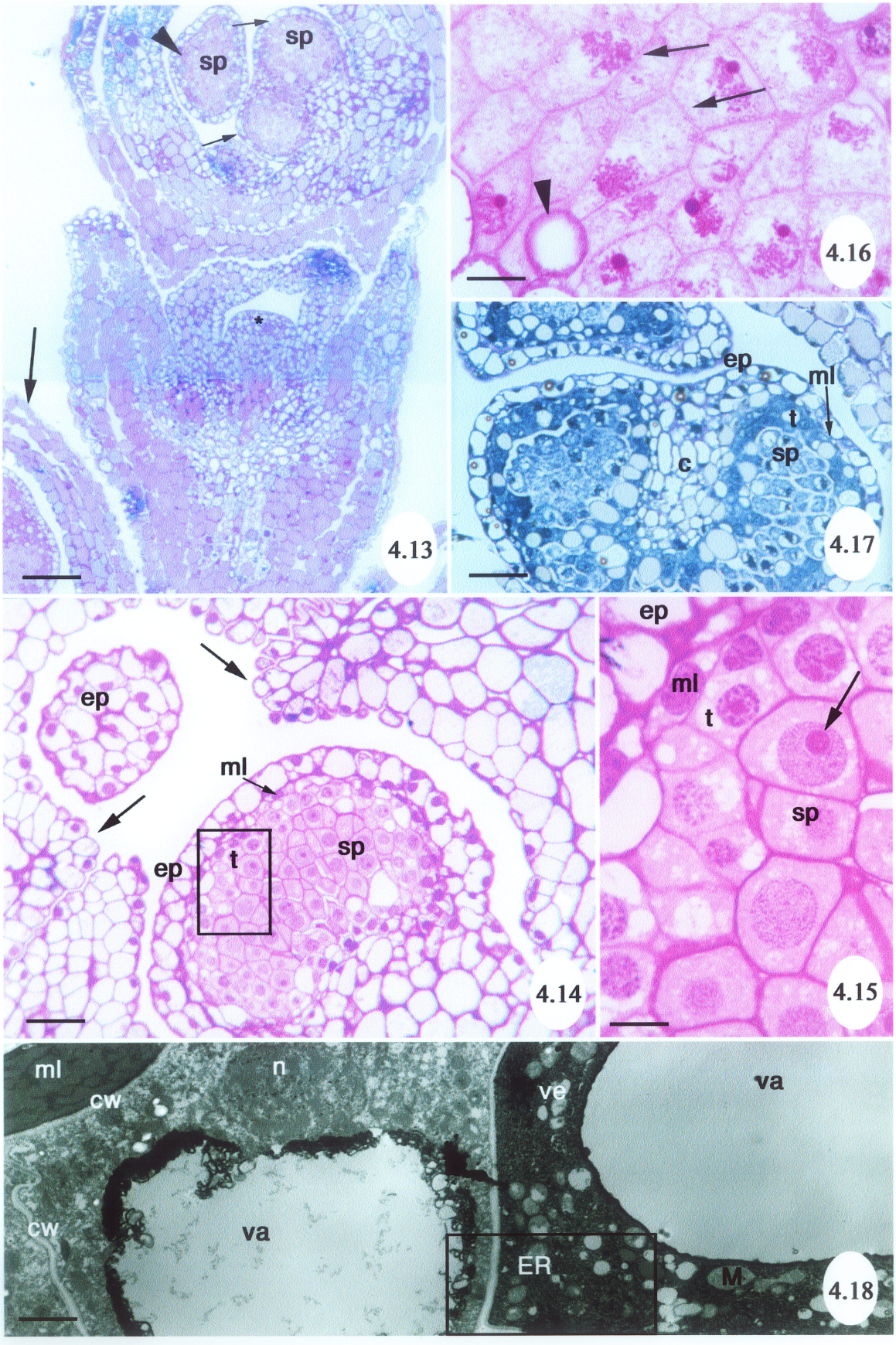
sp
sp
*
4.13
4.16
ep
ml
t
sp
c
4.17
ep
ml
t
sp
4.14
ep
ml
t
sp
4.15
ml
n
cw
ve
va
cw
va
ER
M
4.18

Figure 4.19 Transmission electron micrograph of an anther (LS) showing the cell wall (cw) between two vacuolate tapetal cells containing vesicles (ve), mitochondria (M), endoplasmic reticulum (ER) and a nucleus (n). Uranyl acetate/lead citrate. Scale bar 44 nm.

Figure 4.20 Light micrograph of a floral bud (LS) showing the tapetum (t), middle layer (ml) and epidermis (ep) surrounding the sporogenous cells (sp) in two anthers, one of which contains a well-developed columella (c). Area in the box is enlarged in Figure 4.21. Crystal violet. Scale bar 70 μm.

Figure 4.21 Light micrograph of an anther (LS) showing the tapetum (t), middle layer (ml) and epidermis (ep) surrounding the early prophase I sporogenous cells (sp). Vacuolate cells contain abundant crystalline phenolic-like (medium black arrows) substances. Crystal violet. Scale bar 14 μm.

Figure 4.22 Light micrograph of an anther (LS) showing the sporogenous cells (sp) in early prophase (medium black arrow), tapetum (t), middle layer (ml) and epidermis (ep). A periplasmic space (*) is beginning to develop between the protoplast and cell wall. Crystal violet. Scale bar 10 μm.

Figure 4.23 Light micrograph of an anther (LS) with a well-developed columella (c), showing the tapetum (t), middle layer (ml) and epidermis (ep), all containing vacuolate cells (v). Separation between the tapetum and sporogenous tissue (medium black arrow) is beginning to occur. Crystal violet. Scale bar 14 μm.

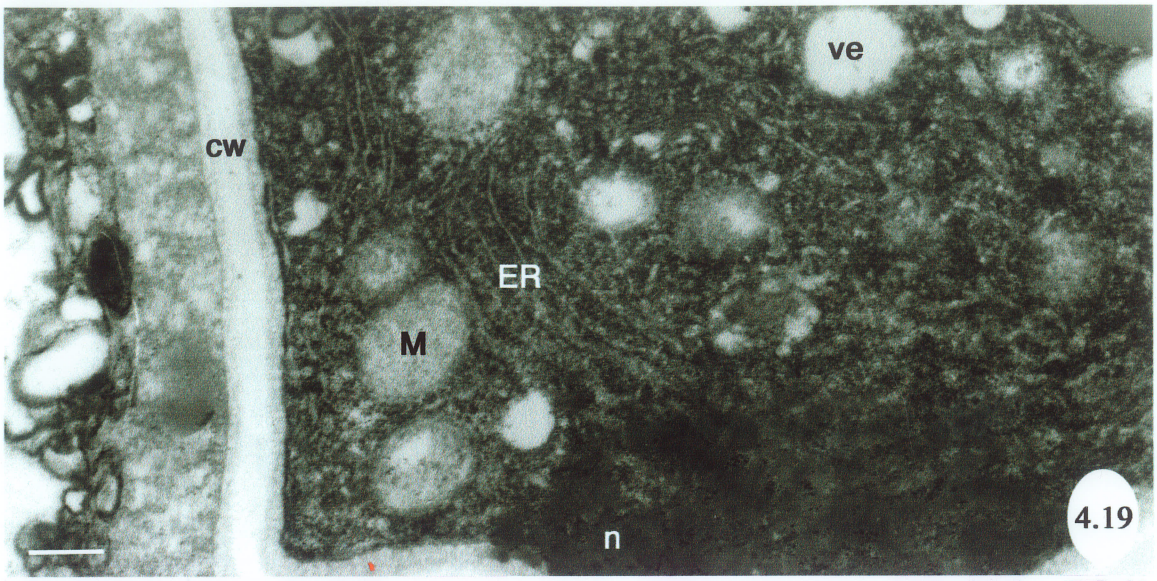
ve
cw
ER
M
n
4.19

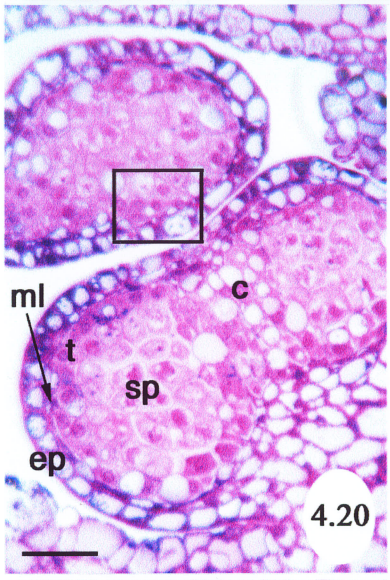
ml
t
sp
c
ep
4.20

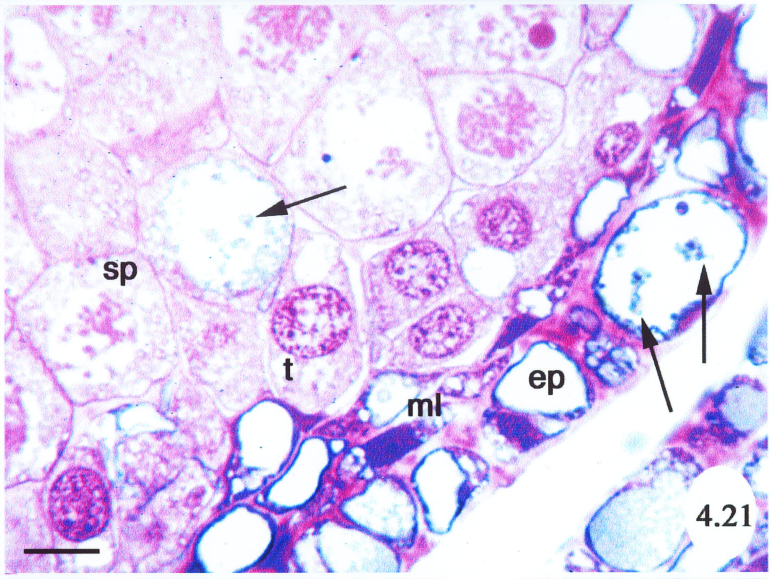
sp
t
ml
ep
4.21

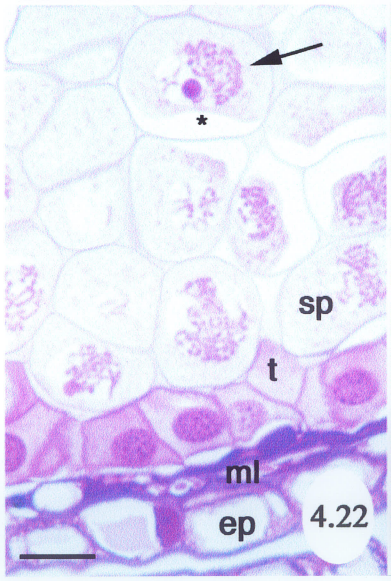
*
sp
t
ml
ep
4.22

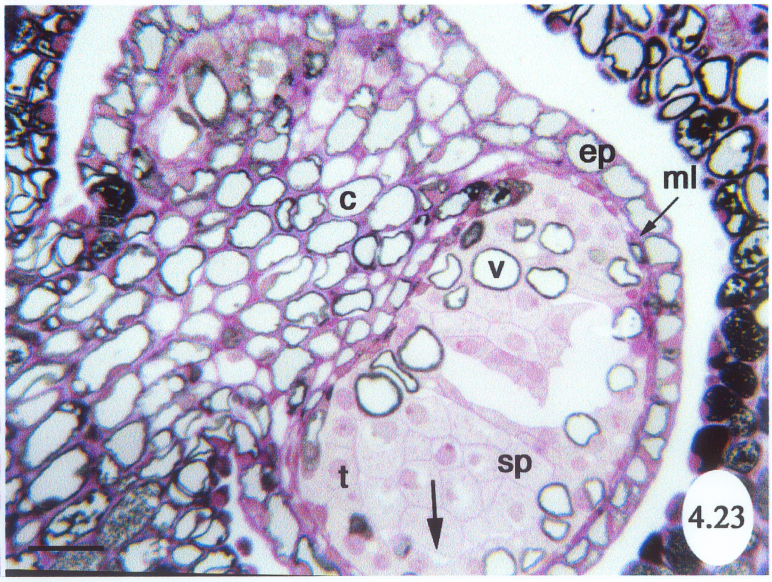
ep
ml
c
v
t
sp
4.23

Figure 4.24 Transmission electron micrograph of the sporogenous cells (CS) containing nuclei (n) with prominent nucleoli (nu) and vescicles (ve). A periplasmic space (*) is present between the protoplast and the cell walls (cw) which contain cytomictic channels (medium black arrows). A vacuolate cell (v) is also in view. Area in the box is enlarged in Figure 4.25. Uranyl acetate/lead citrate. Scale bar 4.5 μm.

Figure 4.25 Transmission electron micrograph of sporogenous cells (CS) containing mitochondria (M), vescicles (ve) and a cell wall (cw) containing a cytomictic channel (medium black arrow). Uranyl acetate/lead citrate. Scale bar 1.4 μm.

Figure 4.26 Transmission electron micrograph of sporogenous cells (LS) containing nuclei (n), starch grains (sg) and cell walls (cw) which contain cytomictic channels (small black arrows). Area in the box is enlarged in Figure 4.27. Uranyl acetate/lead citrate. Scale bar 4.1 μm.

Figure 4.27 Transmission electron micrograph of sporogenous cells (LS) containing mitochondria (M) and and a cell wall (cw) with cytomictic channels (small black arrows). A periplasmic space (*) is also in view. Uranyl acetate/lead citrate. Scale bar 1:2 μm.

Figure 4.28 Transmission electron micrograph of an anther wall (LS) showing tapetal cells (t) containing nuclei (n), vesicles (ve), periplasmic spaces (*) and cytomictic channels (small black arrows) in cell walls (cw). The middle layer (ml) and part of the epidermis (ep) is visible above.. Uranyl acetate/lead citrate. Scale bar 2.2 μm.

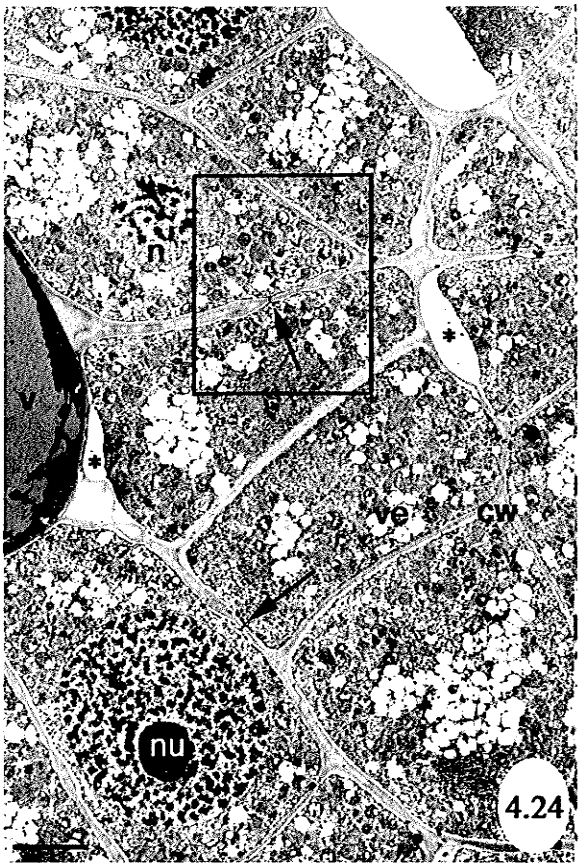
n
v
ve
cw
nu
4.24


M
cw
ve
4.25

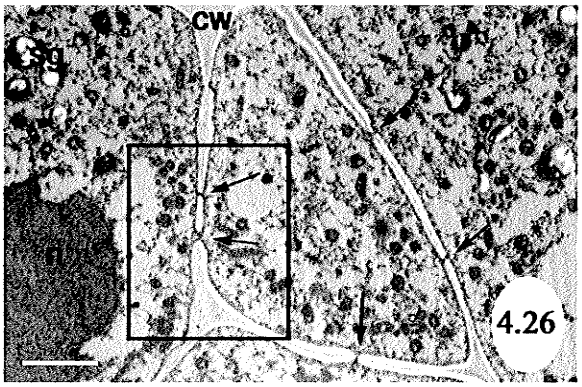
cw
sg
el
4.26

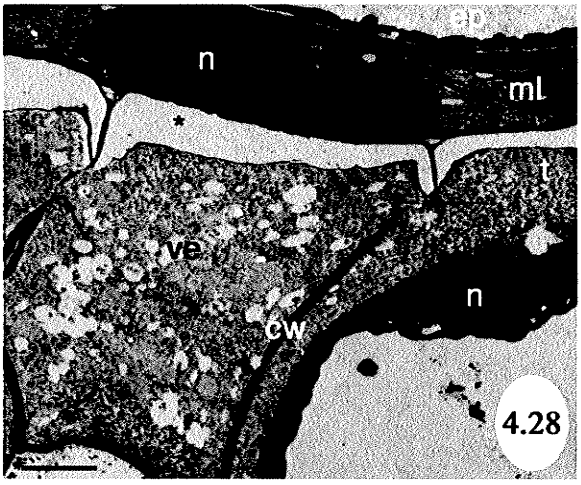
n
ml
t
ve
n
cw
4.28

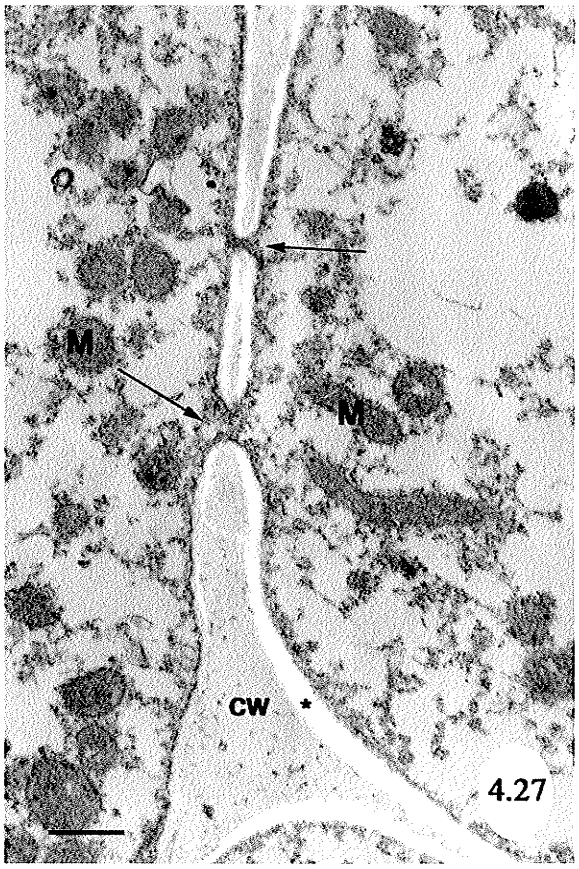
M
M
cw
4.27

Figure 4.29 Light micrograph of an anther (CS) showing microspore mother cells (mmc) separate from one another surrounded by the epidermis (ep), middle layer (ml) and tapetum (t), which extends (large black arrowheads) to the central columella (c). Area in the box is enlarged in Figure 4.30. Crystal violet. Scale bar 47 μm.

Figure 4.30 Light micrograph of an anther (CS) showing microspore mother cells (mmc) with thickened cell walls (medium black arrow) separated from the protoplast by a periplasmic space (*), surrounded by the tapetum (t), which contains a vacuolate cell (v), middle layer (ml) and epidermis (ep). Crystal violet. Scale bar 9 μm.

Figure 4.31 Fluorescence micrograph of an anther (CS) showing microspore mother cells (mmc) with callose positive, thickened cell walls (medium white arrow) separated from cell contents by a periplasmic space (*), surrounded by the tapetum (t), middle layer (ml) and epidermis (ep), all with cellulose walls. Aniline blue and calcofluor white MR2. Scale bar 21 μm.

Figure 4.32 Light micrograph of pollen tetrads (te) containing four tetrahedrally arranged nuclei. The new cell wall can be seen furrowing in (small black arrow). Crystal violet. Scale bar 15 μm.

Figure 4.33 Light micrograph of a possibly cytoplasmically male sterile anther (LS). The epidermis (ep), middle layer (ml) and remaining tapetal (t) tissue is present surrounding an empty locule. Crystal violet. Scale bar 45 μm.

Figure 4.34 Light micrograph of a possibly cytoplasmically male sterile anther (LS). The epidermis (ep), middle layer (ml) and remaining tapetal (t) tissue is present surrounding a few microsporocytes (mmc) in the otherwise empty locule. Crystal violet. Scale bar 45 μm.

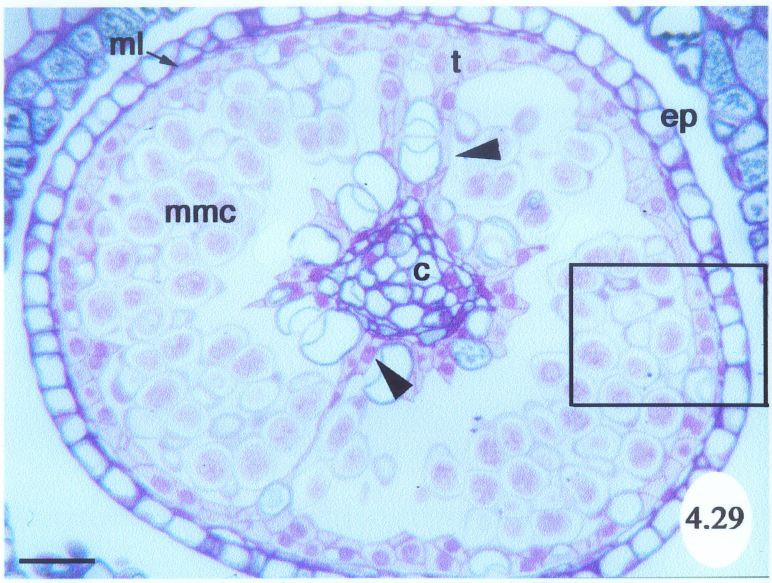
ml
t
ep
mmc
c
4.29

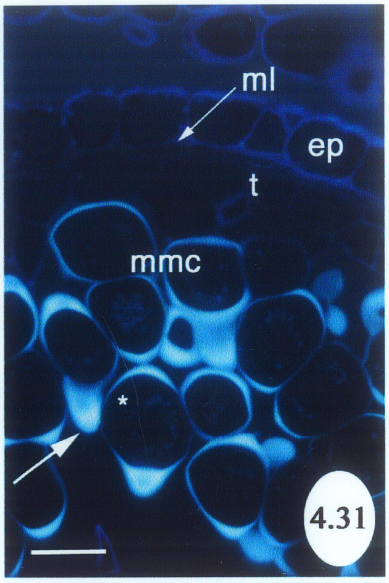
ml
ep
t
mmc
*
4.31

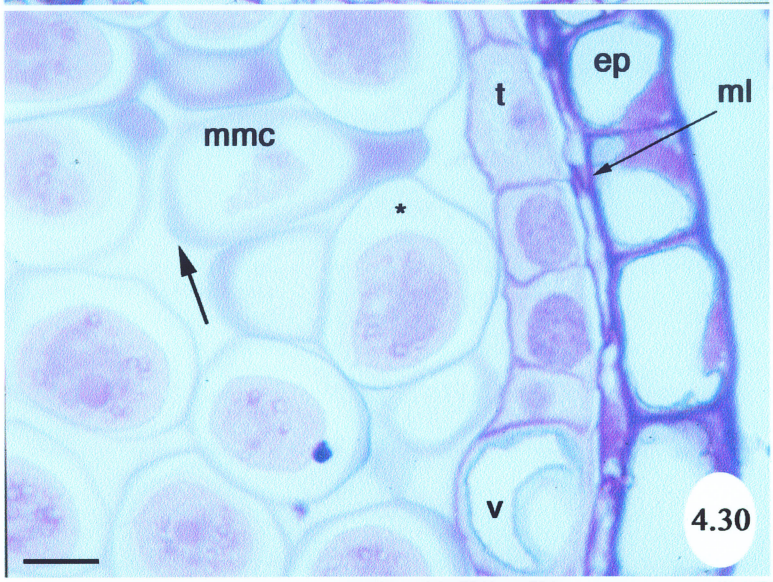
mmc
t
ep
ml
*
v
4.30

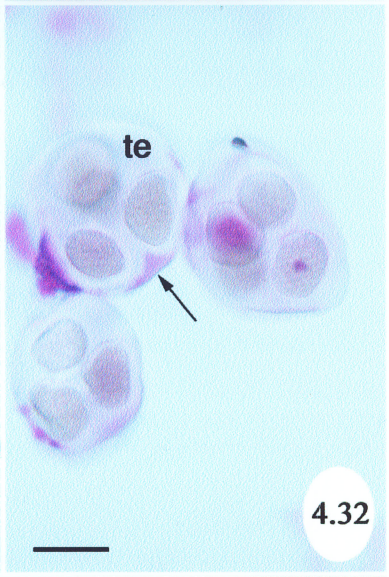
te
4.32

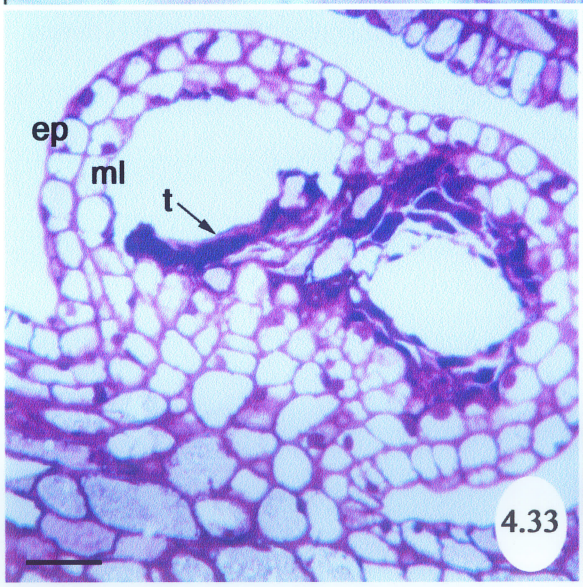
ep
ml
t
4.33

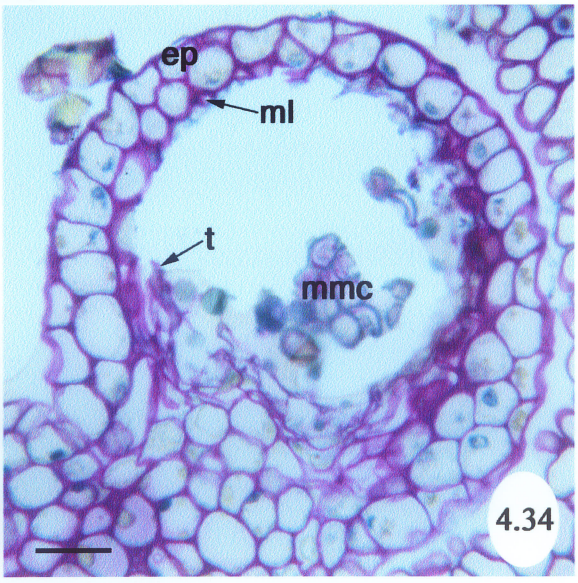
ep
ml
t
mmc
4.34

Figure 4.35 Transmission electron micrograph of an anther wall (LS) showing the epidermis (ep), middle layer (ml), tapetal cells (t) and microsporocytes (mmc) containing nuclei (n), starch grains (sg) and vacuoles (v). Uranyl acetate/lead citrate. Scale bar 3.2 μm.

Figure 4.36 Transmission electron micrograph of two microspore mother cells (mmc) with vesicles (ve), starch grains (sg), nuclei (n), cytomictic channels (small black arrows) and periplasmic spaces (*). Uranyl acetate/lead citrate. Scale bar 0.6 μm.

Figure 4.37 Transmission electron micrograph of a microspore mother cell (CS) showing the cell wall (cw), periplasmic spaces (*), vesicles (ve), starch grains (sg) and nuclei (n), with prominent nucleoli (nu). The original primary cell wall (small black arrow) is much thinner than the inner secondary cell wall (medium black arrow). Uranyl acetate/lead citrate. Scale bar 1.1 μm.

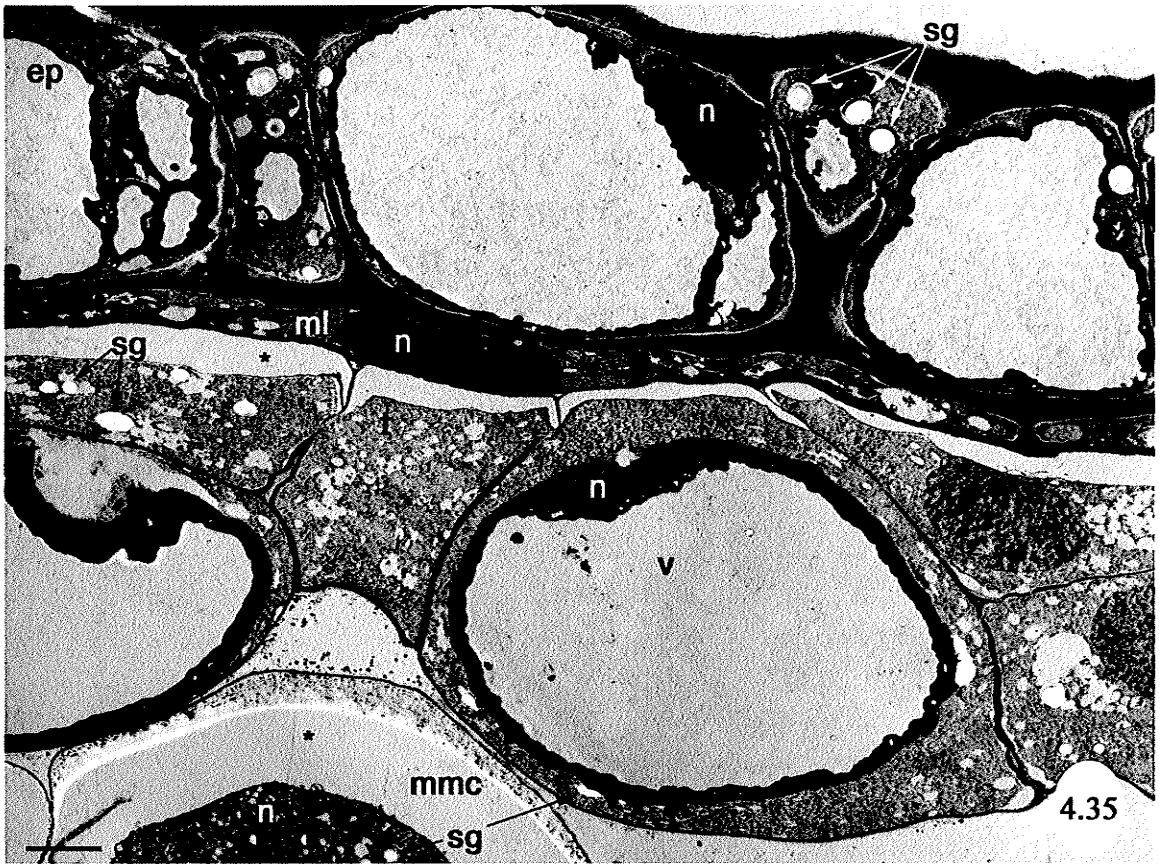

4.35

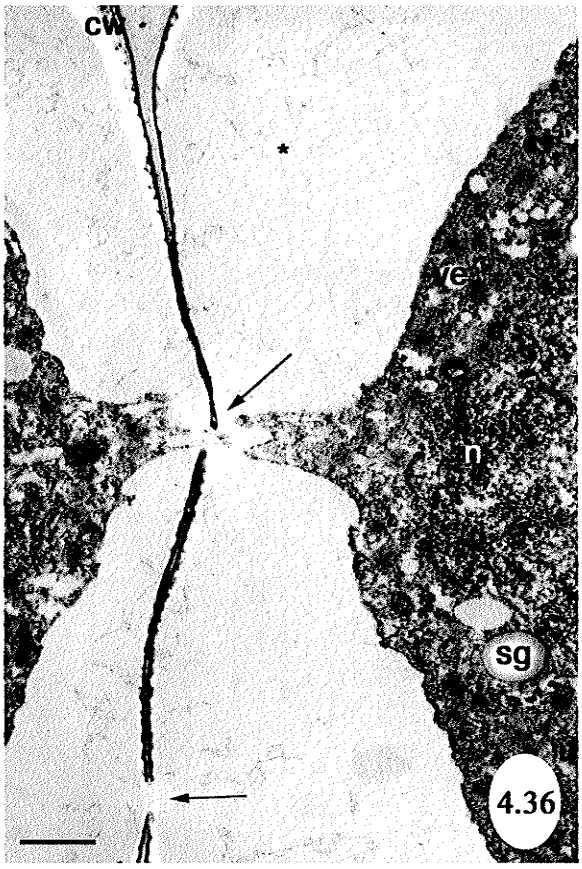

4.36

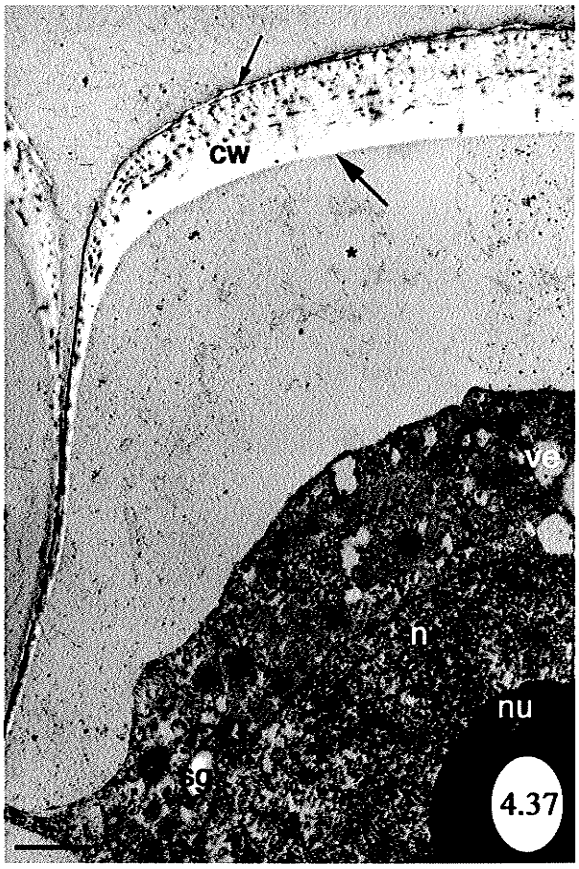

4.37

Figure 4.38 Fluorescence micrograph of two anthers (LS) showing tetrads (te), with callose positive cell walls, surrounded by the tapetum (t), middle layer (ml) and epidermis (ep), all with cellulose walls. The columella (c) is also visible in both anthers. Area in the box is enlarged in Figure 4.39. Aniline blue and calcofluor white MR2. Scale bar 60 μm.

Figure 4.39 Fluorescence micrograph of an anther (LS) showing tetrads (te), with callose positive cell walls, surrounded by the tapetum (t), middle layer (ml) and epidermis (ep), all with cellulose walls. A vacuolate cell (v) is visible within the tapetum. Aniline blue and calcofluor white MR2. Scale bar 14 μm.

Figure 4.40 Light micrograph of two anthers (LS) showing separate microspores (m), with prominent nucleoli (medium black arrows), surrounded by the tapetum (t), middle layer (ml) and epidermis (ep). Vacuolate cells (v) are present within the tapetum. Crystal violet. Scale bar 18 μm.

Figure 4.41 Light micrograph of an anther (LS) showing separate, vacuolate (medium black arrow) microspores (m), with prominent nucleoli (small black arrow) and thickened cell walls (large black arrowhead), bounded by the tapetum (t), also with prominent nucleoli. Crystal violet. Scale bar 10 μm.

Figure 4.42 Light micrograph of an anther to show separate microspores (m) with thin sporopollenin walls (large black arrowhead) and prominent nucleoli (small black arrow). The tapetum (t) also contains prominent nucleoli (small black arrow), many small vacuoles (medium black arrow) and some larger vacuolate cells (v). Crystal violet. Scale bar 15 μm.

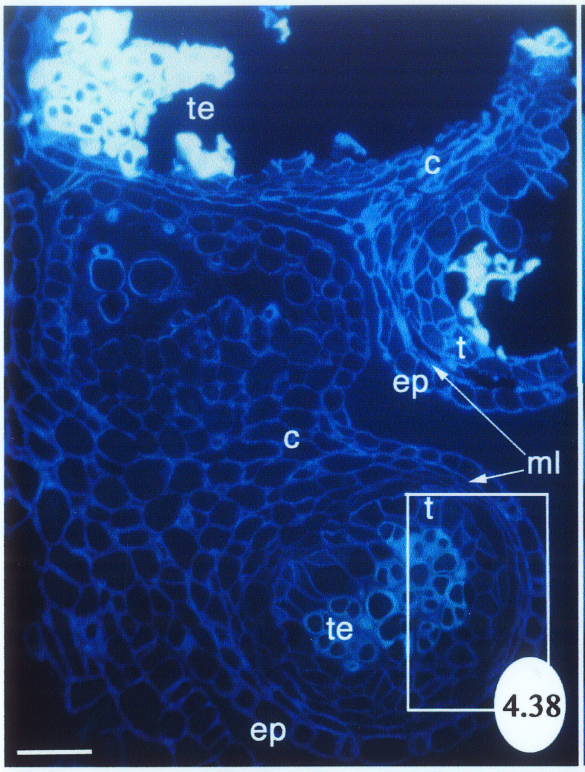
te
c
t
ep
c
ml
t
te
ep
4.38

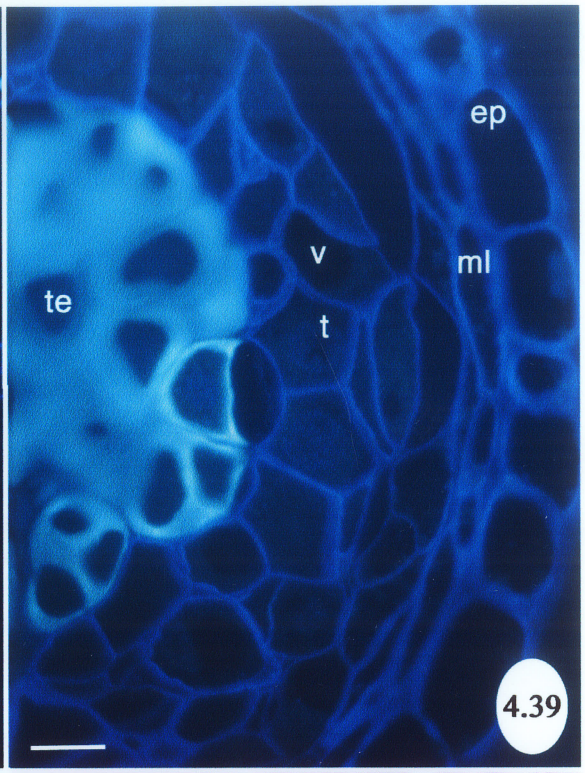
ep
v
ml
te
t
4.39

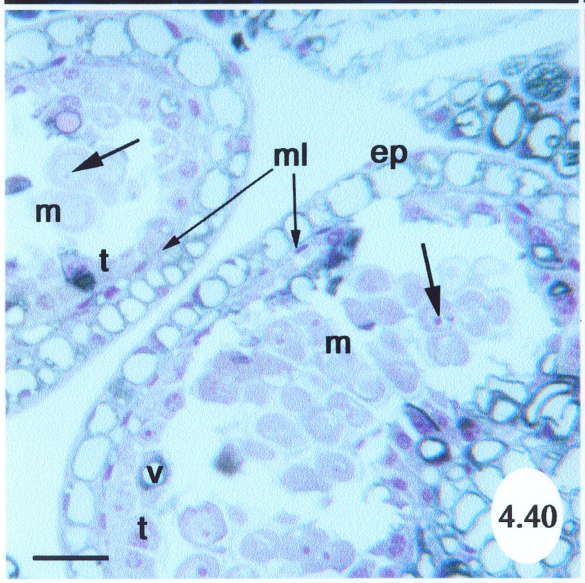
ml
ep
m
t
m
v
t
4.40

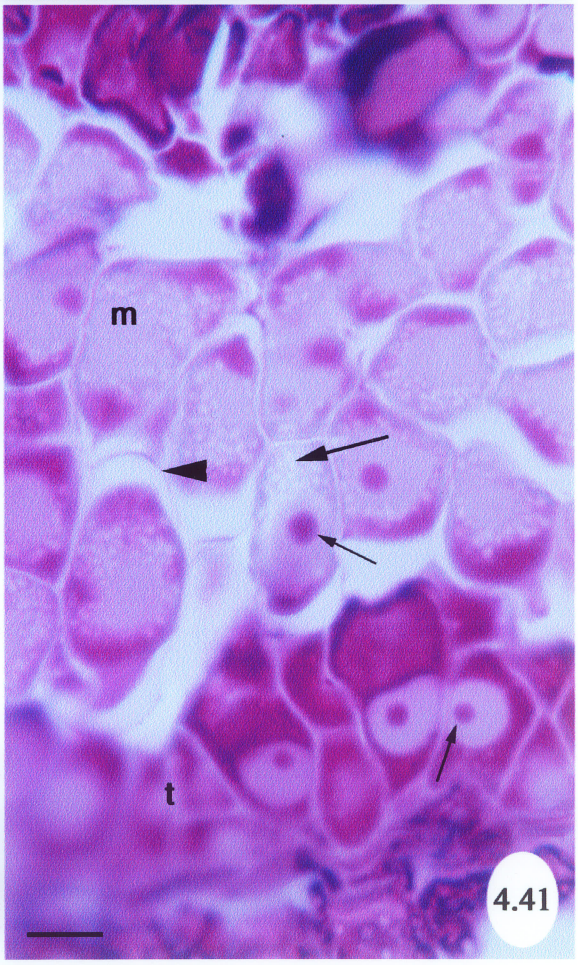
m
t
4.41

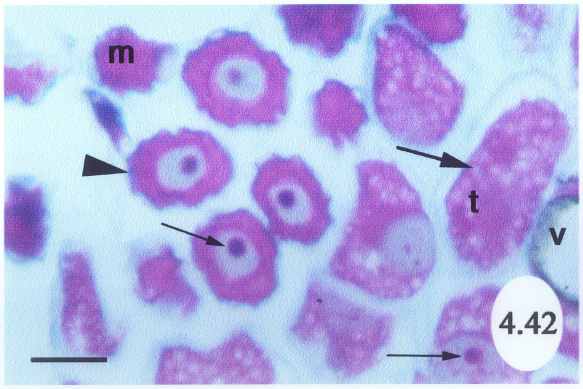
m
t
v
4.42

Figure 4.43 Light micrograph of maturing microspores undergoing the first mitotic division. Some cells contain both the generative nucleus (gn) and vegetative nucleus (vn) with the newly formed generative cell wall (gcw) between the two nuclei. Some degenerated tapetal material (large black arrowhead) is present between cells. Crystal violet. Scale bar 20 μm.

Figure 4.44 Light micrograph of binucleate microspores with a more lenticular vegetative nucleus (vn) and a rounder generative nucleus within the generative cell wall (gcw). Some degenerated tapetal material (t) is present at the periphery and also between cells (large black arrowhead). Crystal violet. Scale bar 20 μm.

Figure 4.45 Light micrograph of a floral bud (LS) to show the three anthers containing young pollen grains (pg) surrounded by a uniseriate epidermis (ep) and degenerating tapetum (t). The perianth segments (large black arrowheads) completely enclose the anthers. Area within the box is enlarged in Figure 4.46. Crystal violet. Scale bar 120 μm.

Figure 4.46 Light micrograph of an (LS) to show young pollen grains (pg) surrounded by a uniseriate epidermis (ep) and degenerating tapetum (t). The perianth segments (large black arrowheads) are also in view. Area within the box is enlarged in Figure 4.47. Crystal violet. Scale bar 45 μm.

Figure 4.47 Phase contrast micrograph of young pollen grains containing a more lenticular vegetative nucleus (vn) and a rounder generative nucleus (gn) with the generative cell wall (gcw) completely surrounding it. A thick intine layer (medium black arrow) is evident beneath the darker staining exine (large arrowhead) in non-apertural regions, as well as degenerated tapetal material (t). Crystal violet. Scale bar 10 μm.

Figure 4.48 Light micrograph of mature pollen grains with a more lenticular vegetative nucleus (vn) and a rounder generative nucleus (gn) with cytoplasmic extensions surrounded by the generative cell wall (gcw). Spines (large black arrowhead) are also evident as well as degenerated tapetal material (t). Crystal violet. Scale bar 10 μm.

Figure 4.49 Light micrograph of mature pollen grains containing starch grains (small black arrows). PAS. Scale bar 15 μm.

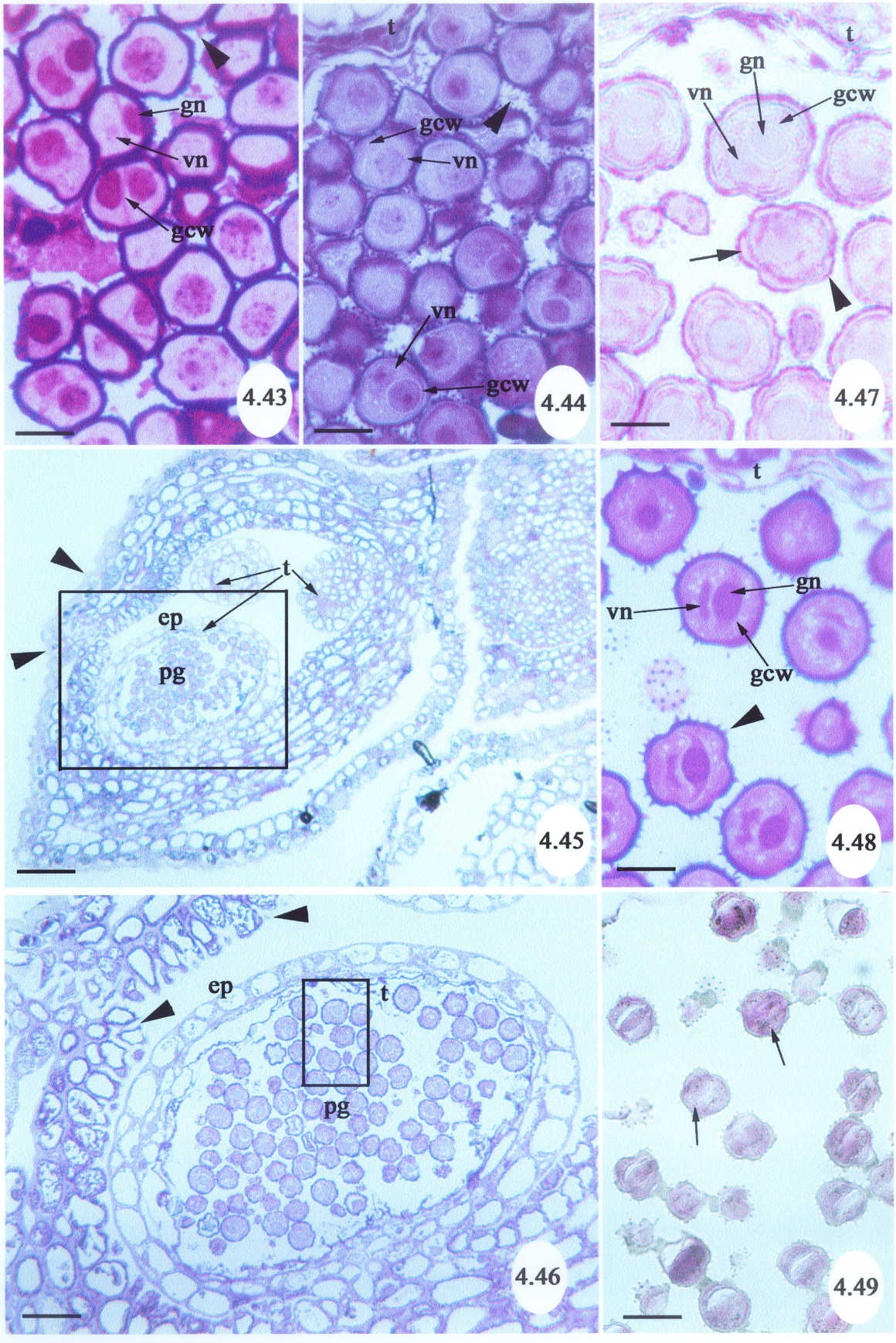
gn
vn
gcw
4.43
t
gcw
vn
vn
gcw
4.44
t
gn
vn
gcw
4.47
t
ep
pg
4.45
t
vn
gn
gcw
4.48
ep
t
pg
4.46
4.49

Figure 4.50 Transmission electron micrograph of a microspore at the uninucleate (n) stage. Three apertures with thickened intine (medium white arrow) and thinned exine (large black arrowhead), alternate with the three pseudocolpae (small black arrows). Area in the box is enlarged in Figure 4.51. Uranyl acetate/lead citrate. Scale bar 2.5 μm.

Figure 4.51 Transmission electron micrograph of the aperture of a microspore at the uninucleate stage. The thickened intine (in) contains electron dense bodies (small black arrow) similar to the inner exine layer (ex). The outer exine layer (large black arrowhead) thins, but is continuous over the apertural region. Uranyl acetate/lead citrate. Scale bar 0.6 μm.

Figure 4.52 Transmission electron micrograph of an orbicules (o) on the inner tapetal cell wall (cw) containing electron dense material (large black arrowhead) and small tubular pieces (small white arrow). Both are surrounded by an electron dense envelope (medium black arrow). Uranyl acetate/lead citrate. Scale bar 293 nm.

Figure 4.53 Transmission electron micrograph of the inner tapetal (t) surface showing tapetal extrusions which contain large electron dense (large black arrowhead) and small tubular (small black arrows) pieces of material. Uranyl acetate/lead citrate. Scale bar 1.6 μm.

Figure 4.54 Transmission electron micrograph of degenerating tapetal material (t) which contains crystalline inclusions (small black arrows). Uranyl acetate/lead citrate. Scale bar 218 nm.

Figure 4.55 Transmission electron micrograph of the apertural region of a binucleate microspore. A thickened intine (in) underlies a plug of tubular electron dense bodies (small white arrow) similar to those above (small black arrow) the exine (ex). The outer exine layer is covered with a layer of material presumed to be pollenkitt (large black arrowhead). Endoplasmic reticulum (ER) and amyloplasts (am) containing starch grains (sg) are present in the cytoplasm. Uranyl acetate/lead citrate. Scale bar 0.6 μm.

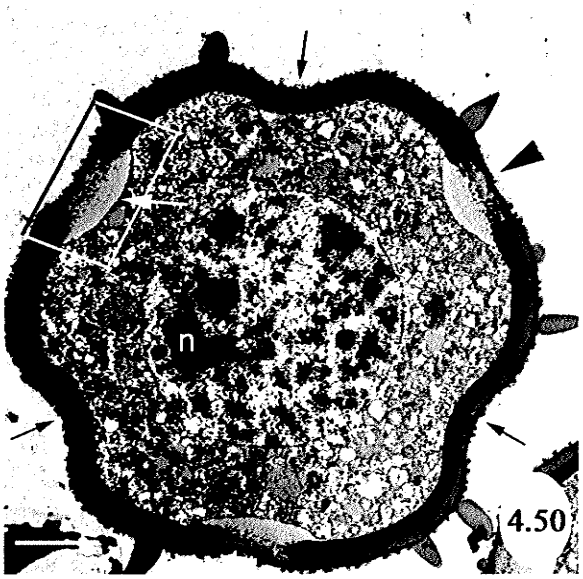

4.50

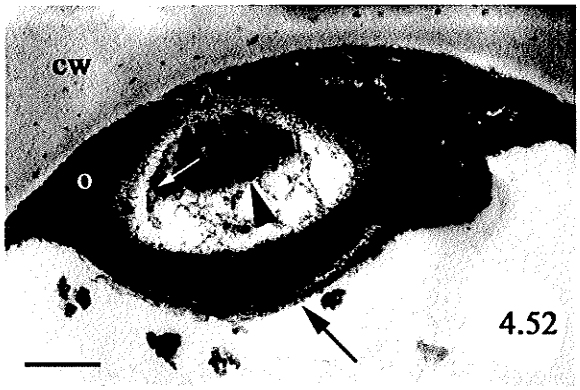

4.52

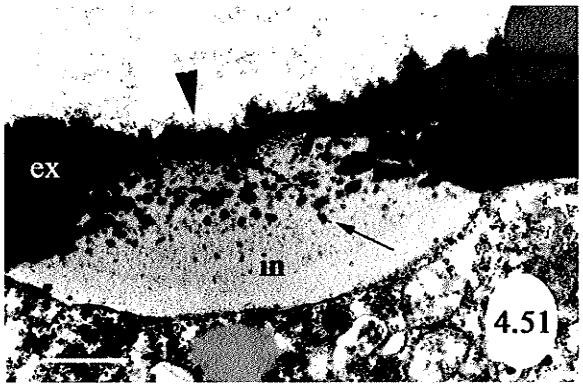

4.51

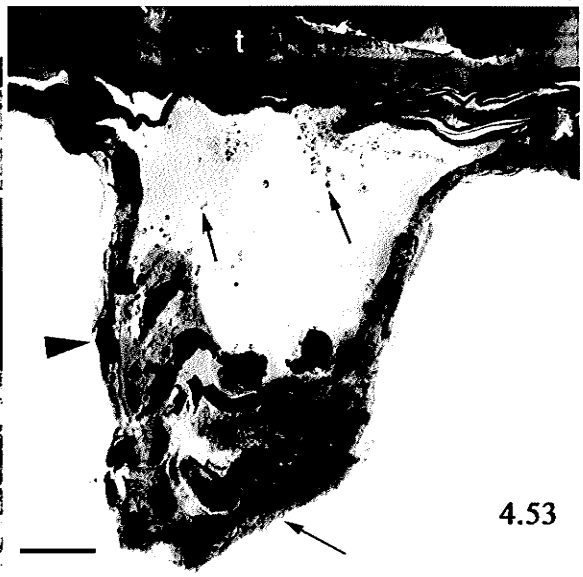

4.53

4.54

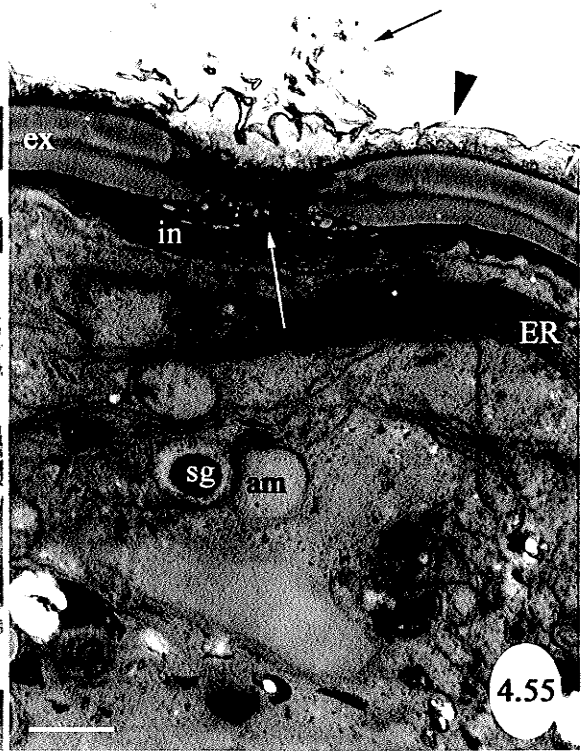

4.55

Figure 4.56 Light micrograph of a floral bud (LS) showing the perianth segments (large black arrowheads) around an anther containing mature pollen grains (pg), tapetal remnants (t) and an intact epidermis (ep). Crystal violet. Scale bar 115 μm.

Figure 4.57 Light micrograph of an anther (LS) showing mature pollen grains consisting of a generative nucleus (gn) within the generative cell wall (gcw) and a vegetative nucleus (vn). Tapetal remnants (t) and epidermal cells (ep) are also in view. Crystal violet. Scale bar 14 μm.

Figure 4.58 Light macrograph of an inflorescence at anthesis with open anthers (large white arrowhead) on a *Pinus banksiana* twig (medium white arrow). Scale bar 3 mm.

Figure 4.59 Light macrograph of an inflorescence at anthesis with open transverse slits (small white arrow) in the anthers. Perianth segments (medium white arrow) and a central nectary (large white arrowhead) are also visible. Scale bar 1.7 mm.

Figure 4.60 Light macrograph of an inflorescence at anthesis with a single terminal, four-parted flower (medium white arrow) and lower lateral trimerous flowers (small white arrow). Scale bar 3 mm.

Figure 4.61 Darkfield light micrograph of whole, mature pollen grains. Scale bar 70 μm.

Figure 4.62 Light micrograph of dehisced pollen grains containing a generative nucleus (gn) within the generative cell wall (gcw) and a vegetative nucleus (vn). The exine (ex) and intine (in) layers are also in view. Toluidine blue O. Scale bar 10 μm.

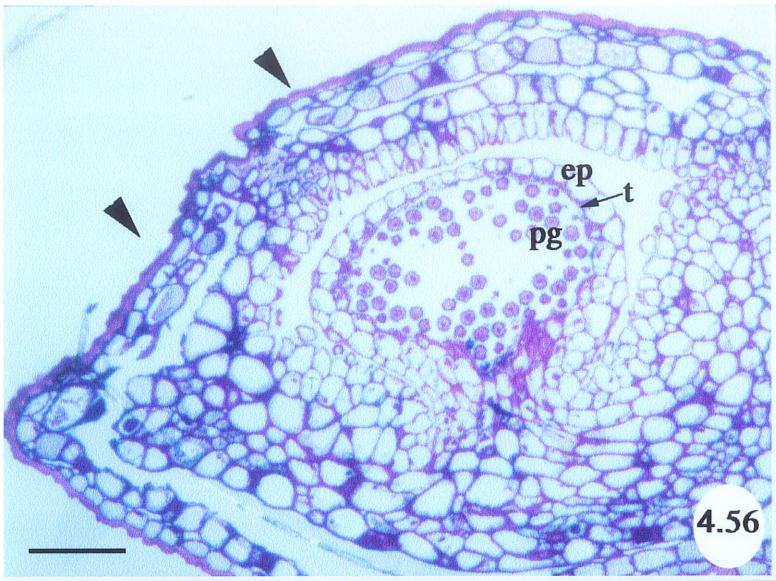
ep
t
pg
4.56

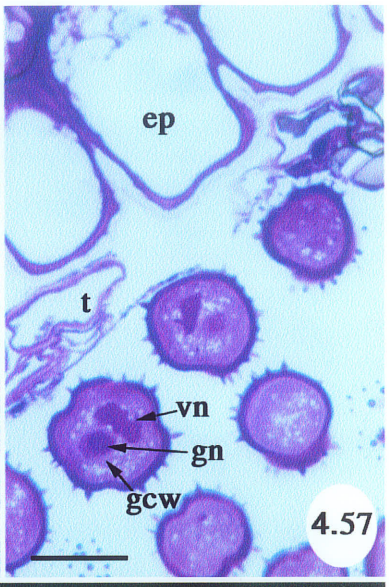
ep
t
vn
gn
gcw
4.57


4.58

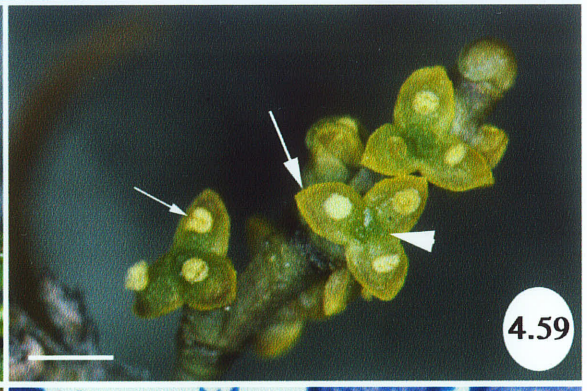
4.59


4.60

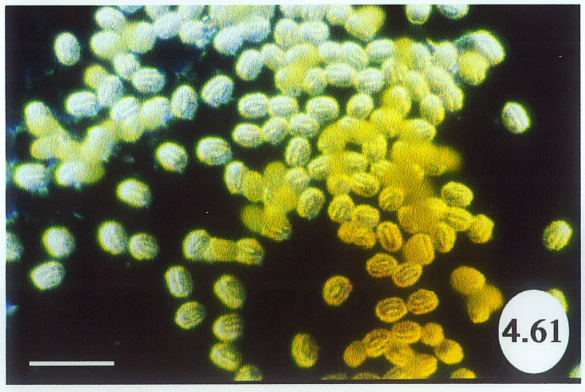
4.61

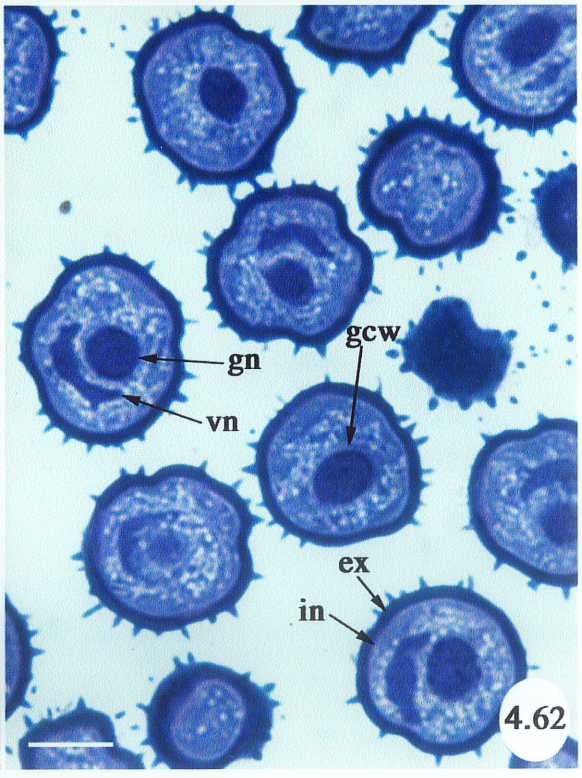
gn
gcw
vn
ex
in
4.62

Figure 4.63 Scanning electron micrograph of a mature pollen grain in equatorial view with spines (small white arrow) distributed over the surface, including within longitudinally oriented colpae (medium black arrow). Area in the box is enlarged in Figure 4.64. Scale bar 10 μm.

Figure 4.64 Scanning electron micrograph of a mature pollen grain in equatorial view spines (small white arrow) distributed over the surface, including within colpae (medium black arrow). Scale bar 5 μm.

Figure 4.65 Scanning electron micrograph of a mature pollen grain in equatorial view showing one each of the three longitudinally oriented colpae (small white arrow) and pseudocolpae (small black arrow). Scale bar 20 μm.

Figure 4.66 Transmission electron micrograph of a mature pollen grain (median CS) showing the vegetative nucleus (vn), generative nucleus (gn) and generative cell wall (gcw). The three apertures (large black arrowheads) within the colpae alternate with the three pseudocolpae (medium black arrows). The bilayered intine (in) thickens beneath the true colpae, whereas the bilayered exine (ex) thins. Uranyl acetate/lead citrate. Scale bar 4 μm.

Figure 4.67 Transmission electron micrograph of a mature pollen grain (OS) showing the generative nucleus (gn), generative cell wall (gcw), vegetative nucleus (vn), and vesicles (ve). Both nuclei contain prominent nucleoli (large black arrowheads). A surface layer of pollenkitt (medium black arrow) is apparent over the bilayered exine (small black arrows). Two thickened layers of intine (small white arrows) are apparent within the aperture. Uranyl acetate/lead citrate. Scale bar 4 μm.

Figure 4.68 Transmission electron micrograph of a pollen grain wall (CS) showing the bilayered nature of both the intine (small white arrows) and exine (small black arrows). A layer of pollenkitt (large black arrowheads) is visible over the papillae (medium black arrow) of the exine. Uranyl acetate/lead citrate. Scale bar 0.5 μm.

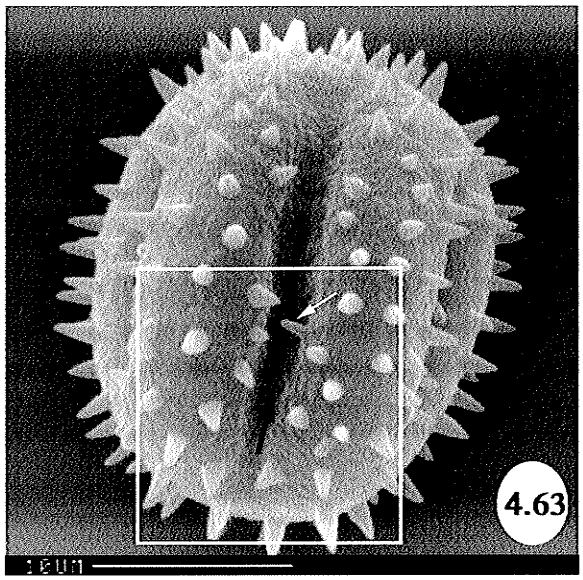
4.63

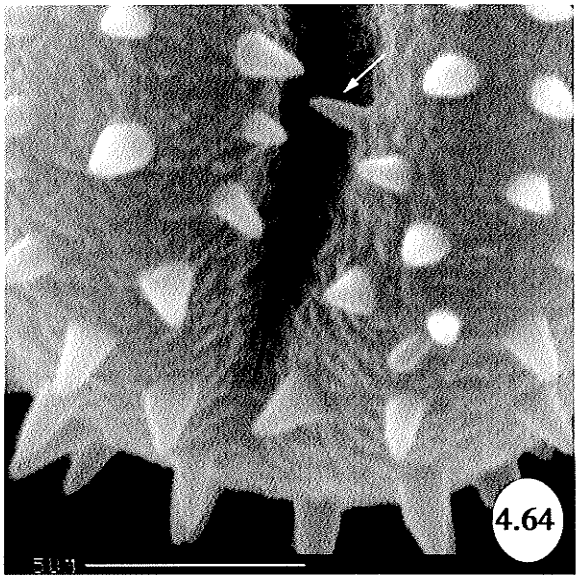
4.64

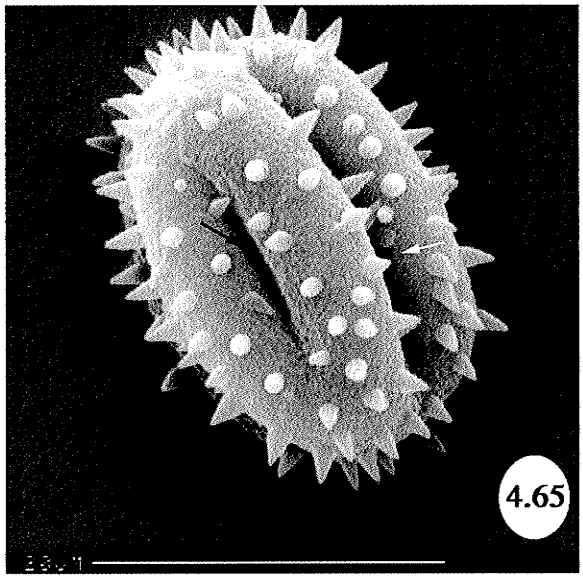
4.65

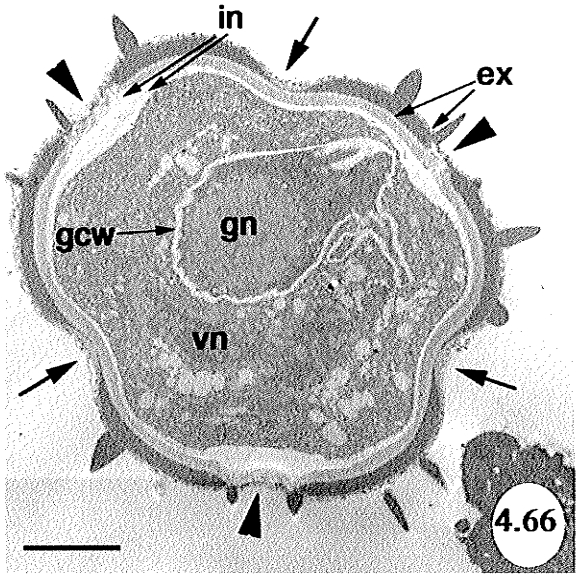
in
ex
gcw
gn
vn
4.66

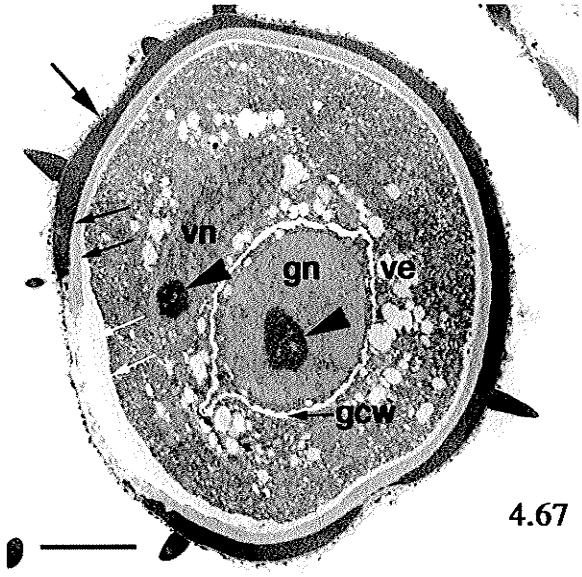
vn
gn
ve
gcw
4.67

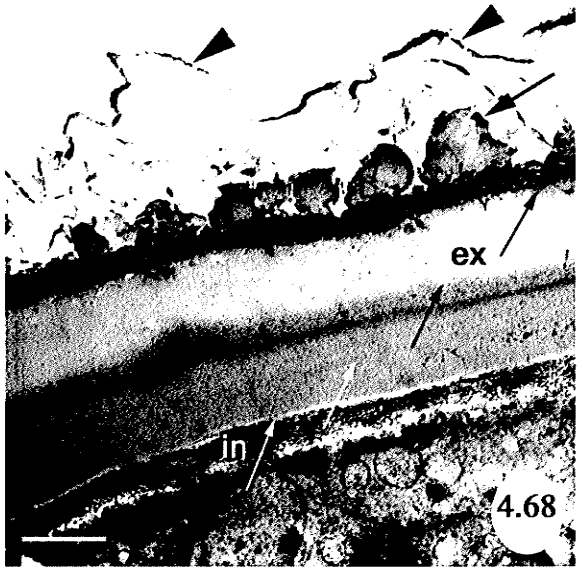
ex
in
4.68

5.0 RESULTS & DISCUSSION--POLLEN GERMINATION

5.1 Pollen Germination Percentages

The germination of mature pollen from open dehiscing anthers show a great deal of variation both at 20°C (Table 5.1) and 30°C (Table 5.2) incubation. This is true for all ten brooms sampled, with both 15 and 20% sucrose added to the medium. Mean germination ranges from 0% in many samples, to a high of 8.7% for a May 4th sample from broom #10, incubated with 15% sucrose at 20°C. Standard deviations tend to be high, and in a few cases, equal or exceed the mean.

Despite the low percent germinability of grains and the high degree of variability, the line graph of the mean germination for each date and treatment combination shows a consistent pattern (Figure 5.1). On all dates, 20°C incubated samples in both 15 and 20% sucrose, have higher germination percentages than samples incubated at 30°C. An analysis of variance (ANOVA) shows the 20°C means for May 4th to be significantly higher ($P = 0.0068$) than the means for all other dates. In addition, both the 15 and 20% sucrose treatments from May 4th at 20°C are significantly different from the 30°C data on the same date ($P = 0.0397$). Sucrose concentration, however, has a weaker effect on germination than temperature. An ANOVA based only on sucrose content fails to show statistical significance between the two concentrations used ($P = 0.15$). Clearly temperature has a stronger influence on germination than sucrose concentration when pollen is germinated *in vitro* under these conditions.

An influence of date on germination is also apparent, and all treatments show the same pattern. From an intermediate range of 1.1 - 2.3% mean germination on April 20th, the mean of most treatments decreases on April 27th to 0.5 - 1.5%, then significantly increases on May 4th ($P = 0.0402$) to a higher range of 1.5 - 3.2%, and subsequently decreases again to 1.3 – 2.0% on May 11th. These results are consistent with Gilbert's (1988) experiments with *Arceuthobium americanum* pollen. In both 1985 and 1987, she found a noticeable increase in germination three and four weeks after flower opening, after an initial low of germination percentages (< 5%).

The trend is robust as it is still observable when the data from all four treatments are combined (Figure 5.2). A decrease in germination percentage on April 27th and May 11th

is, in both cases, preceded by a dip in the daily minimum temperature to below 0°C. Gilbert (1988) also found this pattern of decreasing percent germination following lower ambient temperatures. Decreases, in her study and this one, occur after a four day lag period.

Conversely, an increase in both the minimum and maximum ambient daily temperature (Figure 5.2) precedes the significant increase in germination by pollen samples collected on May 4th (P=0.0402). Some temperate species, such as *Ranunculus adoneus* Gray (snow buttercup, Ranunculaceae), improve pollen germination success by tracking the sun to increase the temperature of maternal tissues through which pollen tubes are penetrating. When these heliotropic movements were restricted, less germinating pollen was found on pistils (Galen & Stanton 2003).

Prior exposure to other conditions also influences germination success. Drought, for example, induces male sterility in *Oryza sativa* probably by the impairment of metabolic pathways involving carbohydrates, since water stress inhibited normal starch accumulation in this study (Sheoran & Saini 1996). As well, a developmental influence has been hypothesized, as the effects on fertility are more pronounced for species such as *Diospyros* if the stress occurs before microsporocyte meiosis (Anjaneyulu & Lakshminarayana 1989).

Site exposure can have a dramatic effect on the local climate of an individual. Despite all ten brooms being in the same macroenvironment, the three brooms with higher germination percentages, # 5, 6 and 10, were all located in sites on the southern side of the infected tree with a more open exposure (Figure 3.1, personal observation). They therefore probably experienced a warmer temperature regime in their own microenvironment. Other brooms were located in more closed forest areas, and may not warm up as much during the day after cooler night temperatures.

Temperature extremes, especially radical temperature differentials between daily minimum and maximums, are likely stressful, and probably adversely affect transpiration and other physiological processes involving enzymes. *Mangifera indica* L. (mango, Anacardiaceae) appears to have a temperature sensitive phase during the development of pollen, as well as an optimum temperature range throughout the entire process. When

temperatures outside the optimal range occur, detrimental effects on pollen germination are observed on this species (Issarakraisila & Considine 1994). *Arceuthobium americanum* likely has optimal temperature range requirements, and particular phases could be more temperature sensitive than others.

Mature and geminating pollen does not exhibit the heat shock response normally seen in vegetative tissues. Specifically, pollen from many angiosperm species either do not produce heat shock proteins at all, or produce them at relatively low levels. These proteins contain abundant proline subunits, and are believed to ameliorate high temperature effects (Mascarhenas & Crone 1996). Even a short exposure to a high temperature such as 40°C decreases the rate of germination of mature *Arceuthobium americanum* pollen (Gilbert 1988).

Some of the variation in germination may be due to differences between individual brooms. When all treatment data is pooled and averaged for each date, pollen from broom #10 consistently germinates more readily, at least under the conditions used (Figure 5.3). Gilbert (1988) also found variability between brooms, and she concluded that this variation might be obscuring treatment effects. Differences could be due to environmental effects such as temperature or involve biotic factors such as host vigor, broom age and therefore age of infection, but when she germinated pollen from differently aged brooms held in growth cabinets at the same temperature, the same variability was observed.

Broom variation could also be genetically based, since *Arceuthobium americanum* has a high degree of genetic diversity (Jerome 2001). The optimal germination temperature can differ for different genotypes within the same species. In a pollen germination experiment on *Betula pendula*, the optimum temperature for germination differed for the five genotypes tested (Pasonen *et al.* 2000). In the present study, however, the pollen germination peaks of *Arceuthobium americanum* occur at the same time in all brooms, despite the variation between brooms. It is therefore more likely that a factor other than genetics is responsible for the variability.

When the pollen of some genera is germinated, more than one pollen tube might emerge from a single grain or tubes can exhibit branching (Khan *et al.* 1991, Pacini

1996). No polysiphony or bifurcated pollen tubes were observed *in vitro* for *Arceuthobium americanum*. This does not agree with reports for dwarf mistletoe by others. The simplest explanation for this discrepancy is that the multiple *in vivo* pollen tubes reported by Ross (2002)were most likely from multiple pollen grains germinating on a single stigma.

Overall, pollen germination percentages are low for all dates and treatments, and a great deal of variability is evident. It is not uncommon for a sample to have no germinated grains, and the highest individual germination percentage observed is 9.3% in a sample from broom #10 on May 4th (Appendix 8.2.3). This agrees with Gilbert (1988) for *Arceuthobium americanum*, although she occasionally had higher rates of germination. She performed a variety of different pollen germination experiments exploring many biotic and abiotic parameters. In an effort to further explore optimal germination conditions it was decided to combine several of these parameters in a single experiment. Indeed, the medium (1.5% agar, 0.01% boric acid with 15 or 20% sucrose) and temperatures (20 or 30°C) chosen for this study were based upon the best results from her study. If several parameters are combined in a single experiment a more direct comparison of their relative effects and interactions is possible.

Each plant species has its own unique requirements for optimal germination. Some species germinate readily in distilled water whereas others require a higher osmolality of the medium (Dafni 1992). The addition of sugars and salts increases germination percentages for some genera. Gilbert (1988) tested a variety of additives as to their ability to promote the germination of *Arceuthobium americanum* pollen. Boric acid and sucrose had small stimulatory effects, whereas salts such as calcium nitrate, potassium nitrate and magnesium sulfate appeared to have no effect.

The most common method of germinating pollen is using a Van Tieghem cell (Dafni 1992). This involves suspending mature grains in a sugar solution and then observing and counting germinated grains under the microscope. Other species benefit from being germinated on the surface of a medium solidified by gelatin or agar (Raghavan 1995). The latter has been found to be the best method of germinating *Arceuthobium americanum* pollen (Gilbert 1988), but pollen germination *in vitro* may not always be a

reflection of the rate *in vivo*. Despite attempts with a range of conditions, *Arabidopsis thaliana* pollen, for example, is always difficult to germinate *in vitro* (Taylor & Hepler 1997). Although good fertilization, seed production and fruit set is observed with pollen showing low *in vitro* germination percentages (Dafni 1992).

5.2 Pollen Tube Lengths

Mean pollen tube length varies from 19.6 - 80.9 μm for grains germinated at 20°C (Table 5.3), and from 19.6 - 64.1 μm for those germinated at 30°C (Table 5.4). As well, standard deviations are high and variable. No single broom or treatment stands out with longer or shorter tube lengths when examining data.

Means for each date and treatment, however, do show a consistent trend (Figure 5.4). Tube length decreases with each successive sampling date from a high on April 20th, through to a low on May 11th. With some exceptions, this is true for all four treatment combinations and is statistically significant ($P \leq 0.0001$). As well, the degree of variation decreases for all treatments on May 11th. Also, pollen germinated at 20°C has significantly longer tubes ($P = 0.0024$) than those incubated at 30°C for both sucrose concentrations. The effect of sucrose concentration alone on tube length is not statistically significant.

The same decrease in pollen tube length is evident when all brooms and treatments are averaged across each date (Figure 5.5). There does not, however, appear to be a relationship between tube length and ambient temperature, as there was for pollen germination percent and ambient temperature. This may or may not hold true *in vivo*, as pollen tube length is apparently influenced by temperature in other species. Flowers of *Ranunculus adoneus* allowed to track the sun had longer pollen tubes within their styles than those which were restrained, and thereby prevented from normal heliotropic movements (Galen & Stanton 2003). *Betula pendula*, however, grows longer tubes at an intermediate temperature, and shorter ones when temperature is either higher or lower than the optimal range (Pasonen *et al.* 2000).

Mean pollen tube lengths calculated for each broom (Figure 5.6) show a stronger correlation with date than with broom number. As previously observed, pollen collected on April 20th have the longest tube lengths, May 11th pollen the shortest, and April 27th

and May 4th means are generally intermediate between these two. Despite the variation, these are statistically significant differences (P = 0.0002).

Arceuthobium americanum has relatively small female flowers. This has implications when considering the distance pollen tubes need to elongate in order to effect fertilization. The stigma to pedicel distance in the pistillate plant is only 1.5 mm in this species (Hawksworth 1996). Even shorter measurements of 0.8 - 1.0 mm (Ross 2002) were reported for the same population of dwarf mistletoe from which the pollen used in this study was collected. Another consideration is the length of time which pollen was allowed to germinate on the agar medium. Hudson (1966) believed it took two months for pollen tubes of *Arceuthobium americanum* to grow through the stylar canals eventually reaching the female reproductive tissues. Ross (2002), on the other hand, only observed a delay of one month between pollination and fertilization. These two factors considered together-short stylar distance and delayed fertilization-might mean a lower rate of pollen tube elongation is normal for this species. If samples had been allowed to incubate for a longer than 48 hours, pollen tube lengths may have been much longer.

Faster growing pollen tubes could have a competitive advantage. This has been hypothesized for other species. Pollen genotype seems to be more important in this instance than either physiological or environmental factors (Hormaza & Herrero 1996). Additionally, pollen with faster growing tubes is believed to result in stronger, more resilient offspring, at least for some species. Pollen density itself could be partially responsible, as it can influence tube growth (Chen *et al.* 2000, Kopp *et al.* 2002). However, pollen density was not controlled for in this experiment.

Overall, date and broom appear to have the strongest effects on pollen tube length. Temperature also affects tube length, but to a lesser degree. However, the two sucrose concentrations tested appear to have no significant effect on the elongation of *Arceuthobium americanum* pollen tubes.

5.3 Correlation of Percent Germination to Pollen Tube Length

A comparison of mean percent germination with mean pollen tube length shows a weak positive relationship (Figure 5.7). Generally, as percent germination increases, the length of pollen tubes also tends to increase. Despite this positive association, the

coefficient of determination (r^2) is only 0.14. In other words, only about 14% of the variation in the germination percentages for each broom is accounted for by the relationship between percent germination and pollen tube length, when the individual means for each broom across all treatments are used.

When the means for each date are examined separately, differences between dates become apparent. The same general trend of increasing pollen tube length with increasing percentage germination holds, but not all dates have as strong a relationship. May 11th ($r^2 = 0.01$) and April 27th ($r^2 = 0.14$) have the weakest correlations, and also are the dates with the lowest overall germination percentages (Figure 5.2). Conversely, April 20th ($r^2 = 0.54$) and May 11th ($r^2 = 0.85$) both have stronger correlations, as well as higher mean germination percentages.

The large amount of variation both within and between samples makes it difficult to come to a definite conclusion as to whether or not there is any relationship between percent germination of pollen and tube length for *Arceuthobium americanum*. Interactions between date, temperature, sucrose concentration and broom for both percent germination (Table 5.5) and pollen tube length (Table 5.6) also complicate the analysis.

When pollen size was factored in, a relationship between percent germination and pollen tube length was found for *Dianthus* (Tejaswini 2002). Mean pollen size was not determined for each sample of *A. americanum* grains in this experiment. An analysis including pollen size might explain some of the variance between brooms and dates.

Future research on the germination of *Arceuthobium americanum* pollen is needed, and could focus on the effects of local environmental conditions on *in vitro* germination success. Aseptic techniques would allow for the incubation of pollen for longer periods, and could perhaps yield better results. Pollen size is another parameter that could be measured simultaneously with percent germination and pollen tube length. A comparison of *in vitro* methods with *in vivo* germination during the same time period might also prove interesting, especially if related to environmental conditions. A continuation of pollen germination research specifically on the Belair, Manitoba population is a logical one because of the groundwork already done, as well as its proximity and ease of access to laboratory facilities.

Table 5.1 Mean ± standard deviation of *in vitro* pollen germination (%) for each of ten subsamples incubated at 20°C. Means by date were calculated from the original data and not from the means within the table.

sucrose (%)	15				20			
sampling date	Apr-20	Apr-27	May-04	May-11	Apr-20	Apr-27	May-04	May-11
1	0.2 ± 0.2	1.8 ± 0.2	0.0	1.3 ± 1.5	1.3 ± 0.0	1.8 ± 0.7	2.7 ± 2.8	4.7 ± 1.2
2	0.0	0.8 ± 0.7	0.5 ± 0.7	2.3 ± 2.1	1.7 ± 1.9	1.0 ± 0.4	1.8 ± 1.6	1.0 ± 1.0
3	0.0	0.2 ± 0.2	1.0 ± 0.0	2.3 ± 2.1	1.3 ± 0.9	0.8 ± 0.7	0.3 ± *	1.0 ± 0.0
4	0.2 ± 0.2	0.0	1.3 ± 1.4	1.7 ± 2.1	0.3 ± 0.5	1.7 ± 0.0	2.5 ± 0.3	0.0
5	0.0	1.2 ± 0.7	1.2 ± 1.2	3.7 ± 0.6	2.5 ± 0.7	1.7 ± 1.4	2.2 ± 0.2	2.7 ± 2.5
6	0.0	0.0	3.2 ± 0.7	1.7 ± 1.2	3.7 ± 0.5	0.8 ± 0.2	3.3 ± 0.5	2.0 ± 2.0
7	0.7 ± 0.0	1.3 ± 0.9	2.0 ± 1.4	1.3 ± 1.2	3.2 ± 4.4	0.8 ± 0.7	2.7 ± 1.4	1.0 ± 1.7
8	2.3 ± 0.9	2.0 ± 0.4	3.7 ± 3.3	0.0	1.2 ± 0.2	1.2 ± 0.2	3.0 ± 0.4	3.0 ± *
9	2.7 ± 1.9	3.0 ± 1.8	8.3 ± 0.9	0.0	3.7 ± 0.5	1.7 ± 0.5	6.0 ± 2.4	2.0 ± *
10	5.0 ± 1.8	4.3 ± 4.2	8.7 ± 0.9	2.7 ± 2.1	3.8 ± 1.2	2.8 ± 2.1	7.2 ± 2.1	2.7 ± 2.3
means by date	1.1 ± 1.7	1.5 ± 1.8	3.0 ± 3.2	2.0 ± 1.6	2.3 ± 1.7	1.4 ± 0.9	3.3 ± 2.2	1.9 ± 1.9

*only one sample counted due to insufficient grains

Table 5.2 Mean ± standard deviation of *in vitro* pollen germination (%) for each of ten subsamples incubated at 30°C. Means by date were calculated from the original data and not from the means within the table.

sucrose (%)	15				20			
sampling date	Apr-20	Apr-27	May-04	May-11	Apr-20	Apr-27	May-04	May-11
1	0.7 ± 0.5	0.0	1.3 ± 0.5	0.3 ± 0.6	2.0 ± 0.4	0.2 ± 0.2	0.0	1.3 ± 2.3
2	0.0	0.0	2.2 ± 0.7	0.3 ± 0.6	0.2 ± 0.2	0.2 ± 0.2	1.3 ± 1.9	1.0 ± 1.0
3	0.0	0.0	0.0 ± *	0.7 ± 0.6	0.8 ± 1.2	0.2 ± 0.2	0.3 ± 0.4	1.0 ± 0.0
4	0.2 ± 0.2	0.0	0.8 ± 0.2	1.3 ± 0.6	0.0	0.0	1.7 ± 2.3	0.7 ± 1.2
5	1.3 ± 0.9	0.2 ± 0.2	2.8 ± 0.2	3.7 ± 2.9	3.5 ± 3.5	0.0	3.2 ± 2.6	3.3 ± 1.5
6	1.7 ± 0.0	0.3 ± 0.5	1.3 ± 1.4	1.7 ± 2.1	3.5 ± 1.1	0.5 ± 0.3	3.0 ± 0.0	3.0 ± 3.0
7	1.8 ± 1.2	0.3 ± 0.5	0.2 ± 0.2	1.3 ± 1.2	1.0 ± 1.0	0.3 ± 0.5	0.5 ± 0.7	0.7 ± 1.2
8	2.8 ± 0.7	0.7 ± 0.5	0.8 ± 1.2	0.0 ± *	1.0 ± 0.4	0.0	1.2 ± 0.2	1.0 ± *
9	2.7 ± 2.3	2.2 ± 2.1	1.7 ± 2.3	3.0 ± *	1.5 ± 1.1	1.0 ± 0.1	1.7 ± 1.4	0.0
10	3.2 ± 1.6	1.0 ± 1.0	4.0 ± 1.4	2.3 ± 1.5	8.0 ± 1.0	4.2 ± 0.2	2.3 ± 0.5	0.7 ± 0.6
means by date	1.4 ± 1.4	0.5 ± 0.9	1.6 ± 1.4	1.5 ± 1.6	2.2 ± 2.5	0.7 ± 0.9	1.5 ± 1.4	1.4 ± 1.6

*only one sample counted due to insufficient grains

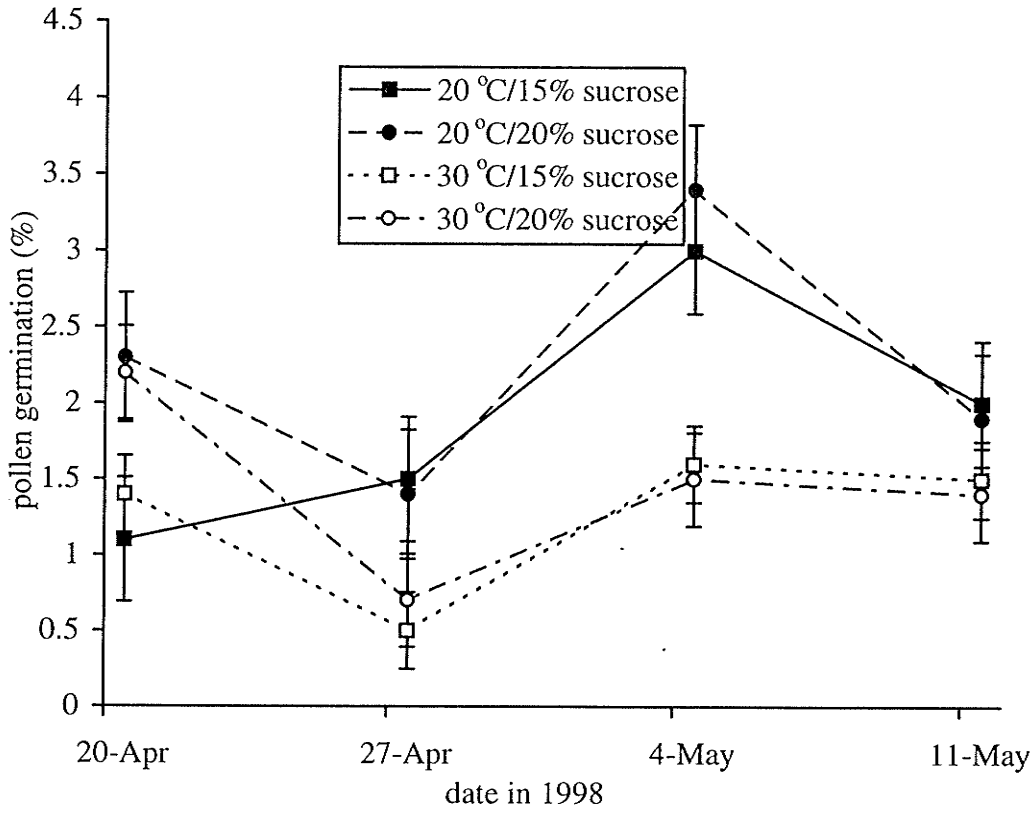

Figure 5.1 *In vitro* mean germination (%) of pollen collected during anthesis in 1998. Standard error bars are shown.

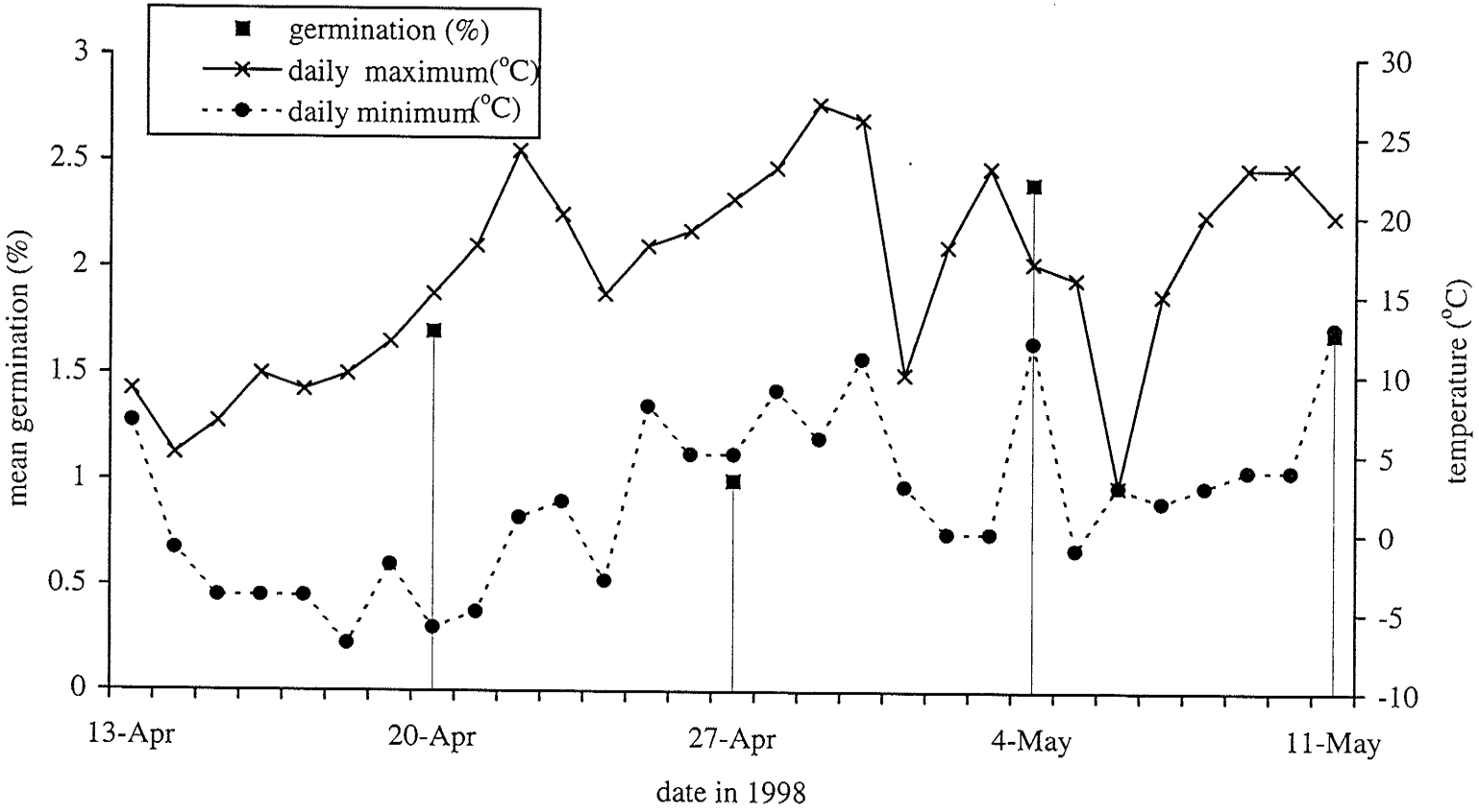

Figure 5.2 *In vitro* mean germination (%) of pollen compared with the daily minimum and maximum temperature (°C) collected during anthesis in 1998.

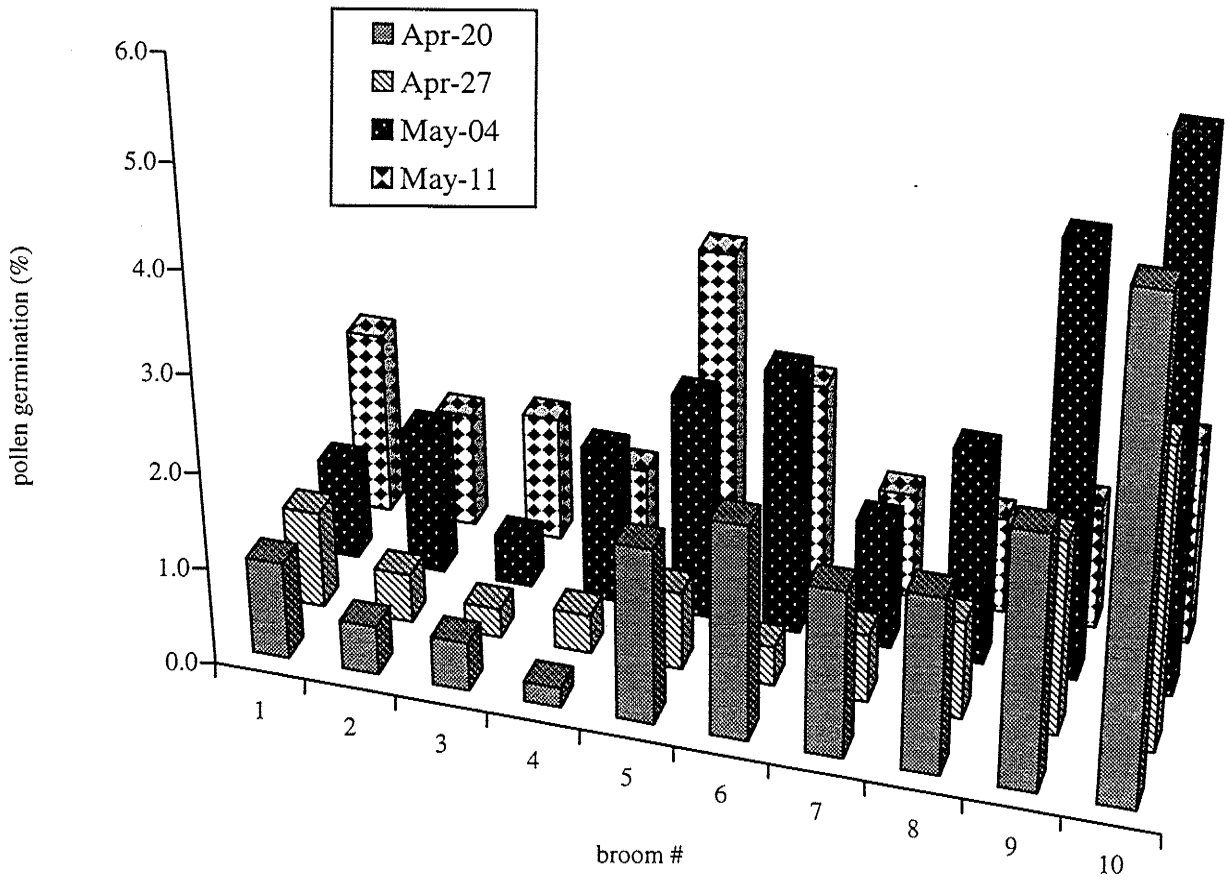

Figure 5.3 *In vitro* mean germination (%) of pollen collected during anthesis in 1998 from ten different brooms.

Table 5.3 Mean ± standard deviation of *in vitro* pollen tube length (μm) for each of ten subsamples incubated at 20°C. Means by date were calculated from the original data and not from the means within the table.

sucrose (%)	15				20			
sampling date	Apr-20	Apr-27	May-04	May-11	Apr-20	Apr-27	May-04	May-11
1	32.7 ± *	33.9 ± 19.8	**	19.6 ± 0.0	52.4 ± 24.6	39.3 ± 21.9	27.4 ± 14.8	22.4 ± 4.2
2	**	30.1 ± 11.0	21.8 ± 3.8	26.2 ± 7.6	39.3 ± 27.8	41.5 ± 22.6	44.8 ± 21.8	21.8 ± 3.8
3	**	19.6 ± *	21.8 ± 5.3	28.1 ± 7.3	50.8 ± 38.9	35.4 ± 17.1	32.7 ± *	19.6 ± 0.0
4	19.6 ± *	**	29.5 ± 10.5	23.6 ± 3.6	55.7 ± 13.9	34.0 ± 14.4	29.7 ± 11.6	**
5	**	37.4 ± 23.8	36.5 ± 14.6	25.6 ± 6.8	47.6 ± 22.7	35.4 ± 16.4	49.9 ± 8.0	27.0 ± 11.3
6	**	**	34.1 ± 16.3	22.3 ± 3.6	39.6 ± 21.5	70.7 ± 19.3	38.3 ± 20.3	24.0 ± 5.3
7	36.0 ± 8.4	32.7 ± 16.0	28.9 ± 9.8	22.9 ± 3.8	34.1 ± 14.1	49.8 ± 32.9	39.3 ± 29.6	39.3 ± 11.3
8	50.1 ± 26.5	41.3 ± 19.4	34.8 ± 14.2	**	40.2 ± 13.8	38.4 ± 19.1	37.8 ± 17.5	24.0 ± 7.6
9	40.1 ± 16.2	37.3 ± 18.9	41.5 ± 20.2	**	54.2 ± 33.8	38.6 ± 26.6	40.5 ± 22.4	19.6 ± 0.0
10	76.0 ± 53.4	65 ± 41.0	48.5 ± 26.7	21.3 ± 4.6	80.9 ± 63.5	43.5 ± 20.3	58.2 ± 27.2	31.1 ± 6.3
means by date	57.8 ± 42.2	44.8 ± 30.0	39.0 ± 20.7	24.1 ± 5.9	51.2 ± 37.1	41.3 ± 21.6	42.4 ± 24.2	25.1 ± 8.1

*only one grain measured **no germinated grains

Table 5.4 Mean ± standard deviation of *in vitro* pollen tube length (μm) for each of ten subsamples incubated at 30°C. Means by date were calculated from the original data and not from the means within the table.

sucrose (%)	15				20			
sampling date	Apr-20	Apr-27	May-04	May-11	Apr-20	Apr-27	May-04	May-11
1	37.7 ± 3.3	**	27.8 ± 9.1	19.6 ± 0.0	32.7 ± 15.8	26.2 ± *	**	24.6 ± 3.3
2	**	**	22.7 ± 5.1	19.6 ± 0.0	13.1 ± *	28.4 ± 15.1	40.0 ± 35.5	34.9 ± 6.5
3	**	**	**	22.9 ± 4.6	49.8 ± 23.4	19.6 ± *	26.2 ± 9.3	24.0 ± 7.6
4	26.2 ± *	26.2 ± *	22.3 ± 3.6	24.6 ± 9.8	26.2 ± *	**	30.8 ± 16.0	19.6 ± 0.0
5	31.9 ± 8.9	19.6 ± *	26.6 ± 10.5	25.0 ± 7.1	44.9 ± 15.2	**	34.8 ± 11.6	26.2 ± 10.2
6	53.0 ± 20.8	29.5 ± 4.6	24.6 ± 5.8	22.3 ± 3.6	36.5 ± 18.6	26.2 ± 6.5	42.2 ± 19.2	25.0 ± 4.9
7	35.7 ± 16.7	19.6 ± 0.0	32.7 ± *	22.9 ± 6.5	36.0 ± 14.2	36.0 ± 23.2	32.7 ± 13.1	26.2 ± 9.3
8	33.1 ± 11.2	50.8 ± 19.6	32.7 ± 19.1	**	43.7 ± 28.9	**	28.1 ± 11.2	26.2 ± *
9	41.7 ± 23.0	32.2 ± 14.3	32.7 ± 13.4	21.8 ± 3.8	37.8 ± 19.0	33.8 ± 12.7	43.9 ± 24.3	**
10	64.1 ± 70.5	24.0 ± 10.0	30.6 ± 11.7	25.3 ± 4.5	51.9 ± 50.2	31.2 ± 10.0	29.5 ± 13.0	29.5 ± 13.9
means by date	44.2 ± 37.5	31.4 ± 14.8	27.9 ± 10.7	23.8 ± 5.8	43.7 ± 33.3	30.8 ± 10.8	35.7 ± 19.0	26.0 ± 8.3

*only one grain measured

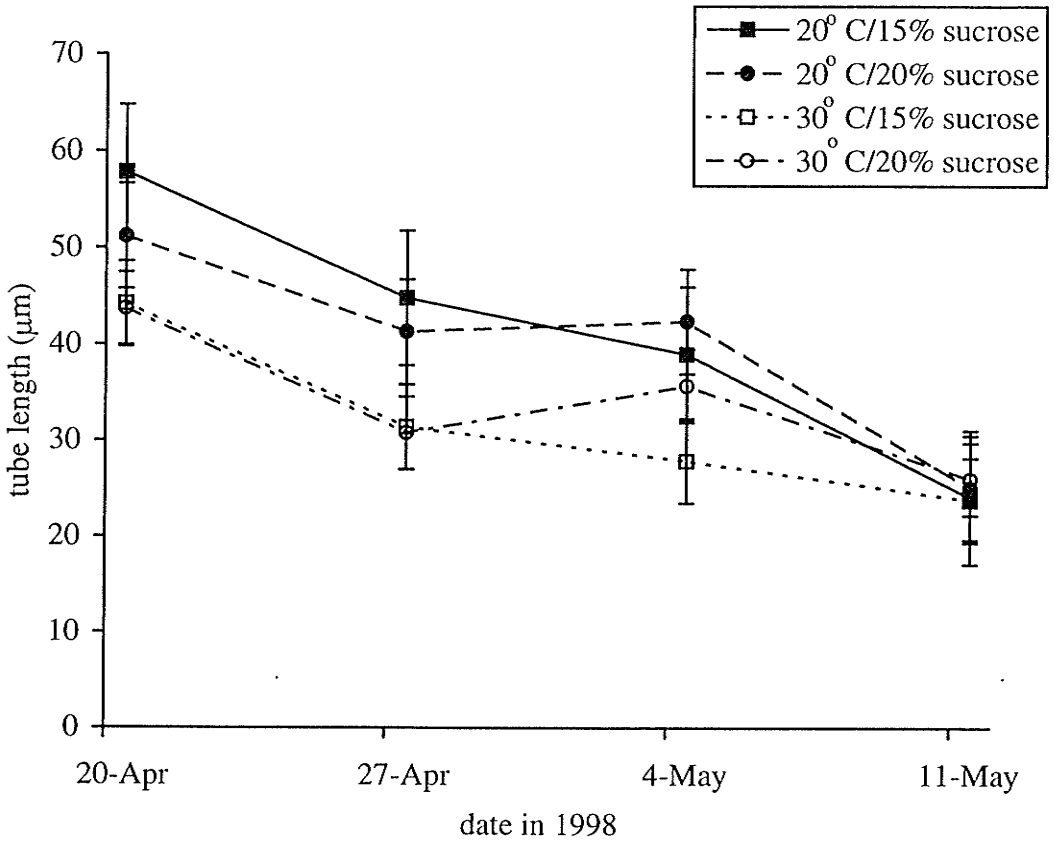

Figure 5.4 *In vitro* mean tube length (μm) of pollen collected during anthesis in 1998. Standard error bars are shown.

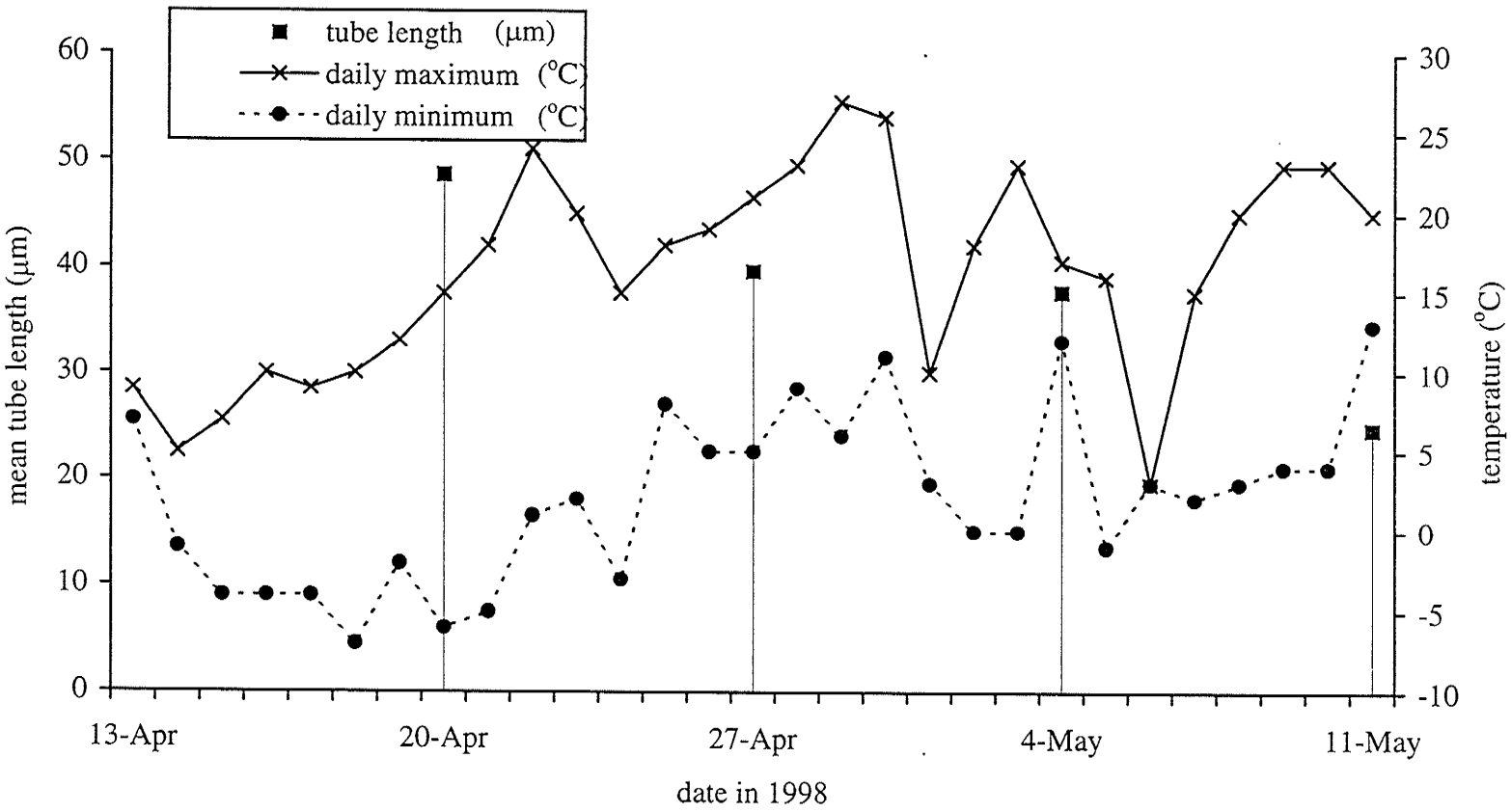

Figure 5.5 *In vitro* mean pollen tube length (μm) compared with the daily minimum and maximum temperature (°C) during anthesis in 1998.

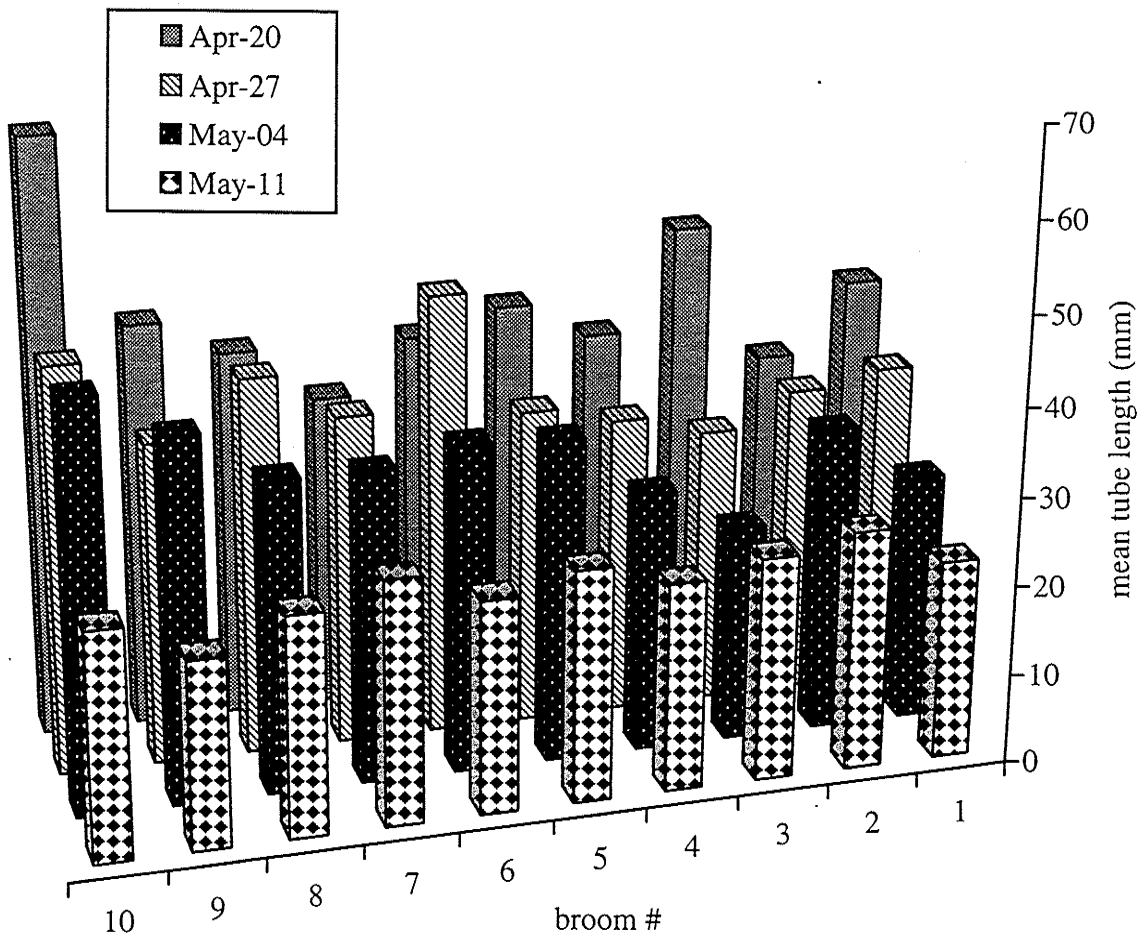

Figure 5.6 *In vitro* mean tube length (μm) of pollen collected during anthesis in 1998 from ten different brooms.

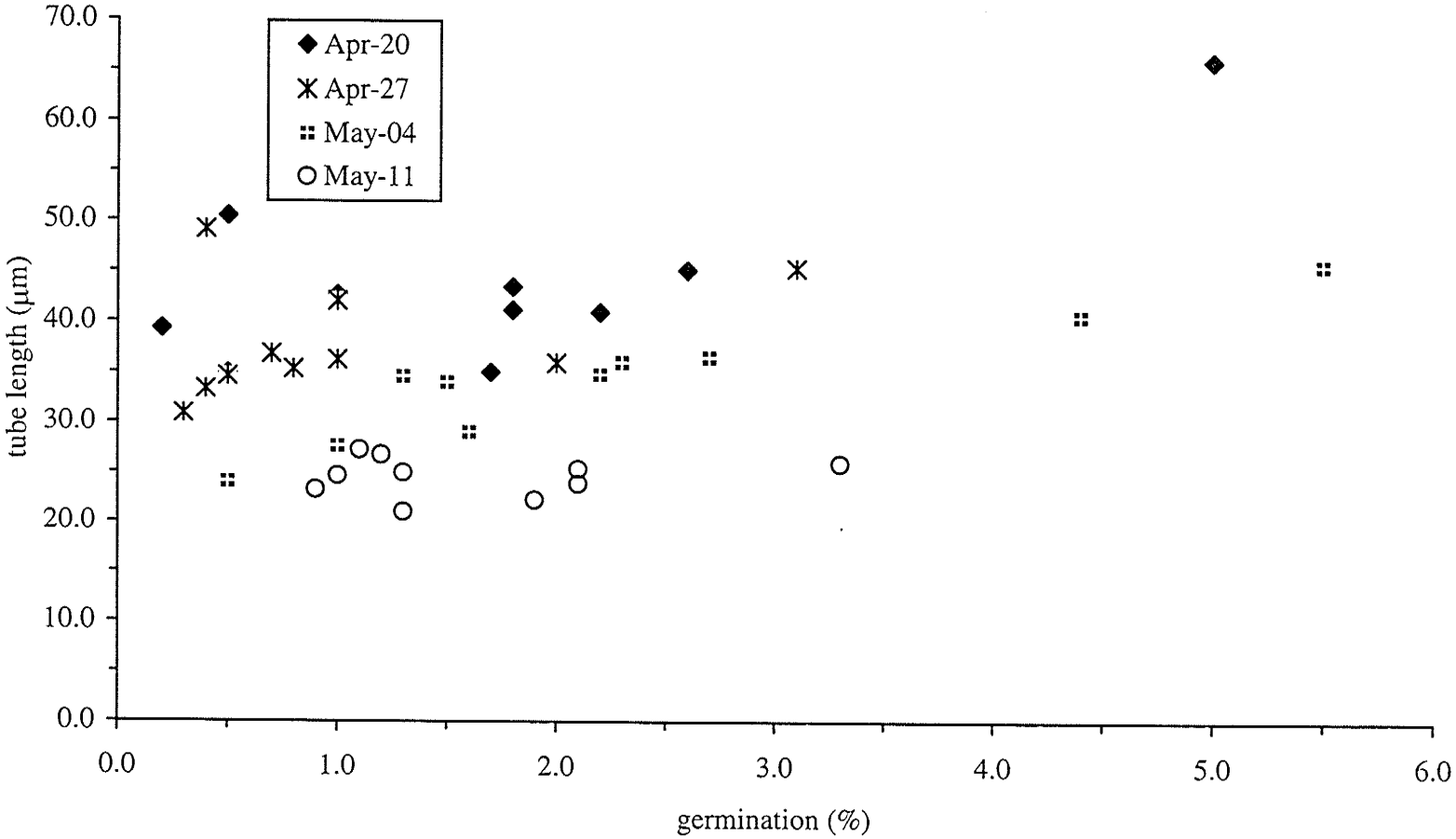

Figure 5.7 Scatterplot of *in vitro* germination (%) versus tube length (µm) of germinated pollen collected during anthesis in 1998. Means for each sample ($r^2 = 0.14$).

Table 5.5 Analysis of variance with interactions for *in vitro* pollen germination (%) of samples collected during anthesis in 1998.

Source	df	Sums of Squares	Mean Square	F-ratio	Probability
constant	1	975.164	975.164	485.21	≤0.0001
date	3	67.9415	22.6472	11.268	≤0.0001
temp	1	47.3875	47.3875	23.578	≤0.0001
date*temp	3	29.1492	9.71639	4.8345	0.0027
% suc	1	4.64379	4.64379	2.3106	0.1296
date*%suc	3	15.3168	5.1056	2.5404	0.0568
temp*%suc	1	0.298857	0.298857	0.1487	0.7001
broom	9	302.5	33.6111	16.724	≤0.0001
date*broom	27	138.415	5.12647	2.5507	≤0.0001
temp*broom	9	36.0184	4.00204	1.9913	0.0404
%suc*broom	9	30.4766	3.38628	1.6849	0.0924
error	275	552.692	2.00979		
total	341	1206.65			

Table 5.6 Analysis of variance with interactions for *in vitro* pollen tube length (μm) of samples collected during anthesis in 1998.

Source	df	Sums of Squares	Mean Square	F-ratio	Probability
constant	1	2138477	2138477	3400.9	≤0.0001
date	3	18769.6	6256.52	9.9499	≤0.0001
temp	1	5803.4	5803.4	9.2293	0.0024
date*temp	3	2721.74	907.247	1.4428	0.2286
% suc	1	805.961	805.961	1.2817	0.2578
date*%suc	3	2068.24	689.414	1.0964	0.3496
temp*%suc	1	162.502	162.502	0.25843	0.6113
broom	9	20288	2254.23	3.585	0.0002
date*broom	27	30019.6	1111.84	1.7682	0.0091
temp*broom	9	13894.7	1543.86	2.4552	0.0090
%suc*broom	9	3501.09	389.01	0.61865	0.7820
error	1295	814297	628.801		
total	1361	1018365			

6.0 CONCLUSIONS

Arceuthobium americanum exhibits a variation of the reduced type of anther wall development. Periclinal division of the primary parietal layer results in an inner secretory tapetum and an outer middle layer. The epidermis becomes an exothecium and no endothecium is present. Although there is some variation in the extent of the columella, the anther is monosporangiate. Differing planes of section and columella variation may have caused the previous confusion in the literature. Cytomictic channels are present between individual microsporocytes at least until the callose-rich walls have begun to be deposited. Channels are also present between tapetal cells at the uninucleate microspore stage, but not between microsporocytes and tapetal cells.

Meiosis results in tetrahedral tetrads of microspores. Released microspores are initially small, become vacuolate and enlarge before the deposition of sporopollenin wall material. This represents the normal type of microgametogenesis. The time of the meiotic event is when presumed cytoplasmically male sterile anthers are first observed.

Mitosis does not appear to be asymmetric. The two nuclei are initially spherical and centrally located. The vegetative nucleus undergoes a shape change to become more elongate and the generative remains fairly spherical. The opposite is reported for most other angiosperms. Both cells were observed to contain mitochondria and amyloplasts. This has implications for the male inheritance of DNA-containing organelles.

Development is completed before winter and pollen overwinters as bicellular grains within intact floral buds. Abundant starch grains, seen within pollen grains in the fall are not as prevalent the following spring at anthesis.

An increased rate of *in vitro* germination and pollen tube length was observed when grains were incubated at 20°C as compared to 30°C. Sucrose concentrations of 15 and 20%, however, had no significant effect on *in vitro* germination. Date of sampling and source of pollen also influenced pollen germination, but the large amount of variation may have obscured any other trends.

7.0 APPENDICES

Fixatives, Stains and Other Recipes

Appendix 8.1.1 Fixatives

Glutaraldehyde

12 mL 25% glutaraldehyde
50 mL 0.05 M potassium phosphate buffer, pH 6.8
DDW up to 100 mL

Mix the above components together and keep refrigerated until use. Final concentrations are 3% glutaraldehyde and 0.025 M phosphate buffer (Hayat 1970).

Karnovsky's Solution

8 grams paraformaldehyde
60 mL DDW

Dissolve the paraformaldehyde in the water warmed to 65°C, in a fumehood. Add 1 N NaOH dropwise to clear the solution, swirling after each addition. Cool the solution to room temperature and add:

40 mL 25% glutaraldehyde

Finally make the solution up to 200 mL with 0.05 M potassium phosphate buffer, pH 6.8. The final pH of the solution should be checked and adjusted to 6.8, if necessary using either 1 N HCl or 1 N NaOH. Final concentrations are 4% paraformaldehyde and 0.025 M phosphate buffer. This solution should be kept in a 2-4°C refrigerator until ready for use (Karnovsky 1965).

Cacodylate-buffered Osmium Tetroxide-Potassium Ferricyanide Fixatives

Primary Fix

0.258 g $CaCl_2 \cdot 2H_2O$
100 mL DDW

Dissolve the $CaCl_2$ in the DDW to make a 20 mM stock solution. Then mix:

7.0 mL 20 mM $CaCl_2$
3.0 mL 25% glutaraldehyde
10 mL 0.05 M cacodylate buffer, pH 7.0

This results in a 0.007 mM $CaCl_2$, 3.75% glutaraldehyde, and 0.025 M cacodylate buffered solution, pH 7.0.

Secondary Fix

1.0 mL 20 mM $CaCl_2$
0.5 mL DDW
0.5 mL 0.2 M cacodylate buffer, pH 7.0

Mix the above three, this will result in 2 mL of a 10 mM $CaCl_2$, 0.05 M cacodylate buffered solution, at pH 7.0. Dissolve in this:

0.032 grams $KFe(CN)_6$

Then add 2 mL of 4% OsO_4. The final solution contains 5 mM $CaCl_2$, 0.8% $KFe(CN)_6$, 2% OsO_4 in a 0.025 M cacodylate buffer, at pH 7.0 (Hepler 1981).

Appendix 8.1.2 Buffers

Potassium Phosphate Buffer

Stock Solution A

13.61 grams KH_2PO_4 (monobasic)
500 mL DDW

Stock Solution B

17.42 grams K_2HPO_4 (dibasic)
500 mL DDW

Use 51 mL of A with 49 mL of B, then dilute to 200 mL with DDW. The final concentration is 0.2 M, pH 6.8. This 0.2 M stock may be diluted further with DDW to make 0.05 M and 0.025 M solutions (Hayat 1970).

Cacodylate Buffer

Stock Solution A

21.4 grams $Na(CH_3)_2AsO_2 \cdot 3H_2O$
500 mL DDW

Stock Solution B

1.0 mL of 12 M HCl, concentrated
DDW up to a final volume of 60 mL for a 0.2 M concentration

Use 50 mL of A with 6.3 mL of B, then dilute this to 200 mL with DDW. The final concentration is 0.2 M, pH 7.0. This 0.2 M stock may be diluted further with DDW to make 0.05 M and 0.025 M solutions (Hayat 1970).

Appendix 8.1.3 Pollen germination media

20% Sucrose Medium

7.5 grams agar
0.05 grams boric acid
100 grams sucrose
500 mL DDW

15% Sucrose Medium

7.5 grams agar
0.05 grams boric acid
75 grams sucrose
500 mL DDW

Measure out the components for each sucrose concentration into a 1 litre Erlenmeyer flask. Heat to 50 °C and using a stir bar, mix until the agar is dissolved. Remove the stir bar and stopper flasks with a cotton plug. Cover the plugs and top of each flask with aluminum foil and autoclave for 15 minutes at 15 psi and 121°C. Allow flasks to cool to 37°C in a water bath, and then pour, using aseptic technique, into 95 mm, 15 mL sterile disposable petri dishes. Once the medium has solidified the dishes should be inverted, and stored in the refrigerator until ready to use.

Appendix 8.1.4 Resins

LR White

A pre-mixed acrylic resin supplied by the London Resin Company. LR White requires the exclusion of oxygen for polymerization, and this was accomplished by carefully floating a second aluminum pan on top of the liquid plastic during thermal curing.

Spurr Resin

10 grams vinylcyclohexene dioxide (ERL 4206 or VCD)

8 grams diglycidyl ether of propylene glycol (DER 736)
26 grams nonenyl sucinnic anhydride (NSA)
0.4 grams dimethylaminoethanol (S-1 or DMAE)

To make up approximately 40 mL, weigh out successive monomer components in a disposable container in the fumehood. Mix thoroughly after each addition. Keep at room temperature until ready for polymerization (Spurr 1969).

Ultra-Low Viscosity Resin

12 grams vinylcyclohexene dioxide (ERL 4206 or VCD)
24 grams *n*-octoenyl succinic anhydride (OSA)
1.2 grams 1,4-butanediol diglycidyl ether (Araldite RD-2)
0.4 grams dimethylaminoethanol (S-1 or DMAE)

To make up approximately 40 mL, weigh out successive monomer components in a disposable container in the fumehood. Mix thoroughly after each addition. Keep at room temperature until ready for polymerization (Mascorro *et al.* 1976).

Appendix 8.1.5 Stains

Aniline Blue

0.05 grams aniline blue
0.025 M potassium phosphate buffer, pH 6.8

Dissolve the aniline blue in the buffer for a 0.05% staining solution, and store in a darkened bottle in the refrigerator. Sections may be mounted directly in the stain for observation. The solution should be discarded if it turns green. This is an excellent counterstain for calcofluor stained slides. Keep slides in the dark until observation. The resin should be removed (Appendix 8.1.6) before staining (O'Brien & McCully 1981).

Aniline Blue Black

7.0 mL acetic acid
DDW up to 100 mL

Dissolve the acetic acid in the water for a 7% solution and add:

1.0 grams aniline blue black

Dissolve the stain in the acetic acid solution and filter with Whatman's No. 1 filter paper before use. Stain for 10 minutes at 50°C and rinse thoroughly with 7% acetic acid. Mount slides in glycerol with a little added 5% acetic acid. This is a good counterstain for the PAS reaction and can be used on epoxy sections without removing the resin (O'Brien & McCully 1981).

Basic Toluidine Blue O

0.1 grams sodium bicarbonate
100 mL DDW

Dissolve the sodium bicarbonate in the water and add:

0.5 grams toluidine blue O

The final pH is around 11.1. Dispense via a syringe equipped with a 0.45 μm millipore filter onto sections on glass slides. Stain for 1 minute on a slide warmer set to 75°C and

rinse thoroughly with water. This solution can be used on epoxy sections without removing the resin (O'Brien & McCully 1981).

Calcofluor White

0.1 grams Calcofluor White M2R
100 mL DDW

Dissolve calcofluor in the water to make a 0.1% stock solution. Store this in the fridge in the dark. For a working solution, dilute the stock solution 1:9 with DDW and use immediately on slides with the resin removed. Stain for one minute and rinse briefly with water. Keep slides in the dark until ready to examine. Mount with glycerol or if counterstaining with aniline blue, use it as the mountant medium. The resin should be removed (Appendix 8.1.6) before staining (O'Brien & McCully 1981).

Crystal Violet

Solution A

2.0 grams crystal violet (gentian violet)
20 mL 95% ethanol

Solution B

0.8 grams ammonium oxalate
80 mL DDW

Mix A and B (pH 6.7) together and filter with No. 1 Whatman filter paper. Dispense via a syringe equipped with a 0.45 μm millipore filter onto sections on glass slides. Stain for 30 seconds to 1 minute on a slide warmer set to 75°C then rinse thoroughly with water. This stain can be used without removing the resin (Sumner 1986).

Lead Citrate

1.33 grams $Pb(NO_3)_2$
1.76 grams $Na_3(C_6H_5O_7)\cdot 2H_2O$
30 mL DDW, boiled and cooled (to remove CO_2)

Dissolve the solids by shaking the above in a 50 mL volumetric flask. Let the solution stand for a further 30 minutes, intermittently shaking it. Leave the stopper in to avoid excess intake of ambient CO_2. Add:

8.0 mL 1N NaOH

Dilute to 50 ml in the volumetric flask. Store the solution in an airtight container at room temperature and filter with a 0.45 μm syringe filter just before using. Staining should be done in a petri dish with KOH pellets, to maintain a CO_2-free atmosphere. The resin does not need to be removed before staining (Reynolds 1963).

Periodic Acid Schiff's Method

Block aldehyde groups by immersing slides in a 5% solution of 2,4-dinitrophenyl-hydrazine in 15% acetic acid in a coplin jar, for 15 minutes at room temperature. Rinse with running tap water for 10 minutes and then transfer slides to 1% periodic acid for 30 minutes. Again wash with tap water for 15 minutes. Now place slides in Schiff's reagent for 40 minutes and wash with running water for 10 minutes, counterstain (if desired) with

aniline blue black, toluidine blue or crystal violet, air dry, mount with glycerol and observe. The resin should be removed (Appendix 8.1.6) before staining (Dufresne 1992).

Sudan Black B

2.0 grams Sudan Black B
100 mL 70% ethanol
50% ethanol

Dissolve the stain in 70% ethanol by warming it to 37°C overnight. The following day filter it twice with Whatman No. 1 filter paper before use. Sections should be preincubated in the 50% ethanol for 2 minutes at room temperature. Then stain by immersing slides in the staining solution in a coplin jar, for 5 minutes at 55°C. Rinse briefly with a stream of 50%, and wash with running water 5 minutes. Air dry and mount with glycerol. The resin should be removed (Appendix 8.1.6) before staining (O'Brien & McCully 1981, Willey 1971).

Uranyl Acetate

3.75 grams uranyl acetate
50 mL 50% methanol

Dissolve the uranyl acetate in the methanol. This results in a saturated solution (7.5%) of uranyl acetate to be used for post-sectioning staining. For *en bloc* staining, dilute 1:14 with 50% methanol. Store the solutions in the dark and filter with a 0.45 μm syringe filter just before using. Staining should be done in an aluminum foil-covered petri dish, in order to keep the stain in the dark. The resin does not need to be removed before staining (Hayat 1970).

Appendix 8.1.6 Miscellaneous Recipes

Haupt's Adhesive

1 grams gelatin
100 mL DDW

Dissolve the gelatin in the water warmed to 30°C, in a fumehood. Add:

15 mL glycerin (glycerol)
1 gram phenol crystals

Stir thoroughly and filter the solution. Pour some into a coplin jar and dip glass slides into the solution using forceps. Let the slides dry vertically and replace them in boxes when completely dry (Willey 1971).

Resin Removal

Immerse slides in a saturated solution of potassium hydroxide in 95% ethanol for 2 minutes. Rinse slides in three changes of 95% ethanol and then five minutes in running tap water. It is best to use sections on gelatin coated slides for this procedure, as there may be problems with section removal with uncoated slides (Sumner 1986).

Appendix 8.2.1 Germination (%) of *Arceuthobium americanum* pollen collected on April 20, 1998 from ten *Pinus banksiana* brooms. Medium contained 1.5% agar, 0.01% boric acid, and 15% or 20% sucrose, and was incubated at either 20 or 30 °C, in the dark.

temperature (°C)	20				30			
% sucrose	15		20		15		20	
	replicates							
Broom #	a	b	a	b	a	b	a	b
1	0.3	0.0	1.3	1.3	0.3	1.0	1.7	2.3
2	0.0	0.0	0.3	3.0	0.0	0.0	0.3	0.0
3	0.0	0.0	0.7	2.0	0.0	0.0	0.0	1.7
4	0.3	0.0	0.7	0.0	0.3	0.0	0.0	0.0
5	0.0	0.0	2.0	3.0	0.7	2.0	1.0	6.0
6	0.0	0.0	3.3	4.0	1.7	1.7	4.3	2.7
7	0.7	0.7	0.0	6.3	1.0	2.7	0.3	1.7
8	3.0	1.7	1.3	1.0	2.3	3.3	1.3	0.7
9	1.3	4.0	4.0	3.3	4.3	1.0	2.3	0.7
10	6.3	3.7	4.7	3.0	2.0	4.3	7.3	8.7

Appendix 8.2.2 Germination (%) of *Arceuthobium americanum* pollen collected on April 27, 1998 from ten *Pinus banksiana* brooms. Medium contained 1.5% agar, 0.01% boric acid, and 15% or 20% sucrose, and was incubated at either 20 or 30 °C, in the dark.

temperature (°C)	20				30			
% sucrose	15		20		15		20	
	replicates							
Broom #	a	b	a	b	a	b	a	b
1	1.7	2.0	1.3	2.3	0.0	0.0	0.0	0.3
2	0.3	1.3	0.7	1.3	0.0	0.0	0.0	0.3
3	0.3	0.0	0.3	1.3	0.0	0.0	0.0	0.3
4	0.0	0.0	1.7	1.7	0.0	0.0	0.0	0.0
5	1.7	0.7	0.7	2.7	0.0	0.3	0.0	0.0
6	0.0	0.0	1.0	0.7	0.0	0.7	0.3	0.7
7	0.7	2.0	0.3	1.3	0.7	0.0	0.0	0.7
8	1.7	2.3	1.3	1.0	1.0	0.3	0.0	0.0
9	4.3	1.7	2.0	1.3	0.7	3.7	0.0	2.0
10	7.3	1.3	4.3	1.3	0.3	1.7	4.3	4.0

Appendix 8.2.3 Germination (%) of *Arceuthobium americanum* pollen collected on May 4, 1998 from ten *Pinus banksiana* brooms. Medium contained 1.5% agar, 0.01% boric acid, and 15% or 20% sucrose, and was incubated at either 20 or 30 °C, in the dark (N/G = no grains).

temperature (°C)	20				30			
% sucrose	15		20		15		20	
	replicates							
Broom #	a	b	a	b	a	b	a	b
1	0.0	0.0	4.7	0.7	1.7	1.0	0.0	0.0
2	1.0	0.0	0.7	3.0	2.7	1.7	2.7	0.0
3	1.0	1.0	0.3	N/G	N/G	0.0	0.0	0.7
4	2.3	0.3	2.7	2.3	1.0	0.7	0.0	3.3
5	0.3	2.0	2.3	2.0	3.0	2.7	5.0	1.3
6	2.7	3.7	3.0	3.7	0.3	2.3	3.0	3.0
7	1.0	3.0	3.7	1.7	0.0	0.3	0.0	1.0
8	6.0	1.3	2.7	3.3	1.7	0.0	1.3	1.0
9	9.0	7.7	7.7	4.3	0.0	3.3	0.7	2.7
10	9.3	8.0	8.7	5.7	5.0	3.0	2.0	2.7

Appendix 8.2.4 Germination (%) of *Arceuthobium americanum* pollen collected on May 11, 1998 from ten *Pinus banksiana* brooms. Medium contained 1.5% agar, 0.01% boric acid, and 15% or 20% sucrose, and was incubated at either 20 or 30 °C, in the dark (N/G = no grains).

temperature (°C)	20						30					
% sucrose	15			20			15			20		
	replicates											
Broom #	a	b	c	a	b	c	a	b	c	a	b	c
1	3.0	1.0	0.0	6.0	4.0	4.0	1.0	0.0	0.0	0.0	0.0	4.0
2	4.0	3.0	0.0	1.0	0.0	2.0	0.0	1.0	0.0	1.0	0.0	2.0
3	3.0	0.0	4.0	1.0	1.0	1.0	1.0	0.0	1.0	1.0	1.0	1.0
4	0.0	4.0	1.0	0.0	0.0	0.0	2.0	1.0	1.0	2.0	0.0	0.0
5	4.0	3.0	4.0	3.0	0.0	5.0	7.0	2.0	2.0	3.0	2.0	5.0
6	1.0	1.0	3.0	2.0	0.0	4.0	1.0	0.0	4.0	3.0	6.0	0.0
7	0.0	2.0	2.0	0.0	0.0	3.0	2.0	0.0	2.0	0.0	2.0	0.0
8	0.0	N/G	N/G	3.0	N/G	N/G	0.0	N/G	N/G	1.0	N/G	N/G
9	0.0	N/G	N/G	2.0	N/G	N/G	3.0	N/G	N/G	0.0	N/G	N/G
10	2.0	1.0	5.0	4.0	4.0	0.0	2.0	1.0	4.0	0.0	1.0	1.0

Appendix 8.3.1 Pollen tube lengths (μm) of *in vitro* germinated *Arceuthobium americanum* pollen collected on April 20, 1998 from ten *Pinus banksiana* brooms. Medium contained 1.5% agar, 0.01% boric acid, and 15% or 20% sucrose, and was incubated at either 20 or 30 °C, in the dark (N/G = no grains).

broom #	temperature (°C)			
	20		30	
	sucrose (%)			
	15	20	15	20
1	32.7	39.3	39.3	19.6
1	N/G	45.8	39.3	26.2
1	N/G	19.6	32.7	32.7
1	N/G	26.2	39.3	19.6
1	N/G	26.2	N/G	52.4
1	N/G	39.3	N/G	52.4
1	N/G	52.4	N/G	19.6
1	N/G	32.7	N/G	32.7
1	N/G	65.5	N/G	32.7
1	N/G	78.6	N/G	39.3
1	N/G	85.1	N/G	65.5
1	N/G	85.1	N/G	19.6
1	N/G	85.1	N/G	N/G
2	N/G	45.8	N/G	13.1
2	N/G	85.1	N/G	N/G
2	N/G	19.6	N/G	N/G
2	N/G	19.6	N/G	N/G
2	N/G	26.2	N/G	N/G
3	N/G	19.6	N/G	65.5
3	N/G	32.7	N/G	78.6
3	N/G	104.8	N/G	26.2
3	N/G	117.9	N/G	26.2
3	N/G	52.4	N/G	52.4
3	N/G	26.2	N/G	N/G
3	N/G	32.7	N/G	N/G
3	N/G	19.6	N/G	N/G
4	19.6	45.8	26.2	N/G
4	N/G	65.5	N/G	N/G
5	N/G	72.0	39.3	32.7
5	N/G	85.1	39.3	45.8
5	N/G	32.7	39.3	45.8
5	N/G	32.7	32.7	58.9
5	N/G	58.9	26.2	32.7

Appendix 8.3.1 continued

5	N/G	45.8	39.3	39.3
5	N/G	45.8	19.6	26.2
5	N/G	19.6	19.6	32.7
5	N/G	39.3	N/G	45.8
5	N/G	26.2	N/G	19.6
5	N/G	32.7	N/G	45.8
5	N/G	32.7	N/G	85.1
5	N/G	58.9	N/G	39.3
5	N/G	98.2	N/G	52.4
5	N/G	32.7	N/G	52.4
5	N/G	N/G	N/G	45.8
5	N/G	N/G	N/G	52.4
5	N/G	N/G	N/G	32.7
5	N/G	N/G	N/G	72.0
5	N/G	N/G	N/G	39.3
6	N/G	32.7	26.2	65.5
6	N/G	26.2	78.6	45.8
6	N/G	85.1	78.6	19.6
6	N/G	32.7	78.6	19.6
6	N/G	52.4	39.3	19.6
6	N/G	19.6	32.7	39.3
6	N/G	26.2	32.7	32.7
6	N/G	26.2	45.8	19.6
6	N/G	39.3	65.5	45.8
6	N/G	72.0	52.4	32.7
6	N/G	78.6	N/G	45.8
6	N/G	19.6	N/G	85.1
6	N/G	32.7	N/G	19.6
6	N/G	32.7	N/G	52.4
6	N/G	39.3	N/G	19.6
6	N/G	45.8	N/G	19.6
6	N/G	19.6	N/G	32.7
6	N/G	85.1	N/G	65.5
6	N/G	19.6	N/G	32.7
6	N/G	32.7	N/G	32.7
6	N/G	32.7	N/G	19.6
6	N/G	19.6	N/G	N/G
7	32.7	26.2	19.6	19.6
7	45.8	19.6	39.3	32.7
7	26.2	45.8	32.7	32.7

Appendix 8.3.1 continued

7	39.3	65.5	19.6	26.2
7	N/G	32.7	26.2	58.9
7	N/G	45.8	65.5	45.8
7	N/G	26.2	45.8	N/G
7	N/G	32.7	19.6	N/G
7	N/G	39.3	19.6	N/G
7	N/G	19.6	45.8	N/G
7	N/G	19.6	58.9	N/G
7	N/G	65.5	N/G	N/G
7	N/G	26.2	N/G	N/G
7	N/G	45.8	N/G	N/G
7	N/G	26.2	N/G	N/G
7	N/G	32.7	N/G	N/G
7	N/G	32.7	N/G	N/G
7	N/G	19.6	N/G	N/G
7	N/G	26.2	N/G	N/G
8	39.3	26.2	26.2	91.7
8	26.2	52.4	45.8	65.5
8	65.5	52.4	19.6	19.6
8	19.6	52.4	19.6	19.6
8	45.8	45.8	32.7	32.7
8	78.6	19.6	39.3	32.7
8	98.2	32.7	39.3	N/G
8	45.8	N/G	32.7	N/G
8	19.6	N/G	32.7	N/G
8	52.4	N/G	52.4	N/G
8	98.2	N/G	19.6	N/G
8	26.2	N/G	32.7	N/G
8	52.4	N/G	26.2	N/G
8	32.7	N/G	19.6	N/G
8	N/G	N/G	52.4	N/G
8	N/G	N/G	26.2	N/G
8	N/G	N/G	45.8	N/G
9	65.5	26.2	32.7	26.2
9	19.6	52.4	26.2	58.9
9	32.7	58.9	78.6	19.6
9	32.7	26.2	26.2	26.2
9	45.8	39.3	32.7	19.6
9	19.6	19.6	39.3	26.2
9	32.7	78.6	19.6	39.3

Appendix 8.3.1 continued

9	32.7	163.7	45.8	52.4
9	65.5	52.4	32.7	72.0
9	52.4	58.9	78.6	N/G
9	39.3	19.6	78.6	N/G
9	65.5	32.7	78.6	N/G
9	52.4	45.8	19.6	N/G
9	19.6	72.0	19.6	N/G
9	26.2	65.5	26.2	N/G
9	39.3	52.4	32.7	N/G
9	N/G	65.5	N/G	N/G
9	N/G	72.0	N/G	N/G
9	N/G	32.7	N/G	N/G
9	N/G	19.6	N/G	N/G
9	N/G	111.3	N/G	N/G
9	N/G	26.2	N/G	N/G
10	32.7	78.6	85.1	45.8
10	32.7	137.5	65.5	19.6
10	32.7	65.5	58.9	52.4
10	196.5	65.5	52.4	19.6
10	150.6	52.4	26.2	32.7
10	32.7	196.5	32.7	32.7
10	183.4	39.3	26.2	39.3
10	32.7	19.6	72.0	39.3
10	117.9	98.2	39.3	26.2
10	32.7	65.5	39.3	45.8
10	39.3	131.0	26.2	26.2
10	85.1	32.7	26.2	39.3
10	131.0	196.5	19.6	26.2
10	137.5	26.2	275.0	19.6
10	137.5	65.5	235.8	19.6
10	131.0	19.6	65.5	52.4
10	124.4	39.3	19.6	19.6
10	52.4	52.4	32.7	32.7
10	32.7	26.2	19.6	19.6
10	137.5	58.9	N/G	196.5
10	26.2	262.0	N/G	32.7
10	19.6	52.4	N/G	32.7
10	52.4	78.6	N/G	19.6
10	65.5	N/G	N/G	19.6
10	32.7	N/G	N/G	203.0

Appendix 8.3.1 continued

10	19.6	N/G	N/G	52.4
10	52.4	N/G	N/G	32.7
10	39.3	N/G	N/G	19.6
10	39.3	N/G	N/G	65.5
10	78.6	N/G	N/G	32.7
10	N/G	N/G	N/G	229.2
10	N/G	N/G	N/G	19.6
10	N/G	N/G	N/G	26.2
10	N/G	N/G	N/G	65.5
10	N/G	N/G	N/G	32.7
10	N/G	N/G	N/G	111.3
10	N/G	N/G	N/G	65.5
10	N/G	N/G	N/G	65.5
10	N/G	N/G	N/G	52.4
10	N/G	N/G	N/G	45.8
10	N/G	N/G	N/G	19.6
10	N/G	N/G	N/G	131.0

Appendix 8.3.2 Pollen tube lengths (µm) of *in vitro* germinated *Arceuthobium americanum* pollen collected on April 27, 1998 from ten *Pinus banksiana* brooms. Medium contained 1.5% agar, 0.01% boric acid, and 15% or 20% sucrose, and was incubated at either 20 or 30 °C, in the dark (N/G = no grains).

broom #	temperature (°C)			
	20		30	
	sucrose (%)			
	15	20	15	20
1	72.0	26.2	N/G	26.2
1	26.2	26.2	N/G	N/G
1	26.2	39.3	N/G	N/G
1	19.6	26.2	N/G	N/G
1	19.6	32.7	N/G	N/G
1	32.7	78.6	N/G	N/G
1	39.3	85.1	N/G	N/G
1	72.0	26.2	N/G	N/G
1	19.6	39.3	N/G	N/G
1	19.6	32.7	N/G	N/G
1	26.2	19.6	N/G	N/G
2	45.8	39.3	N/G	19.6
2	19.6	19.6	N/G	19.6
2	19.6	72.0	N/G	45.8
2	32.7	19.6	N/G	N/G
2	32.7	65.5	N/G	N/G
2	N/G	32.7	N/G	N/G
3	19.6	58.9	N/G	19.6
3	N/G	45.8	N/G	N/G
3	N/G	32.7	N/G	N/G
3	N/G	19.6	N/G	N/G
3	N/G	19.6	N/G	N/G
4	N/G	32.7	26.2	N/G
4	N/G	65.5	N/G	N/G
4	N/G	32.7	N/G	N/G
4	N/G	52.4	N/G	N/G
4	N/G	19.6	N/G	N/G
4	N/G	26.2	N/G	N/G
4	N/G	19.6	N/G	N/G
4	N/G	26.2	N/G	N/G
4	N/G	32.7	N/G	N/G
4	N/G	32.7	N/G	N/G
5	52.4	26.2	19.6	N/G

Appendix 8.3.2 continued

5	85.1	52.4	N/G	N/G
5	19.6	52.4	N/G	N/G
5	26.2	52.4	N/G	N/G
5	26.2	58.9	N/G	N/G
5	32.7	26.2	N/G	N/G
5	19.6	26.2	N/G	N/G
5	N/G	19.6	N/G	N/G
5	N/G	19.6	N/G	N/G
5	N/G	19.6	N/G	N/G
6	N/G	78.6	26.2	26.2
6	N/G	98.2	32.7	32.7
6	N/G	52.4	N/G	19.6
6	N/G	72.0	N/G	N/G
6	N/G	52.4	N/G	N/G
7	19.6	26.2	19.6	52.4
7	19.6	32.7	19.6	19.6
7	26.2	78.6	N/G	N/G
7	32.7	19.6	N/G	N/G
7	39.3	91.7	N/G	N/G
7	26.2	N/G	N/G	N/G
7	65.5	N/G	N/G	N/G
8	85.1	19.6	58.9	N/G
8	52.4	39.3	72.0	N/G
8	32.7	39.3	45.8	N/G
8	19.6	52.4	26.2	N/G
8	26.2	72.0	N/G	N/G
8	52.4	26.2	N/G	N/G
8	26.2	19.6	N/G	N/G
8	32.7	N/G	N/G	N/G
8	32.7	N/G	N/G	N/G
8	39.3	N/G	N/G	N/G
8	65.5	N/G	N/G	N/G
8	19.6	N/G	N/G	N/G
8	52.4	N/G	N/G	N/G
9	26.2	19.6	32.7	19.6
9	32.7	19.6	32.7	52.4
9	26.2	26.2	26.2	26.2
9	19.6	52.4	32.7	45.8
9	19.6	32.7	65.5	32.7
9	19.6	39.3	19.6	26.2

Appendix 8.3.2 continued

9	39.3	104.8	19.6	N/G
9	39.3	52.4	52.4	N/G
9	52.4	19.6	19.6	N/G
9	26.2	19.6	26.2	N/G
9	19.6	N/G	45.8	N/G
9	26.2	N/G	19.6	N/G
9	19.6	N/G	26.2	N/G
9	45.8	N/G	N/G	N/G
9	72.0	N/G	N/G	N/G
9	72.0	N/G	N/G	N/G
9	58.9	N/G	N/G	N/G
9	65.5	N/G	N/G	N/G
10	65.5	98.2	32.7	19.6
10	45.8	52.4	19.6	19.6
10	19.6	52.4	32.7	26.2
10	19.6	32.7	19.6	26.2
10	19.6	19.6	19.6	32.7
10	39.3	26.2	19.6	26.2
10	26.2	32.7	N/G	45.8
10	65.5	52.4	N/G	26.2
10	124.4	26.2	N/G	39.3
10	85.1	26.2	N/G	58.9
10	52.4	78.6	N/G	19.6
10	39.3	32.7	N/G	32.7
10	32.7	32.7	N/G	39.3
10	85.1	45.8	N/G	32.7
10	111.3	45.8	N/G	32.7
10	78.6	52.4	N/G	39.3
10	78.6	32.7	N/G	32.7
10	124.4	N/G	N/G	19.6
10	78.6	N/G	N/G	19.6
10	124.4	N/G	N/G	26.2
10	131.0	N/G	N/G	19.6
10	144.1	N/G	N/G	45.8
10	19.6	N/G	N/G	39.3
10	39.3	N/G	N/G	32.7
10	19.6	N/G	N/G	26.2
10	19.6	N/G	N/G	N/G

Appendix 8.3.3 Pollen tube lengths (µm) of *in vitro* germinated *Arceuthobium americanum* pollen collected on May 4, 1998 from ten *Pinus banksiana* brooms. Medium contained 1.5% agar, 0.01% boric acid, and 15% or 20% sucrose, and was incubated at either 20 or 30 °C, in the dark (N/G = no grains).

broom #	temperature (°C)			
	20		30	
	sucrose (%)			
	15	20	15	20
1	N/G	26.2	19.6	N/G
1	N/G	19.6	19.6	N/G
1	N/G	26.2	26.2	N/G
1	N/G	26.2	19.6	N/G
1	N/G	19.6	32.7	N/G
1	N/G	19.6	32.7	N/G
1	N/G	26.2	45.8	N/G
1	N/G	19.6	26.2	N/G
1	N/G	19.6	N/G	N/G
1	N/G	32.7	N/G	N/G
1	N/G	19.6	N/G	N/G
1	N/G	19.6	N/G	N/G
1	N/G	78.6	N/G	N/G
1	N/G	39.3	N/G	N/G
1	N/G	26.2	N/G	N/G
1	N/G	19.6	N/G	N/G
2	19.6	78.6	19.6	32.7
2	19.6	98.2	19.6	19.6
2	26.2	39.3	32.7	26.2
2	N/G	32.7	26.2	26.2
2	N/G	32.7	19.6	52.4
2	N/G	32.7	19.6	131.0
2	N/G	39.3	19.6	19.6
2	N/G	39.3	32.7	26.2
2	N/G	32.7	19.6	26.2
2	N/G	52.4	19.6	N/G
2	N/G	26.2	26.2	N/G
2	N/G	32.7	19.6	N/G
2	N/G	N/G	19.6	N/G
3	32.7	32.7	N/G	19.6
3	19.6	N/G	N/G	32.7
3	19.6	N/G	N/G	N/G
3	19.6	N/G	N/G	N/G

Appendix 8.3.3 continued

3	19.6	N/G	N/G	N/G
3	19.6	N/G	N/G	N/G
4	26.2	26.2	19.6	19.6
4	32.7	26.2	19.6	19.6
4	19.6	19.6	26.2	26.2
4	52.4	32.7	19.6	32.7
4	19.6	32.7	26.2	19.6
4	26.2	19.6	N/G	52.4
4	26.2	19.6	N/G	32.7
4	32.7	26.2	N/G	19.6
4	N/G	19.6	N/G	19.6
4	N/G	26.2	N/G	65.5
4	N/G	45.8	N/G	N/G
4	N/G	52.4	N/G	N/G
4	N/G	26.2	N/G	N/G
4	N/G	52.4	N/G	N/G
4	N/G	19.6	N/G	N/G
5	65.5	26.2	19.6	32.7
5	32.7	45.8	39.3	52.4
5	26.2	32.7	32.7	19.6
5	19.6	32.7	19.6	32.7
5	39.3	26.2	19.6	32.7
5	39.3	32.7	19.6	39.3
5	32.7	39.3	19.6	32.7
5	N/G	78.6	19.6	19.6
5	N/G	98.2	26.2	45.8
5	N/G	26.2	19.6	32.7
5	N/G	32.7	19.6	32.7
5	N/G	91.7	19.6	26.2
5	N/G	85.1	45.8	45.8
5	N/G	N/G	32.7	19.6
5	N/G	N/G	52.4	26.2
5	N/G	N/G	26.2	19.6
5	N/G	N/G	19.6	45.8
5	N/G	N/G	N/G	52.4
5	N/G	N/G	N/G	52.4
6	26.2	72.0	19.6	32.7
6	19.6	39.3	19.6	45.8
6	32.7	45.8	19.6	26.2
6	19.6	78.6	32.7	45.8

Appendix 8.3.3 continued

6	32.7	19.6	32.7	52.4
6	39.3	19.6	26.2	78.6
6	32.7	19.6	26.2	26.2
6	26.2	91.7	19.6	26.2
6	65.5	26.2	N/G	39.3
6	32.7	32.7	N/G	32.7
6	19.6	32.7	N/G	26.2
6	26.2	32.7	N/G	85.1
6	39.3	39.3	N/G	26.2
6	26.2	52.4	N/G	52.4
6	72.0	32.7	N/G	26.2
6	19.6	19.6	N/G	26.2
6	32.7	32.7	N/G	39.3
6	19.6	26.2	N/G	72.0
6	65.5	26.2	N/G	N/G
6	N/G	26.2	N/G	N/G
7	19.6	19.6	32.7	19.6
7	32.7	19.6	N/G	32.7
7	26.2	32.7	N/G	45.8
7	32.7	124.4	N/G	N/G
7	26.2	26.2	N/G	N/G
7	19.6	32.7	N/G	N/G
7	19.6	52.4	N/G	N/G
7	19.6	19.6	N/G	N/G
7	26.2	19.6	N/G	N/G
7	32.7	65.5	N/G	N/G
7	39.3	26.2	N/G	N/G
7	52.4	19.6	N/G	N/G
7	N/G	19.6	N/G	N/G
7	N/G	85.1	N/G	N/G
7	N/G	39.3	N/G	N/G
7	N/G	26.2	N/G	N/G
8	26.2	32.7	19.6	19.6
8	19.6	19.6	32.7	19.6
8	52.4	39.3	65.5	19.6
8	45.8	19.6	26.2	45.8
8	39.3	26.2	19.6	32.7
8	19.6	26.2	N/G	39.3
8	26.2	26.2	N/G	19.6
8	26.2	19.6	N/G	N/G

Appendix 8.3.3 continued

8	32.7	65.5	N/G	N/G
8	19.6	19.6	N/G	N/G
8	52.4	58.9	N/G	N/G
8	65.5	32.7	N/G	N/G
8	19.6	78.6	N/G	N/G
8	45.8	52.4	N/G	N/G
8	19.6	32.7	N/G	N/G
8	32.7	45.8	N/G	N/G
8	45.8	52.4	N/G	N/G
8	52.4	32.7	N/G	N/G
8	19.6	N/G	N/G	N/G
8	19.6	N/G	N/G	N/G
8	45.8	N/G	N/G	N/G
8	39.3	N/G	N/G	N/G
9	19.6	91.7	19.6	32.7
9	19.6	32.7	19.6	19.6
9	72.0	26.2	52.4	39.3
9	26.2	19.6	45.8	26.2
9	32.7	39.3	26.2	19.6
9	26.2	19.6	26.2	78.6
9	32.7	78.6	19.6	19.6
9	78.6	32.7	39.3	58.9
9	26.2	19.6	52.4	65.5
9	32.7	19.6	26.2	78.6
9	32.7	26.2	N/G	N/G
9	65.5	85.1	N/G	N/G
9	65.5	72.0	N/G	N/G
9	19.6	32.7	N/G	N/G
9	78.6	32.7	N/G	N/G
9	26.2	32.7	N/G	N/G
9	52.4	39.3	N/G	N/G
9	52.4	72.0	N/G	N/G
9	19.6	52.4	N/G	N/G
9	39.3	19.6	N/G	N/G
9	58.9	19.6	N/G	N/G
9	65.5	19.6	N/G	N/G
9	65.5	19.6	N/G	N/G
9	32.7	78.6	N/G	N/G
9	19.6	65.5	N/G	N/G
9	19.6	19.6	N/G	N/G

Appendix 8.3.3 continued

9	65.5	32.7	N/G	N/G
9	65.5	26.2	N/G	N/G
9	32.7	26.2	N/G	N/G
9	52.4	32.7	N/G	N/G
9	19.6	39.3	N/G	N/G
9	78.6	45.8	N/G	N/G
9	78.6	65.5	N/G	N/G
9	39.3	N/G	N/G	N/G
9	45.8	N/G	N/G	N/G
9	65.5	N/G	N/G	N/G
9	72.0	N/G	N/G	N/G
9	32.7	N/G	N/G	N/G
9	39.3	N/G	N/G	N/G
9	19.6	N/G	N/G	N/G
9	26.2	N/G	N/G	N/G
9	45.8	N/G	N/G	N/G
9	45.8	N/G	N/G	N/G
9	26.2	N/G	N/G	N/G
9	26.2	N/G	N/G	N/G
9	39.3	N/G	N/G	N/G
9	19.6	N/G	N/G	N/G
9	19.6	N/G	N/G	N/G
9	19.6	N/G	N/G	N/G
9	19.6	N/G	N/G	N/G
10	32.7	19.6	32.7	26.2
10	19.6	26.2	19.6	19.6
10	78.6	32.7	19.6	19.6
10	19.6	52.4	19.6	32.7
10	32.7	19.6	19.6	65.5
10	32.7	45.8	26.2	32.7
10	65.5	65.5	19.6	45.8
10	104.8	78.6	32.7	19.6
10	32.7	45.8	26.2	19.6
10	19.6	45.8	19.6	32.7
10	19.6	45.8	26.2	26.2
10	39.3	144.1	32.7	32.7
10	78.6	78.6	32.7	19.6
10	98.2	52.4	26.2	19.6
10	32.7	32.7	45.8	N/G
10	52.4	39.3	19.6	N/G

Appendix 8.3.3 continued

10	78.6	45.8	45.8	N/G
10	85.1	52.4	32.7	N/G
10	45.8	65.5	19.6	N/G
10	32.7	72.0	52.4	N/G
10	32.7	39.3	52.4	N/G
10	65.5	32.7	52.4	N/G
10	32.7	65.5	39.3	N/G
10	72.0	65.5	19.6	N/G
10	78.6	78.6	N/G	N/G
10	85.1	72.0	N/G	N/G
10	19.6	45.8	N/G	N/G
10	52.4	52.4	N/G	N/G
10	19.6	45.8	N/G	N/G
10	111.3	131.0	N/G	N/G
10	19.6	72.0	N/G	N/G
10	85.1	78.6	N/G	N/G
10	32.7	52.4	N/G	N/G
10	65.5	65.5	N/G	N/G
10	45.8	19.6	N/G	N/G
10	32.7	78.6	N/G	N/G
10	19.6	98.2	N/G	N/G
10	78.6	N/G	N/G	N/G
10	52.4	N/G	N/G	N/G
10	19.6	N/G	N/G	N/G
10	19.6	N/G	N/G	N/G
10	32.7	N/G	N/G	N/G
10	32.7	N/G	N/G	N/G
10	32.7	N/G	N/G	N/G
10	39.3	N/G	N/G	N/G

Appendix 8.3.4 Pollen tube lengths (µm) of *in vitro* germinated *Arceuthobium americanum* pollen collected on May 11, 1998 from ten *Pinus banksiana* brooms. Medium contained 1.5% agar, 0.01% boric acid, and 15% or 20% sucrose, and was incubated at either 20 or 30 °C, in the dark (N/G = no grains).

broom #	temperature (°C)			
	20		30	
	sucrose (%)			
	15	20	15	20
1	19.6	26.2	19.6	26.2
1	19.6	32.7	N/G	26.2
1	19.6	19.6	N/G	19.6
1	19.6	19.6	N/G	26.2
1	N/G	19.6	N/G	N/G
1	N/G	26.2	N/G	N/G
1	N/G	19.6	N/G	N/G
1	N/G	19.6	N/G	N/G
1	N/G	26.2	N/G	N/G
1	N/G	19.6	N/G	N/G
1	N/G	19.6	N/G	N/G
1	N/G	19.6	N/G	N/G
1	N/G	19.6	N/G	N/G
1	N/G	26.2	N/G	N/G
2	19.6	19.6	19.6	19.6
2	19.6	26.2	N/G	52.4
2	26.2	19.6	N/G	32.7
2	26.2	N/G	N/G	N/G
2	39.3	N/G	N/G	N/G
2	19.6	N/G	N/G	N/G
2	32.7	N/G	N/G	N/G
3	19.6	19.6	19.6	32.7
3	19.6	19.6	26.2	19.6
3	32.7	19.6	N/G	19.6
3	32.7	N/G	N/G	N/G
3	26.2	N/G	N/G	N/G
3	39.3	N/G	N/G	N/G
3	26.2	N/G	N/G	N/G
4	19.6	N/G	19.6	19.6
4	26.2	N/G	19.6	19.6
4	19.6	N/G	39.3	N/G
4	26.2	N/G	19.6	N/G
4	26.2	N/G	N/G	N/G

Appendix 8.3.4 continued

5	19.6	19.6	19.6	19.6
5	32.7	19.6	26.2	19.6
5	19.6	19.6	19.6	26.2
5	19.6	26.2	19.6	26.2
5	32.7	32.7	32.7	52.4
5	32.7	26.2	39.3	19.6
5	19.6	52.4	32.7	19.6
5	32.7	19.6	19.6	32.7
5	32.7	N/G	26.2	26.2
5	19.6	N/G	19.6	19.6
5	19.6	N/G	19.6	N/G
6	26.2	19.6	19.6	19.6
6	26.2	32.7	19.6	32.7
6	19.6	26.2	26.2	26.2
6	19.6	19.6	26.2	19.6
6	19.6	19.6	19.6	19.6
6	N/G	26.2	N/G	32.7
6	N/G	N/G	N/G	26.2
6	N/G	N/G	N/G	26.2
6	N/G	N/G	N/G	26.2
6	N/G	N/G	N/G	26.2
6	N/G	N/G	N/G	19.6
7	19.6	32.7	19.6	32.7
7	19.6	52.4	19.6	19.6
7	26.2	32.7	19.6	N/G
7	26.2	N/G	32.7	N/G
8	N/G	19.6	N/G	26.2
8	N/G	19.6	N/G	N/G
8	N/G	32.7	N/G	N/G
9	N/G	19.6	26.2	N/G
9	N/G	19.6	19.6	N/G
9	N/G	N/G	19.6	N/G
10	19.6	26.2	26.2	19.6
10	19.6	32.7	19.6	39.3
10	19.6	39.3	26.2	N/G
10	32.7	26.2	32.7	N/G
10	19.6	N/G	26.2	N/G
10	19.6	N/G	19.6	N/G
10	19.6	N/G	26.2	N/G
10	19.6	N/G	N/G	N/G

8.0 REFERENCES

Alosi, M.C., and Calvin, C.L. 1984. The anatomy and morphology of the endophytic system of Arceuthobium spp. *In* Biology of Dwarf Mistletoes: Proceedings of the Symposium. *Edited by* F.G. Hawksworth and R.F. Scharf. USDA For. Serv. Gen Tech. Rep. RM-111, Fort Collins Colorado. 40-52.

Alosi, M.C., and Calvin, C.L. 1985. The ultrastructure of dwarf mistletoe (*Arceuthobium* spp.) sinker cells in the region of the host secondary vasculature. Can. J. Bot. **63**: 889-898..

Anjaneyulu, C., and Lakshminarayana, K. 1989. Microsporogenesis and the development of male gametophyte in two species of *Diospyros* L. Taiwania, **34**: 187-191.

Aouali, N., Laporte, P., and Clément, C. 2001. Pectin secretion and distribution in the anther during pollen development in *Lilium*. Planta, **213**: 71-79.

Baker, F.A. 1981. Biology and control of the eastern dwarf mistletoe. Ph. D. thesis, University of Minnesota, Minnesota. 254 pp.

Baltz, R., Schmit, A.-C., Kohnen, M., Hentges, F., and Steinmetz, A. 1999. Differential localization of the LIM domain protein PLIM-1 in microspores and mature pollen grains from sunflower. Sex. Plant Reprod. **12**: 60-65.

Bannikova, V.P., and Khvedynich, O.A. 1977. Violation of growth of incompatible pollen tubes. Phytomorphol. **27**: 225-230.

Baranyay, J.A., and Safranyik, L. 1970. Effect of dwarf mistletoe on growth and mortality of lodgepole pine in Alberta. Can. Dept. Fish. For., Can. Serv. Publ. 1285, 19 pp.

Barlow, B.A. 1983. Biogeography of Loranthaceae and Viscaceae. *In* The Biology of Mistletoes. *Edited by* M. Calder and P. Bernhardt. Academic Press, Australia. 19-46.

Barnes, S.H., and Blackmore, S. 1988. Pollen ontogeny in *Catananche caerulea* L. (Compositae: Lactuceae) II. Free microspore stage to the formation of the male germ unit. Ann. Bot. **62**: 615-623.

Bedinger, P. 1992. The remarkable biology of pollen. Plant Cell, **4**: 879-887.

Bernhard, A., and Endress, P.K. 1999. Androecial development and systematics in Flacourtiaceae s. l. Plant Syst. Evol. **215**: 141-155.

Bhandari, N.N. 1984. The microsporagium. *In* Embryology of Angiosperms. *Edited by* B.M. Johri. Springer-Verlag, New York. 53-121.

Bhandari, N.N., and Nanda, K. 1968. Studies in Viscaceae. I. Morphology and embryology of the Indian dwarf mistletoe--*Arceuthobium minutissiumum*. Phytomorphol. **18**: 435-450.

Bhandari, N.N., and Vohra, S.C.A. 1983. Embryology and affinities of Viscaceae. *In* The Biology of Mistletoes. *Edited by* M. Calder & P. Bernhardt. Academic Press, Australia. 69-85.

Bhojwani, S.S., and Bhatnagar, S.P. 1988. The Embryology of Angiosperms. Vikas Publishing House PVT Ltd, New Delhi, India. 284 pp.

Billings, F.H. 1932. Microsporogenesis in *Phoradendron*. Ann. Bot. **46**: 979-992.

Blackmore, S., and Barnes, S.H. 1988. Pollen ontogeny in *Catananche caerulea* L. (Compositea: Lactuceae) I. Premeiotic phase to establishment of tetrads. Ann. Bot. **62**: 605-614.

Blasiak, J., Mulcahy, D.L., and Musgrave, M.E. 2001. Oxytropism: a new twist in pollen tube orientation. Planta, **213**: 318-322.

Brown, R.C., and Lemmon, B.E. 1991a. Pollen development in orchids. 1. Cytoskeleton and the control of division plane in irregular patterns of cytokinesis. Protoplasma, **163**: 9-18.

Brown, R.C., and Lemmon, B.E. 1991b. Pollen development in orchids. 2. The cytokinetic apparatus in simultaneous cytokinesis. Protoplasma, **165**: 155-166.

Brown, R.C., and Lemmon, B.E. 1991c. Pollen development in orchids. 3. A novel generative pole microtubule system predicts unequal pollen mitosis. J. Cell Sci. **99**: 273-281.

Brown, R.C., and Lemmon, B.E. 1992a. Control of division plane in normal and griseofulvin-treated microsporocytes of *Magnolia*. J. Cell Sci. **103**: 1031-1038.

Brown, R.C., and Lemmon, B.E. 1992b. Pollen development in orchids. 4. Cytoskeleton and ultrastructure of the unequal pollen mitosis in *Phalaenopsis*. Protoplasma, **167**: 183-192.

Brown, R.C., and Lemmon, B.E. 2000. The cytoskeleton and polarization during pollen development in *Carex blanda* (Cyperaceae). Am. J. Bot. **87**: 1-11.

Brumfield, R.T. 1941. Asymmetrical spindles in the first microspore division of certain angiosperms. Am. J. Bot. **28**: 713-722.

Calder, D.M. 1983. Mistletoes in focus: an introduction. *In* The Biology of Mistletoes. *Edited by* M. Calder and P. Bernhardt. Academic Press, Australia. 1-18.

Calvin, C.L., Hawksworth, F.G., and Knutson, D.M. 1984. Phloem in *Arceuthobium globosum* (Viscaceae). Bot. Gaz. **145**: 461-464.

Calvin, C.L., and Wilson, C.A. 1996. Endophytic system. *In* Dwarf Mistletoes: Biology, Pathology, and Systematics. *Edited by* F.G. Hawksworth and D. Wiens. Agriculture Handbook 709, USDA For. Serv., Washington, D. C. 113-122.

Chaubal, R., Zanella, C., Trimnell, M.R., Fox, T.W., Albertsen, M.C., and Bedinger, P. 2000. Two male-sterile mutants of *Zea mays* (Poaceae) with an extra cell division in the anther wall. Am. J. Bot. **87**: 1193-1201.

Chen, Y.-F., Matsubayashi, Y., and Sakagami, Y. 2000. Peptide growth factor phytosulfokine-α contributes to the pollen population effect. Planta, **211**: 752-755.

Cigan, A.M., Unger, E., Xu, R.-j., Kendall, T., and Fox, T.W. 2001. Phenotypic complementation of *ms45* maize requires tapetal expression of MS45. Sex. Plant Reprod. **14**: 135-142.

Clément, C., Laporte, P., and Audran, J.C. 1998. The loculus content and tapetum during pollen development in *Lilium*. Sex. Plant Reprod. **11**: 94-106.

Cohen, L.I. 1963a. Studies on the ontogeny of the dwarf mistletoes, *Arceuthobium*. I. Embryogeny and histogenesis. Am. J. Bot. **50**: 400-407.

Cohen, L.I. 1963b. Studies on the ontogeny of the dwarf mistletoes, *Arceuthobium*. II. Homology of the endophytic system. Am. J. Bot. **50**: 409-417.

Cohen, L.I. 1965. Studies on the ontogeny of the dwarf mistletoes, *Arceuthobium*. III. Development of the inflorescence. Am. J. Bot. **52**: 455-463.

Cohen, L.I. 1968. Development of the staminate flower in the dwarf mistletoe *Arceuthobium*. Am. J. Bot. **55**: 187-193.

Coppola, J. 1989. Wind dispersal of *Arceuthobium americanum* pollen. Southwest. Nat. **34**: 291-293.

Corriveau, J.L., and Coleman, A.W. 1988. Rapid screening method to detect potential biparental inheritance of plastid DNA and results for over 200 angiosperm species. Am. J. Bot. **75**: 1443-1458.

Dafni, A. 1992. Pollination Ecology-A Practical Approach. Oxford University Press, New York. 250 pp.

Davis, G.L. 1966. Systematic Embryology of the Angiosperms. John Wiley & Sons, New York. 528 pp.

De Martinis, D., Cotti, G., te Lintel Hekker, S., Harren, F.J.M., and Mariani, C. 2002. Ethylene response to pollen tube growth in *Nicotiana tabacum* flowers. Planta, **214**: 806-812.

Derksen, J., Knuiman, B., Hoedemaekers, K., Guyon, A., Bonhomme, S., and Pierson, E.S. 2002. Growth and cellular organization of *Arabidopsis* pollen tubes *in vitro*. Sex. Plant Reprod. **15**: 133-139.

Derksen, J., van Wezel, R., Knuiman, B., Ylstra, B., and van Tunen, A. 1999. Pollen tubes of flavonol-deficient *Petunia* show striking alterations in wall structure leading to tube disruption. Planta, **207**: 575-581.

Dickinson, H.G. 1976. Common factors in exine deposition. *In* The Evolutionary Significance of the Exine. Linnean Society Symposium Series Number 1. *Edited by* I.K. Ferguson and J. Muller. Academic Press, London. 67-89.

Dickinson, H.G., Elleman, C.J., and Doughty, J. 2000. Pollen coatings-chimaeric genetics and new functions. Sex. Plant Reprod. **12**: 302-309.

Dowding, E.S. 1929. The vegetation of Alberta. III. The sandhill areas of central Alberta with particular reference to the ecology of *Arceuthobium americanum* Nutt. J. Ecol. **17**: 82-110.

Dowding, E.S. 1931. Floral morphology of *Arceuthobium americanum*. Bot. Gaz. **91**: 42-54.

Dufresne, A.G. 1992. Aspects of embryogenesis in *Brassica napus* L. *cv.* Regent: a light and electron microscopic investigation from anthesis to the quadrant stage of proembryo development. M.Sc. thesis, University of Manitoba, Winnipeg, Manitoba. 146 pp.

Dunbar, A. 1973. A review of the ultrastructure and ontogeny of some angiosperm pollen. Grana, **13**: 85-92.

Duvall, M.R. 2001. An anatomical study of anther development in *Acorus* L.: phylogenetic implications. Plant Syst. Evol. **228**: 143-152.

Dwivedi, N.K., Suryanarayana, N., and Susheelamma, B.N. 1988. A note on the microsporogenesis and male gametophyte in *Cudrania javanensis* Trecul. Act. Bot. Indica, **16**: 278-280.

Echlin, P. 1971. The role of the tapetum during microsporogenesis of angiosperms. *In* Pollen: Development and Physiology. *Edited by* J. Heslop-Harrison. Appleton-Century-Crofts, New York. 41-61.

Esau, K. 1965. The flower. *In* Plant Anatomy. John Wiley & Sons, New York. 529-535.

Fei, H., and Sawhney, V.K. 1999. *MS32*-regulated timing of callose degradation during microsporogenesis in *Arabidopsis* is associated with the accumulation of stacked rough ER in tapetal cells. Sex. Plant Reprod. **12**: 188-193.

Ferguson, C., Teeri, T.T., Siika-aho, M., Read, S.M., and Bacic, A. 1998. Location of cellulose and callose in pollen tubes and grains of *Nicotiana tabacum*. Planta, **206**: 452-460.

Feuer, S., and Kuijt, J. 1978. Fine structure of mistletoe pollen. I. Eremolepidaceae, *Lepidoceras*, and *Tupeia*. Can. J. Bot. **56**: 2853-2864.

Foster, A.S., and Gifford, E.M. 1974. Comparative Morphology of Vascular Plants, 2nd ed. W.H. Freeman and Company, San Franciso. 751 pp.

French, D.W. & Baker, F.A. 1982. Summary of research on *Arceuthobium americanum* on jack pine in Manitoba. Progress Report No. 2, Cooperative Aid Agreement #13-706 with Department of Plant Pathology, University of Minnesota, Minnesota. 16 pp.

Furness, C.A., and Rudall, P.J. 1999. Inaperturate pollen in monocotyledons. Int. J. Plant Sci. **160**: 395-414.

Furness, C.A., and Rudall, P.J. 2001. The tapetum in basal angiosperms: early diversity. Int. J. Plant Sci. **162**: 375-392.

Galen, C., and Stanton, M.L. 2003. Sunny-side up: flower heliotropism as a source of parental environmental effects on pollen quality and performance in the snow buttercup, *Ranunculus adoneus* (Ranunculaceae). Am. J. Bot. **90**: 724-729.

Gilbert, J.A. 1984. The biology of dwarf mistletoes (*Arceuthobium* spp.) in Manitoba. M.Sc. thesis, University of Manitoba, Winnipeg, Manitoba. 138 pp.

Gilbert, J. A. 1988. Some aspects of the reproductive biology of Arceuthobium americanum in Manitoba. Ph.D. thesis, University of Manitoba, Winnipeg, Manitoba. 179 pp.

Gilbert, J. & Punter, D. 1990. Release and dispersal of pollen from dwarf mistletoe on jack pine in Manitoba in relation to microclimate. Can. J. For. Res. **20**: 267-273.

Gilbert, J. & Punter, D. 1991. Germination of pollen of the dwarf mistletoe *Arceuthobium americanum*. Can. J. Bot. **69**: 685-688.

Gill, L.S. 1935. *Arceuthobium* in the United States. Conn. Acad. Arts Sci. Trans. **32**: 111-245.

Goldberg, R.B., Beals, T.P., and Sanders, P.M. 1993. Anther development: basic principles and practical applications. Plant Cell, **5**: 1217-1229.

González-Melendi, P., Testillano, P.S., Ahmadian, P., Reyes, J., and Risueño, M.C. 2000. Immunoelectron microscopy of PCNA as an efficient marker for studying replication times and sites during pollen development. Chromosoma, **109**: 397-409.

Gregor, S., Wiens, D., Stevens, R.E., and Hawksworth, F.G. 1974. Pollination studies of *Arceuthobium americanum* in Utah and Colorado. Southwest. Nat. **19**: 65-73.

Greyson, R.I. 1994. The Development of Flowers. Oxford University Press, New York. 314 pp.

Guilford, W.J., Schneider, D.M., Labovitz, J., and Opella, S.J. 1988. High resolution solid state ^{13}C NMR spectroscopy of sporopollenins from different plant taxa. Plant Physiol. **86**: 134-136.

Hanácková, Z., and Piñeyro-López, A. 1997. Microsporogenesis in *Karwinskiaparvifolia* (Rhamnaceae). Bull. Pol. Acad. Sci. Biol. Sci. **45**: 135-144.

Hardy, C.R., Stevenson, D.W., and Kiss, H.G. 2000. Development of the gametophytes, flower, and floral vasculature in *Dichorisandra thyrsiflora* (Commelinaceae). Am. J. Bot. **87**: 1228-1239.

Hawksworth, F.G. 1961. Dwarfmistletoe of ponderosa pine in the southwest. . USDA For. Serv. Tech. Bul. 1246. 109 pp.

Hawksworth, F.G., and Geils, B.W. 1996. Biotic associates. *In* Dwarf Mistletoes: Biology, Pathology, and Systematics. *Edited by* F.G. Hawksworth and D. Wiens. Agriculture Handbook 709, USDA For. Serv., Washington, D.C. 73-89.

Hawksworth, F.G., and Wiens, D. 1972. Biology and Classification of Dwarf Mistletoes (*Arceuthobium*). Agriculture Handbook 401, USDA For. Serv., Washington, D.C. 234 pp.

Hawksworth, F.G., and Wiens, D. 1996. Dwarf Mistletoes: Biology, Pathology, and Systematics. Agriculture Handbook 709, USDA For. Serv., Washington, D.C. 410 pp.

Hayat, M.A. 1970. Principles and Techniques of Electron Microscopy Biological Applications Volume 1. Van Nostrand Reinhold Company, New York. 412 pp.

Hayat, M.A. 1978. Introduction to Biological Scanning Electron Microscopy. University Park Press, Baltimore. 323 pp.

Hepler, P.K. 1981. The structure of endoplasmic reticulum as revealed by osmium tetroxide-potassium ferricyanide staining. Eur. J. Cell Biol. **26**: 102-110.

Hermann, P., and Palser, B.F. 2000. Stamen development in the Ericaceae. I. Anther wall, microsporogenesis, inversion, and appendages. Am. J. Bot. **87**: 934-957.

Heslop-Harrison, J. 1971. The pollen wall: structure and development. *In* Pollen: Development and Physiology. *Edited by* J. Heslop-Harrison. Appleton-Century-Crofts, New York. 75-98.

Heslop-Harrison, J. 1976. The adaptive significance of the exine. *In* The Evolutionary Significance of the Exine. Linnean Society Symposium Series Number 1. *Edited by* I.K. Ferguson and J. Muller. Academic Press, London. 27-37.

Hormaza, J.I., and Herrero, M. 1996. Dynamics of pollen tube growth under different competition regimes. Sex. Plant Reprod. **9**: 153-160.

Hudson, D.N. 1966. The megasporogenesis of *Arceuthobium americanum* Engelm. M.Sc. thesis, University of Montana, Montana. 38 pp.

Huijuan, L., and Yaozhi, W. 1994. Microsporogenesis and the development of male gametophyte and *Gentiana macrophylla*. Phytomorphol. **44**: 37-42.

Issarakraisila, M., and Considine, J.A. 1994. Effects of temperature on pollen viability in mango *cv.* 'Kensington'. Ann. Bot. **73**: 231-240.

Izhar, S., and Frankel, R. 1971. Mechanism of male sterility in *Petunia*: the relationship between pH, callase activity in the anthers, and the breakdown of the microsporogenesis. Theor. Appl. Genet. **41**: 104-108.

Jerome, C.A. 2001. Evolutionary biology of the parasitic angiosperm *Arceuthobium americanum* (Viscaceae) as determined by genetic analysis and infectivity experiments. Ph.D. thesis, University of Manitoba, Winnipeg, Manitoba. 192 pp.

Jin-Hui, Z., Zhe, T., Zu-Keng, C., and Fu, Zhou. 1994. Ultrastructural studies on microsporogenesis in the photoperiod-sensitive genic male-sterile rice. Chinese J. Bot. **6**: 129-133.

Johnson, T. 1888. *Arceuthobium oxycedri*. Ann. Bot. **2**: 137-160.

Karnovsky, M.J. 1965. A formaldehyde-glutaraldehyde fixative of high osmolarity for use in electron microscopy. J. Cell Biol. **27**: 137A.

Karrenberg, S., Kollman, J., and Edwards, P.J. 2002. Pollen vectors and inflorescence morphology in four species of *Salix*. Plant Syst. Evol. **235**: 181-188.

Kaul, M.L.H., and Nirmala, C. 1991. Male sterile gene action diversity in barley and pea. Nucleus (Calcutta), **34**: 32-39.

Kelly, J.K., Rasch, A., and Kalisz, S. 2002. A method to estimate pollen viability from pollen size variation. Am. J. Bot. **89**: 1021-1023.

Khan, F.A., Ahmad, S., and Siddiqui, S.A. 1991. Microsporogenesis and development of male gametophyte in some *Solanum* species. Beitr. Biol. Pflanzen, **66**: 1-7.

Knox, R.B. 1984. The pollen grain. *In* Embryology of Angiosperms. *Edited by* B.M. Johri. Springer-Verlag, New York. 197-271.

Kopp, R.F., Maynard, C.A., Rocha De Niella, P., Smart, L.B., and Abrahamson, L.P. 2002. Collection and storage of pollen from *Salix* (Salicaceae). Am. J. Bot. **89**: 248-252.

Korstian, C.F., and Long, W.H. 1922. The western yellow pine mistletoe. USDA Tech. Bull. 1112, 35 pp.

Kreunen, S.S., and Osborn, J.M. 1999. Pollen and anther development in *Nelumbo* (Nelumbonaceae). Am. J. Bot. **86**: 1662-1676.

Ku, S., Yoon, H., Suh, H.S., and Chung, Y.-Y. 2003. Male-sterility of thermosensitive genic male-sterile rice is associated with premature programmed cell death of the tapetum. Planta, 10.1007/s00425-003-1030-7.

Kudlicka, K., and Rodkiewicz, B. 1990. Organelle coatings of meiotic nuclei during microsporgenesis in Malvaceae. Phytomorphol. **40**: 33-41.

Kuijt, J. 1955. Dwarf mistletoes. Bot. Rev. **21**: 569-627.

Kuijt, J. 1982. The Viscaceae in the southeastern United States. J. Arn. Arb. **63**: 401-410.

Laitiainen, E., Nieminen, K.M., Vihinen, H., and Raudaskoski, M. 2002. Movement of generative cell and vegetative nucleus in tobacco pollen tubes is dependent on microtubule cytoskeleton but independent of the synthesis of callose plugs. Sex. Plant Reprod. **15**: 195-204.

Lalonde, S., Beebe, D.U., and Saini, H.S. 1997. Early signs of disruption of wheat anther development associated with the induction of male sterility by meiotic-stage water deficit. Sex. Plant Reprod. **10**: 40-48.

Lancucka-Srodoniowa, M. 1980. Macroscopic remains of the dwarf mistletoe *Arceuthobium* Bieb. (Loranthaceae) in the Neogene of Poland. Act. Palaeobot. **21**: 61-66.

Lankinen, Å. 2000. Effects of soil pH and phosphorus on *in vitro* pollen competitive ability and sporophytic traits in clones of *Viola tricolor*. Int. J. Plant Sci. **161**: 885-893.

Lippi, M.M., Cimoli, F., Maugini, E., and Tani, G. 1994. A comparative study of the tapetal behaviour in male fertile and male sterile *Iris pallida* Lam. during microsporogenesis. Caryologia, **47**: 109-120.

Lynch, S.P., and Webster, G.L. 1975. A new technique of preparing pollen for scanning electron microscopy. Grana, **15**: 127-136.

Mascarhenas, J.P. 1989. The male gametophyte of flowering plants. Plant Cell, **1**: 657-664.

Mascarhenas, J.P., and Crone, D.E. 1996. Pollen and the heat shock response. Sex. Plant Reprod. **9**: 370-374.

Mascorro, J.A., Ladd, M.W., and Yates, R.D. 1976. Rapid infiltration of biological tissues utilizing *n*-hexenyl succinic anhydride (HXSA)/vinyl cyclohexene (VCD), an ultra-low viscosity embedding medium. Ann. Proc. Electron Microsc. Soc. Am. **34**: 346-347.

Mathew, C.J. 1978. Development of male and female gametophytes in *Camellia sasanqua*. Phytomorphol. **28**: 262-269.

Mathiasen, R.L. 1996. Dwarf mistletoes in forest canopies. Northwest Sci. **70**: 61-71.

Mauseth, J.D. 1988. Plant Anatomy. The Benjamin/Cummings Publishing Company, Menlo Park, California. 559 pp.

McConchie, C.A., Jobson, S., and Knox, R.B. 1985. Computer-assisted reconstruction of the male germ unit in pollen of *Brassica campestris*. Protoplasma, **127**: 57-63.

Meyerowitz, E.M. 1994. The genetics of flower development. Sci. Am. **271**: 56-65.

Mogami, N., Shiota, H., and Tanaka, I. 2002. LP28, a lily pollen-specific LEA-like protein, is located in the callosic cell wall during male gametogenesis. Sex. Plant Reprod. **15**: 57-63.

Mogensen, H.L., and Rusche, M.L. 2000. Occurrence of plastids in rye (Poaceae) sperm cells. Am. J. Bot. **87**: 1189-1192.

Moore, P.D., Webb, J.A., and Collinson, M.E. 1991. Pollen Analysis, 2nd ed. Blackwell Scientific Publications, Oxford. 216 pp.

Moscatelli, A., Cai, G., Liu, G.-Q., Tiezzi, A., and Cresti, M. 1996. Dynein-related polypeptides in pollen and pollen tubes. Sex. Plant Reprod. **9**: 312-317.

Nickerson, A.W., Bulla, Jr., L.A., and Kurtzman, C.P. 1970. Spores. *In* Principles and Techniques of Scanning Electron Microscopy, Biological Applications Volume 1. *Edited by* M.A. Hayat. Van Nostrand Reinhold Company, New York. 159-180.

Nickrent, D.L. 1996. Molecular systematics. *In* Dwarf Mistletoes: Biology, Pathology, and Systematics. *Edited by* F.G. Hawksworth and D. Wiens. Agriculture Handbook 709, USDA For. Serv., Washington, D.C. 155-172.

Nitta, T., Takahata, Y., and Kaizuma, N. 1997. Scanning electron microscopy of microspore embryogenesis in *Brassica* spp. Plant Cell Rep. **16**: 406-410.

O'Brien, T.P., and McCully, M.E. 1981. The Study of Plant Structure Principles and Selected Methods. Termarcarphi Pty. Ltd., Melbourne, Australia. 353 pp.

Okada, T., and Toriyama, K. 2001. Pollen vegetative cell-specific expression of *Bra r 1*: useful tool for observation of the vegetative nucleus and identification of transgenic pollen by nuclear-targeted GFP. Sex. Plant Reprod. **13**: 301-307.

Omori, Y., and Ohba, H. 1996. Pollen development of *Rheum nobile* Hook.f. and Thomson (Polygonaceae), with reference to its sterility induced by bract removal. Bot. J. Linn. Soc. **122**: 269-278.

Osborn, J.M., El-Ghazaly, G., and Cooper, R.L. 2001. Development of the exineless pollen wall in *Callitriche truncata* (Callitrichaceae) and the evolution of underwater pollination. Plant Syst. Evol. **228**: 81-87.

Pacini, E. 1996. Types and meaning of pollen carbohydrate reserves. Sex. Plant Reprod. **9**: 362-366.

Pacini, E., Bellani, L.M., and Lozzi, R. 1986. Pollen, tapetum and anther development in two cultivars of sweet cherry (*Prunus avium*). Phytomorphol. **36**: 197-210.

Pacini, E., Franchi, G.G., and Hesse, M. 1985. The tapetum: its form function, and possible phylogeny in Embryophyta. Plant Syst. Evol. **149**: 155-185.

Pasonen, H.L., Käpylä, M., and Pulkkinen, P. 2000. Effects of temperature and pollination site on pollen performance in *Betula pendula* Roth-evidence for genotype-environment interactions. Theor. Appl. Genet. **100**: 1108-1112.

Penfield, F.B., Stevens, R.E., and Hawksworth, F.G. 1976. Pollination ecology of three Rocky Mountain dwarf mistletoes. For. Sci. **22**: 473-484.

Pérez-Muñoz, C.A., Jernstedt, J.A., and Webster, B.D. 1993. Pollen wall development in *Vigna vexillata* II. Ultrastructural studies. Am. J. Bot. **80**: 1193-1202.

Piffanelli, P., Ross, J.H.E., and Murphy, D.J. 1998. Biogenesis and function of the lipidic structures of pollen grains. Sex. Plant Reprod. **11**: 65-80.

Piven, N.M., Barredo-Pool, F.A., Borges-Argáez, I.C., Herrera-Alamillo, M.A., Mayo-Mosqueda, A., Herrera-Herrera, J.L., and Robert, M.L. 2001. Reproductive biology of henequén (*Agave fourcroydes*) and its wild ancestor *Agave angustifolia* (Agavaceae). 1. Gametophyte development. Am. J. Bot. **88**: 1966-1976.

Player, G. 1979. Pollination and wind dispersal of pollen in *Arceuthobium*. Ecol. Monogr. **49**: 73-87.

Poulton, J.L., Koide, R.T., and Stephenson, A.G. 2001. Effects of mycorrhizal infection and soil phosphorus availability on *in vitro* and *in vivo* pollen performance *in Lycopersicon esculentum* (Solanaceae). Am. J. Bot. **88**: 1786-1793.

Prasad, T., Prasad, K., and Singh, D. 1990. Embryology and seed development in *Cyphomandra betacea* Sendt. (Solanaceae). J. Phytol. Res. **3**: 79-84.

Punter, D., and Gilbert, J. 1989. Animal vectors of *Arceuthobium americanum* seed in Manitoba. Can. J. For. Res. **19**: 865-869.

Punter, D., and Gilbert, J. 1991. Explosive discharge of jack pine dwarf mistletoe (*Arceuthobium americanum*) seed in Manitoba. Can. J. For. Res. **21**: 434-438.

Raghavan, V. 1995. Manipulation of pollen grains for gametophytic and sporophytic types of growth. *In* Methods in Cell Biology. *Edited by* D.W. Galbraith, H.J. Bohnert, and D.P. Bourque. Academic Press, New York. 367-375.

Ranganath, R.M., and Nagashree, N.R. 2000. Selective cell elimination during microsporogenesis in sedges. Sex. Plant Reprod. **13**: 53-60.

Ressayre, A., Raquin, C., Mignot, A., Godelle, B., and Gouyon, P.-H. 2002. Correlated variation in microtubule distribution, callose deposition during male post-meiotic cytokinesis, and pollen aperture number across *Nicotiana* species (Solanaceae). Am. J. Bot. **89**: 393-400.

Reynolds, E.S. 1963. The use of lead citrate at high pH as an electron opaque stain in electron microscopy. J. Cell Biol. **17**: 208-212.

Rodkiewicz, B., Bednara, F., and Szczuka, E. 1992. The organelle aggregation, plastid division and incipient cytokinesis I in simultaneous sporo- and microsporogenesis. Ukr. Botan. Zh. **49**: 75-80.

Rodkiewicz, B., Duda, E., and Bednara, J. 1989. Organelle aggregations during microsporogenesis in *Nymphaea*. Flora (Jena), **183**: 397-404.

Rodríguez-García, M.I., and Majewska-Sawka, A. 1992. Is the special callose wall of microsporocytes an impermeable barrier? J. Exp. Bot. **43**: 1659-1663.

Ross, C.M. 2002. Development in the female flowere/fruit of the dwarf mistletoe *Arceuthobium americanum* (Viscaceae): reproductive development, viscin tissue development, and cytogenetic analysis of tissue regions within the fruit. Ph.D. thesis, University of Manitoba, Winnipeg, Manitoba. 517 pp.

Rowley, J.R. 1976. Dynamic changes in pollen wall morphology. *In* The Evolutionary Significance of the Exine. Linnean Society Symposium Series Number 1. *Edited by* I.K. Ferguson and J. Muller. Academic Press, London. 39-65.

Russell, S.D. 1984. Ultrastructure of the sperm of *Plumbago zeylanica*: 2. Quantitative cytology and three dimensional reconstruction. Planta, **162**: 385-391.

Russell, S.D., and Cass, D.D. 1981. Ultrastructure of the sperm of *Plumbago zeylanica*: 1. Cytology and association with the vegetative nucleus. Protoplasma, **107**: 85-107.

Russell, S.D., Strout, G.W., Stramski, A.K., Mislan, T.W., Thompson, R.A., and Schoemann, L.M. 1996. Microgametogenesis in *Plumbago zeylanica*

(Plumaginaceae). 1. Descriptive cytology and three-dimensional organization. Am. J. Bot. **83**: 1435-1453.

Saito, C., Nagata, N., Sakai, A., Mori, K., Kuroiwa, H., and Kuroiwa, T. 2000. Unequal distribution of DNA-containing organelles in generative and sperm cells of *Erythrinacrista-galli* (Fabaceae). Sex. Plant Reprod. **12**: 296-301.

Santos, R.P., Mariath, J.E.A., and Hesse, M. 2003. Pollenkitt formation in *Ilexparaguariensis* A.St.Hil. (Aquifoliaceae). Plant Syst. Evol. **237**: 185-198.

Sheoran, I.S., and Saini, H.S. 1996. Drought-induced male sterility in rice: changes in carbohydrate levels and enzyme activities associated with the inhibition of starch accumulation in pollen. Sex. Plant Reprod. **9**: 161-169.

Sodmergen, Zhang, Q., Zhang, Y., Sakamoto, W., and Kuroiwa, T. 2002. Reduction in amounts of mitochondrial DNA in the sperm cells as a mechanism for maternal inheritance in *Hordeum vulgare*. Planta, DOI 10.1007/s00425-002-0853-y.

Song, C.P., An, G.Y., Cao, G.S., Du, Z.L., Wang, X.C., and Yen, L.F. 1998. Involvement of Ca^{+2} in 1-aminocyclopropane-1-carboxylic acid-stimulated pollen germination. J. Plant Growth Regul. **17**: 95-99.

Southworth, D. 1986. Substructural organization of pollen exines. *In* Pollen and Spores Form and Function: Linnean Society Symposium Series. *Edited by* S. Blackmore and I.K. Ferguson. Academic Press, Orlando, Florida. 61-69.

Southworth, D. 1996. Gametes and fertilization in flowering plants. Curr. Top. Dev. Biol. **34**: 259-279.

Speranza, A., Calzoni, G.L., and Pacini, E. 1997. Occurrence of mono- or disaccharides and polysaccharide reserves in mature grains. Sex. Plant Reprod. **10**: 110-115.

Spurr, A.R. 1969. A low-viscosity epoxy resin embedding medium for electron microscopy. J. Ultrastruct. Res. **26**: 31-43.

Srivastava, L.M., and Esau, K. 1961. Relation of dwarfmistletoe (*Arceuthobium*) to the xylem tissue of conifers. I. Anatomy of parasite sinkers and their connection with host xylem. Am. J. Bot. **48**: 159-167.

Stanley, R.G. 1971. Pollen chemistry and tube growth. *In* Pollen: Development and Physiology. *Edited by* J. Heslop-Harrison. Appleton-Century-Crofts, New York. 131-155.

Stanley, R.G., and Linskens, H.F. 1974. Pollen: Biology, Biochemistry, and Management. Springer-Verlag, New York. 306 pp.

Stepka, M., Ciampolini, F., Charzynska, M., and Cresti, M. 2000. Localization of pectins in the pollen tube wall of *Ornithogalum virens* L. Does the pattern of pectin distribution depend on the growth rate of the pollen tube? Planta, **210**: 630-635.

Stevens, R.E., and Hawksworth, F.G. 1970. Insects and mites associated with dwarf mistletoes. USDA For. Serv. Res. Pap. RM-59, Fort Collins, Colorado. 12 pp.

Straatman, K.R., Nijsse, J., Kieft, H., van Aelst, A.C., and Schel, J.H.N. 2000. Nuclear pore dynamics during pollen development and androgenesis in *Brassica napus*. Sex. Plant Reprod. **13**: 43-51.

Sumner, M.J. 1986. Ovule development and zygote formation in *Brassica campestris* L. *cv*. Candle. Ph.D. thesis, University of Manitoba, Winnipeg, Manitoba. 184 pp.

Sussex, I.M. 1989. Developmental programming of the shoot meristem. Cell, **56**: 225-229.

Suzuki, K., Takeda, H., Tsukaguchi, T., and Egawa, Y. 2001. Ultrastructural study on degeneration of tapetum in anther of snap bean (*Phaseolus vulgaris* L.) under heat stress. Sex. Plant Reprod. **13**: 293-299.

Tanaka, I. 1997. Differentiation of generative and vegetative cells in angiosperm pollen. Sex. Plant Reprod. **10**: 1-7.

Tanaka, I., Ono, K., and Fukuda, T. 1998. The developmental fate of angiosperm pollen is associated with a preferential decrease in the level of histone H1 in the vegetative nucleus. Planta, **206**: 561-569.

Taylor, L.P., and Hepler, P.K. 1997. Pollen germination and tube growth. Ann. Rev Plant Physiol. Plant Mol. Biol. **48**: 461-491.

Taylor, P.E., Glover, J.A., Lavithis, M., Craig, S., Singh, M.B., Knox, R.B., Dennis, E.S., and Chaudhury, A.M. 1998. Genetic control of male fertility in *Arabidopsis thaliana*: structural analyses of postmeiotic developmental mutants. Planta, **205**: 492-505.

Tejaswini. 2002. Variability of pollen grain features: a plant strategy to maximize reproductive fitness in two species of *Dianthus*? Sex. Plant Reprod. **14**: 347-353.

Thoday, D., and Johnson, E.T. 1930. On *Arceuthobium pusillum*, Peck. II. Flowers and fruit. Ann. Bot. **44**: 813-824.

Tian, H.Q., Zhang, Z., and Russell, S.D. 2001. Sperm dimorphism in *Nicotiana tabacum* L. Sex. Plant Reprod. **14**: 123-125.

Tsou, C.-H., Fu, Y.-L. 2002. Tetrad pollen formation in *Annona* (Annonaceae): proexine formation and binding mechanism. Am. J. Bot. **89**: 734-747.

Van Tieghem, P. 1895. Observations sur la structure et la déhiscence des anthères des Loranthacées, suivies de remarques sur la structure et la déhiscence de l'anthère en génèral. Bull. Soc. bot. Fr. **42**: 363-368.

Weber, W.A. 1976. Rocky Mountain Flora. A field guide for the identification of the Ferns, Conifers, and Flowering Plants of the Southern Rocky Mountains from Pikes Peak to Rocky Mountain National Park and from the Plains to the Continental Divide. Colorado Associated University Press, Boulder, Colorado. 479 pp.

West, G. 1971. Studying the Past by Pollen Analysis. *Edited by* J.J. Head and O.E. Lowenstein. Oxford University Press, London. 16 pp.

Wiens, D. 1968. Chromosomal and flowering characteristics in dwarf mistletoes (*Arceuthobium*). Am. J. Bot. **55**: 325-334.

Willey, R.L. 1971. Microtechniques: A Laboratory Guide. Macmillan Publishing Co., Inc., New York. 99 pp.

Wilson, C.A., and Calvin, C.L. 1996. Anatomy of the dwarf mistletoe shoot system. *In* Dwarf Mistletoes: Biology, Pathology, and Systematics. *Edited by* F.G. Hawksworth and D. Wiens. Agriculture Handbook 709, USDA For. Serv., Washington, D. C. 95-111.

Wyatt, R. 1998. Richards II. Some things do remain quite the same. Am. J. Bot. **85**: 1502-1505.

Xu, P., Vogt, T., and Taylor, L.P. 1997. Uptake and metabolism of flavonols during *in vitro* germination of *Petunia hybrida* (L.) pollen. Planta, **202**: 257-265.

Yoder, J.I. 1999. Parasitic plant responses to host plant signals: a model for subterranean plant-plant interactions. Curr. Opin. Plant Biol. **2**: 65-70.

Zonia, L., Cordeiro, S., and Feijó, J.A. 2001. Ion dynamics and hydrodynamics in the regulation of pollen tube growth. Sex. Plant Reprod. **14**: 111-116